



---

Dissertations

Theses and Dissertations


---

1990

## Multinuclear Magnetic Resonance Studies of Arenesulfonates: Substituent, Concentration, Counterion, and Solvent Effects

David C. French  
*Loyola University Chicago*

Follow this and additional works at: [https://ecommons.luc.edu/luc\\_diss](https://ecommons.luc.edu/luc_diss)

 Part of the [Chemistry Commons](#)

---

### Recommended Citation

French, David C., "Multinuclear Magnetic Resonance Studies of Arenesulfonates: Substituent, Concentration, Counterion, and Solvent Effects" (1990). *Dissertations*. 3171.  
[https://ecommons.luc.edu/luc\\_diss/3171](https://ecommons.luc.edu/luc_diss/3171)

This Dissertation is brought to you for free and open access by the Theses and Dissertations at Loyola eCommons. It has been accepted for inclusion in Dissertations by an authorized administrator of Loyola eCommons. For more information, please contact [ecommons@luc.edu](mailto:ecommons@luc.edu).



This work is licensed under a [Creative Commons Attribution-Noncommercial-No Derivative Works 3.0 License](#).  
Copyright © 1990 David C. French

**MULTINUCLEAR MAGNETIC RESONANCE STUDIES OF ARENESULFONATES:  
SUBSTITUENT, CONCENTRATION, COUNTERION, AND SOLVENT EFFECTS**

by

**David C. French**

A Dissertation Submitted to the Faculty of the Graduate School of  
Loyola University of Chicago in Partial Fulfillment of the Requirements  
for the Degree of Doctor of Philosophy

August 1990

## ACKNOWLEDGEMENTS

I am extremely grateful to Dr. David S. Crumrine for his direction of this project, for his encouragement, and for his guidance in the preparation of the manuscripts for publication. I would like to thank Dr. A. Keith Jameson, Dr. Duarte Mota de Freitas, and Dr. Charles M. Thompson for their helpful suggestions.

My thanks are due to the faculty, staff, and graduate students in the Chemistry Department for their support. I would like to thank the Chemistry Department for the award of a First Year Graduate Student Scholarship, and the Graduate School for the award of a University Fellowship.

I gratefully acknowledge Patricia S. Ryan, my wife, for her patience and encouragement during the completion of this study. Special thanks are due to Eileen J. French for assisting in the care of her grandson, Eric D. French, during my last year of study.

## DEDICATION

Dedicated to the memory of Romaine C. French

## VITA

The author, David C. French, is the son of Romaine C. French and Eileen J. French. He was born November 4, 1952, in East Chicago, Indiana.

His secondary education was completed June 1970 at Thornridge High School in Dolton, Illinois. He did not pursue an education in chemistry until several years after high school. Mr. French attended Southern Illinois University at Carbondale where he received the degree of Bachelor of Science in chemistry December 1981.

While at SIU-C, Mr. French worked for Dr. G. V. Smith in the Molecular Sciences Program as a undergraduate researcher from January 1981 to December 1981. After receiving his degree, he was employed by Travenol Laboratories, Inc. as a Research Assistant until July 1985. In August 1985, he entered the graduate chemistry program at Loyola University, and was awarded a First Year Graduate Student Scholarship. In April 1989, Mr. French was awarded a University Fellowship.

### List of Publications

"Concentration And Solvent Dependence of  $^{33}\text{S}$  Nuclear Magnetic Relaxation In Benzenesulfonic Acid" French, D. C.; Crumrine, D. S. *J. Magn. Reson.* **1989**, *84*, 548.

"Improved Correlation of  $^{33}\text{S}$  Chemical Shifts With  $\text{pK}_a$ 's of Arenesulfonic Acids: Use of  $^{33}\text{S}$  NMR For  $\text{pK}_a$  Determination" French, D. C.; Crumrine, D. S. *J. Org. Chem.* **1990**, *55*, 5494.

## TABLE OF CONTENTS

	Page
ACKNOWLEDGEMENTS . . . . .	ii
DEDICATION . . . . .	iii
VITA . . . . .	iv
LIST OF TABLES . . . . .	vii
LIST OF FIGURES . . . . .	ix
LIST OF SYMBOLS AND ABBREVIATIONS . . . . .	xi
CONTENTS OF APPENDIX . . . . .	xv
 <b>CHAPTER</b>	
<b>I. STATEMENT OF PROBLEMS</b>	
I.1 Use of $^{33}\text{S}$ NMR For the Determination of $\text{pK}_a$ 's of Arenesulfonic Acids . . . . .	1
I.2 Concentration, Counterion, And Solvent Dependence of $^{33}\text{S}$ Quadrupolar Relaxation In Benzenesulfonates . . . . .	1
 <b>II. REVIEW OF THE RELATED LITERATURE</b>	
II.1 $^{33}\text{S}$ NMR Spectroscopy of Sulfonic Acids And Sulfonate Salts . . . . .	3
II.2 Use of $^{33}\text{S}$ NMR For the Determination of $\text{pK}_a$ 's of Arenesulfonic Acids . . . . .	7
II.3 Quadrupolar Relaxation of Ionic Nuclei In Electrolyte Solutions . . . . .	9
II.3.1 Introduction . . . . .	9
II.3.2 The Ion-Solvent Contribution to Quadrupolar Relaxation of Monoatomic Ions In Electrolyte Solution . . . . .	11
II.3.3 The Ion-Ion Contribution to Quadrupolar Relaxation of Monoatomic Ions In Electrolyte Solution . . . . .	14
II.3.4 $^{33}\text{S}$ Relaxation of Inorganic Ions In Aqueous Solution . . . . .	16
 <b>III. RESULTS AND DISCUSSION</b>	
III.1 Use of $^{33}\text{S}$ NMR For the Determination of $\text{pK}_a$ 's of Arenesulfonic Acids . . . . .	18
III.2 Concentration And Counterion Dependence of $^{33}\text{S}$ Quadrupolar Relaxation In Aqueous Benzenesulfonates . . . . .	27

CHAPTER	Page
III.2.1 Concentration Dependence of $^{23}\text{Na}$ Relaxation In Dilute Aqueous Benzenesulfonates . . . . .	44
III.2.2 Concentration And Counterion Dependence of $^{33}\text{S}$ Relaxation In Concentrated Aqueous Benzenesulfonates . . . . .	51
III.3 Concentration, Counterion, And Solvent Dependence of $^{33}\text{S}$ Quadrupolar Relaxation In Benzenesulfonates . . . . .	58
 IV. CONCLUSIONS	
IV.1 Use of $^{33}\text{S}$ NMR For the Determination of $\text{pK}_a$ 's of Arenesulfonic Acids . . . . .	70
IV.2 Concentration, Counterion, And Solvent Dependence of $^{33}\text{S}$ Quadrupolar Relaxation In Benzenesulfonates . . . . .	71
 V. EXPERIMENTAL SECTION	
V.1 Use of $^{33}\text{S}$ NMR For the Determination of $\text{pK}_a$ 's of Arenesulfonic Acids . . . . .	73
V.2 Concentration, Counterion, And Solvent Dependence of $^{33}\text{S}$ Quadrupolar Relaxation In Benzenesulfonates . . . . .	75
 SELECTED SPECTRA . . . . .	78
 APPENDIX . . . . .	104
 REFERENCES . . . . .	108

## LIST OF TABLES

Table	Page
1. NMR Properties of Nuclei Used In This Investigation . . . . .	4
2. $^{33}\text{S}$ Chemical Shifts And Linewidths of Arenesulfonates ( $\text{ZC}_6\text{H}_4\text{SO}_3^- \text{ Cat}^+$ ). . . . .	20
3. Taft Substituent Constants Used And Calculated $^{33}\text{S}$ Chemical Shifts of Arenesulfonates ( $\text{ZC}_6\text{H}_4\text{SO}_3^-$ ) In Aqueous Solution At $20^\circ$ And $39^\circ$ C . . . . .	22
4. $\text{pK}_a$ 's of Arenesulfonic Acids ( $\text{ZC}_6\text{H}_4\text{SO}_3\text{H}$ ) Determined By Three Methods. . . . .	23
5. $^{33}\text{S}$ NMR Data For Lithium Benzenesulfonate In Aqueous Solution . . . . .	29
6. $^{33}\text{S}$ NMR Data For Sodium Benzenesulfonate In Aqueous Solution . . . . .	30
7. $^{33}\text{S}$ NMR Data For Potassium Benzenesulfonate In Aqueous Solution . . . . .	31
8. $^{33}\text{S}$ NMR Data For Benzenesulfonic Acid In Aqueous Solution. . . . .	32
9. $^{33}\text{S}$ NMR Data For Magnesium Benzenesulfonate In Aqueous Solution . . . . .	32



Table	Page
10. Linear Regression Results For $^{33}\text{S}$ $R_Q$ vs Counterion Concentration: Five Benzenesulfonates In Aqueous Solution At 20°C . . . .	33
11. Physical Constants of the Metal Counterions Used . . . .	42
12. $^{23}\text{Na}$ Relaxation Data For Sodium Benzenesulfonate In Aqueous Solution . . . . .	46
13. Linear Regression Results For $^{23}\text{Na}$ $1/T_1$ vs Concentration of Sodium Benzenesulfonate In Aqueous Solution At 20°C . . . .	50
14. $^7\text{Li}^+$ Relaxation Data For Lithium Benzenesulfonate In Aqueous Solution . . . . .	52
15. Linear Regression Results For $^7\text{Li}^+$ $1/T_1$ vs Concentration For Aqueous Lithium Benzenesulfonate At 20° C . . . . .	54
16. $^{13}\text{C}$ Relaxation Data For Lithium Benzenesulfonate In Aqueous Solution . . . . .	55
17. $^{33}\text{S}$ NMR Data For Benzenesulfonates In Formamide Solution. . . .	59
18. $^{33}\text{S}$ NMR Data For Benzenesulfonates In Formamide Plus 18 Mole% Water Solution . . . . .	60
19. $^{33}\text{S}$ NMR Data For Benzenesulfonates In N-Methylformamide Solution . . . . .	61
20. Linear Regression Results For $^{33}\text{S}$ $R_Q$ vs Concentration: Four Benzenesulfonates In Formamide, Formamide Plus 18 Mole% Water, And N-Methylformamide At 20° C. . . . .	65
21. Some Physical Properties of the Pure Solvents Used (at 25° C) . . . . .	66

## LIST OF FIGURES

Figure	Page
1.	Structure of the Fifteen Arenesulfonates Studied . . . . . 18
2.	pK <sub>a</sub> 's of Arenesulfonic Acids Determined By Three Methods vs <sup>33</sup> S Chemical Shifts At 20° C . . . . . 25
3.	pK <sub>a</sub> 's of Arenesulfonic Acids Determined By Three Methods vs <sup>33</sup> S Chemical Shifts At 39° C . . . . . 26
4.	<sup>33</sup> S R <sub>Q</sub> vs Concentration For Lithium Benzenesulfonate In H <sub>2</sub> O At 20° C . . . . . 34
5.	<sup>33</sup> S R <sub>Q</sub> vs Concentration For Sodium Benzenesulfonate In H <sub>2</sub> O At 20° C . . . . . 35
6.	<sup>33</sup> S R <sub>Q</sub> vs Concentration For Potassium Benzenesulfonate In H <sub>2</sub> O At 20° C . . . . . 36
7.	<sup>33</sup> S R <sub>Q</sub> vs Concentration For Benzenesulfonic Acid In H <sub>2</sub> O At 20° C . . . . . 37
8.	<sup>33</sup> S R <sub>Q</sub> vs Concentration For Magnesium Benzenesulfonate In H <sub>2</sub> O At 20° C . . . . . 38
9.	<sup>33</sup> S R <sub>Q</sub> vs Concentration For (PhSO <sub>3</sub> ) <sub>n</sub> M In H <sub>2</sub> O At 20° C. . . . . 39
10.	<sup>33</sup> S R <sub>Qrel</sub> vs Concentration For (PhSO <sub>3</sub> ) <sub>n</sub> M In H <sub>2</sub> O At 20° C . . . . . 40

Figure	Page
11. $^{23}\text{Na}^+$ $1/T_1$ vs Concentration For Sodium Benzenesulfonate In $\text{H}_2\text{O}$ At $20^\circ\text{C}$ . . . . .	47
12. $^{23}\text{Na}^+$ $1/T_1$ vs Concentration (<0.2 M) For Sodium Benzenesulfonate In $\text{H}_2\text{O}$ At $20^\circ\text{C}$ . . . . .	48
13. $^{23}\text{Na}^+$ $1/T_1$ vs Square Root of Concentration For Sodium Benzenesulfonate In $\text{H}_2\text{O}$ At $20^\circ\text{C}$ . . . . .	49
14. $^7\text{Li}^+$ $1/T_1$ vs Concentration For Lithium Benzenesulfonate In $\text{H}_2\text{O}$ At $20^\circ\text{C}$ . . . . .	53
15. $^{13}\text{C}$ $1/T_1$ vs Concentration For Lithium Benzenesulfonate In $\text{H}_2\text{O}$ At $20^\circ\text{C}$ . . . . .	56
16. $^{33}\text{S}$ $R_Q$ vs Concentration For Benzenesulfonates In Formamide At $20^\circ\text{C}$ . . . . .	62
17. $^{33}\text{S}$ $R_Q$ vs Concentration For Benzenesulfonates In Formamide-Water At $20^\circ\text{C}$ . . . . .	63
18. $^{33}\text{S}$ $R_Q$ vs Concentration For Benzenesulfonates In N-Methylformamide At $20^\circ\text{C}$ . . . . .	64

## LIST OF SYMBOLS AND ABBREVIATIONS

### Roman Symbols

$a$	distance of closest approach between the relaxing nucleus in ion $i$ and the center of ion $j$
$b$	radius of the second solvation sphere
$c$	concentration in mol/liter solvent or mol/kg solvent
$c'$	concentration in particles per $\text{cm}^3$
$c_{\text{solv}}$	solvent dipole concentration in particles per $\text{cm}^3$
$d$	ion-solvent contribution to the local field gradient
$d_1$	ion-solvent contribution to the local field gradient in the FRD Model
$d_2$	ion-solvent contribution to the local field gradient in the NOS Model
$d_3$	ion-solvent contribution to the local field gradient in the FOS Model
$d^*(b)$	ion-solvent contribution to the local field gradient from solvent dipoles beyond the first solvation sphere
$e$	charge of the proton
$ez_j$	charge on ion $j$
$f_r$	microviscosity factor
$h$	Planck's constant
$\hbar$	$h/2\pi$
$I$	nuclear spin quantum number
$J(0)$	spectral density function at zero frequency
$k$	1. a reaction rate constant 2. Boltzmann's constant
$n_s$	number of solvent dipoles in the first solvation sphere of an ion
$P$	the polarization factor accounting for ion-ion cross-correlations

$P_{CR}$	the polarization factor accounting for solvent-solvent cross-correlations [ = $(2\epsilon + 3) / 5\epsilon$ ]
$Q$	nuclear electric quadrupole moment
$q_{ij}$	electric field gradient (efg) tensor element $ij$ in the molecular frame
$r$	correlation coefficient
$R^C$	receptivity of the observed nucleus relative to $^{13}\text{C}$
$R_Q$	quadrupolar relaxation rate ( = $1/T_{Q,2}$ ) at the extreme narrowing limit
$R_Q^0$	quadrupolar relaxation rate at the limit of infinite dilution
$r_0$	distance of closest approach between the center of an ion and the point dipole of a solvent molecule
$r_{ion}$	effective ionic radius
$T$	Kelvin temperature
$T_1$	longitudinal, or spin-lattice, relaxation time
$T_2$	transverse, or spin-spin, relaxation time
$T_{Q,1}$	longitudinal, or spin-lattice, relaxation time of a quadrupolar nucleus
$T_{Q,2}$	transverse, or spin-spin, relaxation time of a quadrupolar nucleus
$T_1^0$	$T_1$ at the limit of infinite dilution
$V$	molecular volume
$V_m^{(2)}(t)$	components of the electric field gradient tensor in the laboratory frame
$WF$	nuclear linewidth function
$ez_j$	charge on an ion

### Greek Symbols

$\delta$	chemical shift in ppm
$\delta(^{33}\text{S})$	$^{33}\text{S}$ chemical shift
$\delta(^{33}\text{S}_m)$	$^{33}\text{S}$ chemical shift of a <i>meta</i> -substituted benzenesulfonate

$\delta(^{33}\text{S}_p)$	$^{33}\text{S}$ chemical shift of a <i>para</i> -substituted benzenesulfonate
$\Delta$	ion-ion contribution to the local field gradient at the relaxing nucleus
$\Delta\nu_{\frac{1}{2}}$	NMR linewidth at half-height
$\epsilon$	static dielectric constant of the solvent
$\gamma$	magnetogyric ratio of the observed nucleus
$\eta$	1. asymmetry of efg tensor 2. viscosity
$\Lambda$	local field gradient quenching parameter
$\lambda$	distribution width parameter
$\mu$	dipole moment of solvent molecule
$\overline{\mu^2}$	fully random mean square of the electric dipole moment ( $= 5\mu^2 / 9$ )
$\nu_j$	stoichiometric number of ion $j$
$\Xi$	nuclear resonance frequency
$\sigma$	Hammett substituent constant
$\sigma_I$	Taft substituent constant for inductive contribution to $\sigma$
$\sigma_p$	paramagnetic part of the chemical shift
$\sigma_R$	Taft substituent constant for resonance contribution to $\sigma$
$\tau_c$	isotropic molecular reorientational correlation time
$\tau_{\text{eff}}$	effective correlation time
$\tau(\text{H}_2\text{O})$	correlation time of a water molecule in the first hydration sphere of an ion
$\tau_{\parallel}$	correlation time for molecular reorientation parallel to the principle symmetry axis
$\tau_{\perp}$	correlation time for molecular reorientation perpendicular to the principle symmetry axis

## Abbreviations

Cat <sup>+</sup>	cation
DMF	dimethylformamide
DMSO	dimethyl sulfoxide
efg	electric field gradient
FA	formamide
FID	free induction decay
FOS	Fully Oriented Solvation Model
FRD	Fully Random Distribution Model
HMPT	hexamethylphosphoric triamide
N. A.	natural abundance of observed nucleus
NMF	N-methylformamide
NMR	nuclear magnetic resonance
NOS	Non-Oriented Solvation Model
o. d.	outside diameter
ppm	parts per million
UV	ultraviolet

## CONTENTS OF APPENDIX

### $^{33}\text{S}$ NMR SPECTRA OF TWO SYNTHETIC MIXTURES OF SULFONIC ACIDS AND SULFONATE SALTS DISSOLVED IN WATER

	Page
Mixture 1 . . . . .	105
Mixture 2 . . . . .	106
Results And Discussion . . . . .	107



## CHAPTER I

### STATEMENT OF PROBLEMS

#### I.1 Use of $^{33}\text{S}$ NMR For the Determination of $\text{pK}_a$ 's of Arenesulfonic Acids

Substituent effects on the  $^{33}\text{S}$  NMR spectra of an extended series of arenesulfonates were studied. Arenesulfonic acids are almost completely ionized in aqueous solution below 1 M concentration at 20° C. The  $^{33}\text{S}$  NMR chemical shift must be related to the electron density on sulfur. The application of  $^{33}\text{S}$  NMR to the determination of  $\text{pK}_a$ 's of arenesulfonic acids, which largely depend on electron density at the sulfonate group, was investigated.

#### I.2 Concentration, Counterion, And Solvent Dependence of $^{33}\text{S}$ Quadrupolar Relaxation In Benzenesulfonates

The purpose of this investigation was to study the ion-ion and ion-solvent contributions to  $^{33}\text{S}$  quadrupolar relaxation rates in benzenesulfonates. Specific counterion effects were examined by studying the  $^{33}\text{S}$  quadrupolar relaxation rates of lithium, sodium, potassium, and magnesium benzenesulfonates and benzenesulfonic acid dissolved in water as a function of concentration at 20° C. The  $^{33}\text{S}$  NMR relaxation rates were extrapolated to zero solute concentration in order to determine the extent to which ion-ion and ion-solvent interactions contribute to the quadrupolar relaxation of  $^{33}\text{S}$ . The  $^{33}\text{S}$  relaxation rates of lithium, sodium, and potassium benzenesulfonates

dissolved in the solvents formamide, N-methylformamide, and a binary mixture of formamide plus 18 mole% water were also studied to determine if the specific ion-ion contribution to  $^{33}\text{S}$  relaxation follows the same trend as in the aqueous systems. These data were extrapolated to zero concentration in order to compare the ion-solvent contribution to  $^{33}\text{S}$  quadrupolar relaxation rates in the solvents studied.

## CHAPTER II

### REVIEW OF THE RELATED LITERATURE

#### II.1 $^{33}\text{S}$ NMR Spectroscopy of Sulfonic Acids And Sulfonate Salts

The only naturally occurring isotope of sulfur with a non-zero nuclear spin quantum number is  $^{33}\text{S}$  ( $I = 3/2$ ). The field of  $^{33}\text{S}$  NMR has grown rapidly, and a review of the subject has appeared.<sup>1</sup> The NMR properties of  $^{33}\text{S}$  are listed in Table 1, along with those of the other more frequently studied nuclei which were used in this investigation.<sup>2a</sup>

Due to several of the properties of  $^{33}\text{S}$ , it is an intrinsically insensitive nucleus for NMR investigation. For instance, its low natural abundance and low magnetogyric ratio give  $^{33}\text{S}$  an NMR receptivity of  $9.78 \times 10^{-2}$  relative to  $^{13}\text{C}$ .<sup>2</sup> Additionally, the moderate nuclear electric quadrupole moment of  $^{33}\text{S}$  gives rise to NMR signals which, in many cases, may be very broad (i. e. hundreds to thousands of hertz).<sup>2b</sup>

**Table 1.** NMR Properties of Nuclei Used In This Investigation.<sup>a</sup>

Property	Nucleus			
	<sup>33</sup> S	<sup>23</sup> Na	<sup>7</sup> Li	<sup>13</sup> C
I	3/2	3/2	3/2	1/2
N. A. (%)	0.76	100	92.58	1.1
$\gamma$ ( $10^7 \text{ rad s}^{-1} \text{ T}^{-1}$ )	2.0557	7.0704	10.3976	6.7283
Q ( $10^{-30} \text{ m}^2$ )	-6.4	10	-3.7	-----
$\epsilon$ (MHz @ 7.05 T)	23.01	79.29	116.60	75.44
R <sup>C</sup>	$9.78 \times 10^{-2}$	$5.24 \times 10^2$	$1.54 \times 10^3$	1.00
WF ( $10^{-59} \text{ m}^4$ )	5.5	13	1.8	-----

<sup>a</sup> values taken from reference 2a.

The linewidth at half-height,  $\Delta\nu_{\frac{1}{2}}$ , of an NMR signal with a Lorentzian line shape is related to the transverse, or spin-spin, relaxation time,  $T_2$ , by the expression:<sup>3</sup>

$$\Delta\nu_{\frac{1}{2}} = 1/\pi T_2 \quad [1]$$

In the limit of extreme motional narrowing, when isotropic molecular tumbling is rapid on the NMR time scale (i. e. when  $\omega\tau_c \ll 1$ ), the relaxation rate for a covalently bound quadrupolar nucleus is given by the expression:<sup>4</sup>

$$\frac{1}{T_2} = \frac{1}{T_1} = \frac{3}{40} \cdot \frac{2I+3}{I^2(2I-1)} \left[ \frac{1+\eta^2}{3} \right] \left[ \frac{eq_{zz}eQ}{\hbar} \right]^2 \tau_c \quad [2]$$

Here,  $T_1$  is the longitudinal, or spin-lattice, relaxation time,  $I$  is the spin of the relaxing nucleus,  $e$  is the charge of the proton,  $Q$  is the nuclear electric quadrupole moment, and  $\hbar$  is the modified Planck constant. The term  $eq_{zz}$  is the maximum component of the electric field gradient tensor, and the correlation time  $\tau_c$  is the time constant which describes the motional modulation of the quadrupole interaction inducing nuclear relaxation. The term  $\eta$  is the asymmetry parameter where:

$$\eta = \frac{q_{yy} - q_{xx}}{q_{zz}} \quad [3]$$

The conventional choice of axes is such that  $0 \leq \eta \leq 1$  with:

$$|q_{xx}| \leq |q_{yy}| \leq |q_{zz}| \quad [4]$$

By combining Eqns. [1] and [2], a nuclear linewidth function may be defined by:

$$WF = \frac{Q^2(2I+3)}{I^2(2I-1)} \quad [5]$$

This expression affords an estimate of the susceptibility of a nucleus to line-broadening due to rapid quadrupolar relaxation.<sup>2a</sup> The linewidth functions for the quadrupolar nuclei used in this study are listed in Table I.

Faure *et al.*<sup>5</sup> reported the <sup>33</sup>S NMR spectra of several sulfonic acids, but little else had appeared on the subject until Crumrine and Gillice-Castro<sup>6</sup> investigated the <sup>33</sup>S NMR spectra of a series of sulfonic acids and sulfonate salts dissolved in water at 6.104 MHz (1.879 T). The <sup>33</sup>S resonances of aromatic sulfonates were found upfield from those of aliphatic sulfonates. Similar results were observed for the <sup>33</sup>S NMR spectra of sulfones.<sup>7</sup> The <sup>13</sup>C NMR of the carboxylic carbon of carboxylic acids and carboxylic acid derivatives,<sup>8</sup> and the <sup>14</sup>N NMR of aromatic and aliphatic nitro compounds<sup>9</sup> both follow a similar trend.

The linewidth at half-height of the <sup>33</sup>S resonance for a given sulfonate was found to respond, in some cases dramatically, to changes in temperature, concentration, and solution pH.<sup>6</sup> However, <sup>33</sup>S chemical shifts were found to change very little with respect to changes in concentration and pH. Linewidths were also found to be sensitive to changes in solvent. The <sup>33</sup>S NMR linewidth of benzenesulfonic acid was 24 Hz in water, 59 Hz in formamide, and 200 Hz in methanol. However, no signal was observed in dimethyl sulfoxide (DMSO), dimethylformamide (DMF), acetonitrile, ethylene glycol, or formic acid.<sup>6</sup>

Sulfonic acids are known to be almost completely ionized at 1 to 3 M concentration in water.<sup>10</sup> Therefore, the narrow linewidths observed for sulfonic acids and sulfonate salts result from a high degree of symmetry in the electric field at the sulfur nucleus of the sulfonate anion. Increased ion-ion interaction at higher concentrations, formation of solvated ion aggregates, as well as changes in proton transfer rate are expected to broaden the  $^{33}\text{S}$  NMR resonance due to a concomitant decrease in the symmetry of the electric field at the sulfur nucleus. Indeed, the  $^{33}\text{S}$  linewidth for benzenesulfonic acid changed from 24 Hz at a concentration of 2.7 M in water and pH 1 to  $410 \pm 30$  Hz when dissolved in 12 M hydrochloric acid at a solute concentration of 3.3 M.<sup>6</sup>

## II.2 Use of $^{33}\text{S}$ NMR For the Determination of $\text{pK}_a$ 's of Arenesulfonic Acids

Previous studies of substituent effects on the acidities of arenesulfonic acids, including 1, 2, 8-10, and the first  $\text{pK}_a$ 's of 3 and 13 (Figure 1, page 18), have been conducted by measuring their degree of ionization in solutions of varying Hammett acidity ( $H_0$ ) using UV or  $^1\text{H}$  NMR methods.<sup>11</sup> It has been necessary to carry out these  $\text{pK}_a$  determinations in concentrated sulfuric acid solution, where significant amounts of the free sulfonic acid and its conjugate base are both present. Experimental difficulties limited these methods to sulfonic acids showing an isolated B band in the UV spectrum, and to the determination of first ionizations of disulfonic acids only. Therefore, the  $\text{pK}_a$ 's of 4, 5, 15, and 3,5-bis(trifluoro)methylbenzenesulfonic acid have previously been calculated from a Hammett plot of  $\text{pK}_a$  vs  $\sigma$ , using the experimentally determined  $\text{pK}_a$ 's of 1, 2, 8, 10, and the first ionization of 3.<sup>12</sup>

Cassidei and Sciacovelli<sup>13</sup> correlated the  $^{33}\text{S}$  chemical shifts of a series of sodium sulfonates with the  $^{13}\text{C}$  chemical shifts of the carboxylic carbon in related

sodium carboxylates. Hinton and Buster<sup>14</sup> found a linear relationship between the <sup>33</sup>S chemical shifts of arenesulfonic acids 1, 8, 11, 15 and Hammett  $\sigma$  constants. For the cases of *meta*- and *para*-ZC<sub>6</sub>H<sub>4</sub>Y, the Hammett equation is:<sup>15a</sup>

$$\log \frac{k}{k_0} = \sigma\rho \quad [6]$$

Here,  $k_0$  is the rate constant or equilibrium constant for Z = H,  $k$  is the respective constant for the group Z,  $\rho$  is a constant for a given reaction under a given set of conditions, and  $\sigma$  is a constant characteristic of the group Z.

The  $\sigma$  values account for the total electrical effects (i. e. resonance plus field) of a group Z attached to a benzene ring. A positive  $\sigma$  corresponds to an "electron-withdrawing" group and a negative  $\sigma$  corresponds to an "electron-donating" group. The slope  $\rho$  measures the susceptibility of the given reaction (eg. ionization, electrophilic substitution, nucleophilic substitution) to electronic effects. Reactions with a positive  $\rho$  are promoted by electron-withdrawing groups (eg. ionization of acids); reactions with a negative  $\rho$  are promoted by electron-donating groups (eg. electrophilic substitution).

Crumrine *et al.*<sup>16</sup> reported a linear correlation between the <sup>33</sup>S NMR chemical shifts of sulfonic acids 1, 2, 4, 5, 8, 10, 15 and their pK<sub>a</sub>'s. A Hammett plot of  $\delta(^{33}\text{S})$  vs  $\sigma$  followed the relationship of Eqn. [7]. The fit was found to be greatly improved by using a dual-substituent parameter fit to  $\sigma_{\text{I}}$  and  $\sigma_{\text{R}}$  (Eqns. [8] and [9]).<sup>17</sup>

$$\delta(^{33}\text{S}) = -8.75\sigma - 11.89 \quad (r = 0.986) \quad [7]$$

$$\delta(^{33}\text{S}_{\text{m}}) = -6.39\sigma_{\text{I}} - 10.08\sigma_{\text{R}} - 11.98 \quad (r = 0.997) \quad [8]$$

$$\delta(^{33}\text{S}_{\text{p}}) = -7.37\sigma_{\text{I}} - 11.6\sigma_{\text{R}} - 112.43 \quad (r = 0.994) \quad [9]$$



Here,  $\sigma_I$  accounts for the field, or inductive, contribution to  $\sigma$  and  $\sigma_R$  accounts for the resonance contribution.<sup>15b</sup>

Chemical shifts were calculated from Eqns. [8] and [9] and plotted against the experimental values. Excellent agreement was obtained between calculated and experimental values ( $r = 0.997$ ), and the slope of the plot obtained (0.978) was within experimental error of the theoretical value of 1.00.

Changes in the  $^{33}\text{S}$  chemical shifts of the arenesulfonates were found to be related to the  $\text{pK}_a$ 's of the arenesulfonic acids. A linear relationship was obtained using:

$$\text{pK}_a = 0.0725\delta(^{33}\text{S}) - 5.787 \quad (r = 0.996) \quad [10]$$

However, this method was found to be applicable only to arenesulfonic acids.

## II.3 Quadrupolar Relaxation of Ionic Nuclei In Electrolyte Solutions

### II.3.1 Introduction

Various models have been proposed to explain the origin of the electric field gradient which induces quadrupolar relaxation of ions possessing spherical electronic symmetry in electrolyte solutions.<sup>18</sup> According to the collision model, in dilute solutions of strong electrolytes where ion-ion contributions to the electric field gradient may be neglected, the field gradient arises upon each ion-solvent molecule collision, with concomitant loss of electronic symmetry for the ion.<sup>19</sup> Since a contribution to the paramagnetic part of the chemical shift,  $\sigma_p$ , is also caused by loss of electronic symmetry, Deverell reported a relationship between  $(1/T_1)^{1/2}$  and  $\sigma_p$ .<sup>19b</sup> The theory of Deverell assumes that modulation of the field gradient arising from ion-solvent molecule collision is solely responsible for nuclear relaxation. However, the

correlation time for this "electronic contribution" should be on the order of a collision time and such extremely short correlation times would reduce the efficiency of this mechanism.<sup>18</sup> Therefore, this contribution to nuclear relaxation is neglected in other models for simple electrolyte solutions at normal temperatures and densities.

In the electrostatic model of Hertz,<sup>20</sup> the electric field gradient arises from the electric point dipoles of the surrounding solvent molecules and the point charges of other ions in solution. Hertz developed expressions for relaxation rates of quadrupolar nuclei in electrolyte solutions, at finite concentration as well as at infinite dilution, which account for the ion-ion and ion-solvent contributions to the electric field gradient at the relaxing nucleus. The electrostatic model accounts successfully for a wide variety of experimentally observed relaxation rates of quadrupolar nuclei centered in ions of spherical electronic symmetry in both aqueous and nonaqueous electrolyte solutions.<sup>20a,21,22</sup>

In the limit of extreme motional narrowing the quadrupolar relaxation rate  $R_Q$  ( $= 1/T_{Q,1} = 1/T_{Q,2}$ ) is given by:<sup>4</sup>

$$R_Q = \frac{1}{8} \frac{2I+3}{I^2(2I-1)} \left[ \frac{eQ}{\hbar} \right]^2 J(0) \quad [11]$$

Here,  $J(0)$  is the spectral density function at zero frequency given in Eqn. [12] with  $m = 0, \pm 1, \text{ or } \pm 2$ , and the other symbols have their usual meaning.

$$J(0) = 2 \int_0^{\infty} \langle V_m^{(2)}(0) [V_m^{(2)}(t)]^* \rangle dt \quad [12]$$

The  $V_m^{(2)}(t)$  are defined as the laboratory frame components of the electric field gradient tensor at the relaxing nucleus, \* denotes the complex conjugate, and  $\langle \rangle$  denotes the average value. The field gradient at the nucleus is referred to as the

local field gradient, and the integrand is the time correlation function of the gradient.

The electrostatic theory assumes that in a strong electrolyte solution the relaxation mechanism arises from purely electrostatic interactions consisting of a contribution from solvent dipoles,  $d$ , and a contribution from the point charges of the surrounding ions,  $\Delta$ .<sup>20b,21a</sup> Neglecting cross-correlations, the observed relaxation rate is given by:<sup>23</sup>

$$R_Q^{\text{obsd}} = F_Q(d + \Delta) \quad [13]$$

Here,  $F_Q$  is a constant comprised of the nuclear properties of interest;  $d$  and  $\Delta$  are the so-called ion-solvent and ion-ion contributions to the local field gradient, respectively. The constant  $F_Q$  is:

$$F_Q = \frac{27}{10} \frac{2I+3}{I^2(2I-1)} \left[ \frac{eQ(1+\gamma_\infty)}{\hbar} \right]^2 \quad [14]$$

The term  $(1+\gamma_\infty)$  is the Sternheimer antishielding factor<sup>24</sup> which accounts for the amplification of external field gradients due to distortion from spherical symmetry of closed shell electrons close to the nucleus produced by a charge,  $e$ , external to the ion.<sup>25,26</sup>

### II.3.2 The Ion-Solvent Contribution to Quadrupolar Relaxation of Monoatomic Ions In Electrolyte Solution

In the limit of infinite dilution, the ion-ion contribution to the local field gradient,  $\Delta$ , becomes negligibly small since it is proportional to the electrolyte concentration. Thus, the fluctuating field gradient at the nucleus of a solvated ion in the limit of zero concentration is caused by the electric dipoles of the solvent

molecules. In order to evaluate the integral in Eqn. [12], models for the solvation sphere of the ion must be introduced. Therefore, a general expression for the relaxation rate can be written:<sup>22</sup>

$$R_Q = F_Q \cdot d \quad [15]$$

Hertz *et al.*<sup>21a,22</sup> have discussed three models for the state of solvation of the relaxing ion which determines the ion-solvent contribution to the local field gradient. The first is the "Fully Random Distribution" (FRD) Model:

$$d = d_I = \frac{4\pi}{9} \frac{\mu^2 c_{\text{solv}} P^2 \tau_c}{r_0^5} \quad [16]$$

where  $\mu$  is the dipole moment of the solvent molecule,  $c_{\text{solv}}$  is the dipole concentration in particles per  $\text{cm}^3$ ,  $r_0$  is the closest distance of approach between the center of the ion and the point dipole, taken as the sum of the ionic and solvent molecular radii, and  $\tau_c$  is the reorientational correlation time of the solvent molecules. The term P is a polarization factor defined as:<sup>20a</sup>

$$P_{\text{CR}} = \frac{2\epsilon + 3}{5\epsilon} \quad [17]$$

Here,  $\epsilon$  is the static dielectric constant of the solvent, and  $P_{\text{CR}}$  is introduced to account for the many-body cross-correlation contributions to the spectral density  $J(0)$ .<sup>20a,21a</sup> The FRD model assumes uniform distribution of the centers of mass and random orientation of the solvent dipoles over the whole of space up to the surface of the ion. Therefore, a solvation sphere in the usual sense is absent.

The factor  $4\pi/9$  is split into two parts for convenience:

$$\frac{4\pi}{9} = \frac{4\pi}{5} \cdot \frac{5}{9}$$

Here, the first term corresponds to radially uniform distribution and the second term corresponds to fully random dipole orientation. Therefore, Eqn. [16] may be written as:

$$d_1 = \frac{4\pi}{5} \frac{\overline{\mu^2} c_{\text{solv}} P^2 r_c}{r_0^5} \quad [16a]$$

Here,  $\overline{\mu^2} = 5\mu^2 / 9$  is the fully random mean square of the electric dipole moment.

The "Non-Oriented Solvation" (NOS) Model gives:

$$d = d_2 = \frac{5}{9} \frac{\mu^2 n_s r_c}{r_0^8} + d^*(b) = \frac{\overline{\mu^2} n_s r_c}{r_0^8} + d^*(b) \quad [18]$$

In this model a first solvation sphere is defined with  $n_s$  molecules at constant distance of approach  $r_0$  and the dipoles randomly oriented. The term  $d^*(b)$  allows for the effect of solvent dipoles beyond the first solvation sphere. Since there is an essentially random distribution of solvent molecules outside the first solvation sphere,  $d^*(b)$  is given by Eqn. [16] if  $r_0$  is replaced by  $b$ , which is the radius of the second solvation sphere.

The "Fully Oriented Solvation" (FOS) Model gives:

$$d = d_3 = \frac{\mu^2 n_s \tau_c}{r_0^8} \Lambda + d^*(b) \quad [19]$$

In this model, a well defined first solvation sphere with radial orientation of solvent dipoles exists. The factor  $\Lambda = (1 - e^{-6\lambda})$  describes a varying degree of quenching of the field gradient caused by cubic symmetry of the solvation sphere. A lateral Gaussian distribution of solvent dipoles around positions corresponding to cubic symmetry is assumed which is characterized by a distribution width parameter  $\lambda$ . For a random lateral distribution  $\lambda \rightarrow \infty$  and no quenching occurs, whereas for strictly cubic symmetry  $\lambda \rightarrow 0$  and the field gradient at the central nucleus due to the first coordination sphere vanishes.

### II.3.3 The Ion-Ion Contribution to Quadrupolar Relaxation of Monoatomic Ions In Electrolyte Solution

According to the electrostatic theory, point charges arising from all of the ions in strong electrolyte solutions may contribute to the local field gradient. However, to a first approximation it is assumed that the relaxing nucleus is located in an ion of type  $i$ , and that the ion-ion contribution,  $\Delta$ , arises from oppositely charged ions of type  $j$ . Struis *et al.* reported the following expression for the ion-ion contribution developed by Hertz:<sup>23</sup>

$$\Delta = \frac{4\pi\nu_j(P)^2(z_j e)^2 c' \tau_c}{27a^3} \quad [20]$$

Here,  $c' = 10^{-3}cN_A$  is the concentration of the  $j$  ions in particles per cubic centimeter,  $c$  is the molar concentration of the electrolyte in F.W./dm<sup>3</sup> of solution,

and  $N_A$  is Avogadro's number. The term  $z_j e$  is the charge on ion  $j$ ,  $\nu_j$  is its stoichiometric number,  $a$  is the distance of closest approach between the relaxing nucleus in ion  $i$  and the center of ion  $j$ , and  $\tau_c$  is the correlation time describing the relative translational diffusion between the ions. The  $P$  denotes a polarization factor which should not be confused with the polarization factor  $P_{CR}$  previously introduced in Eqn. [16] and defined in Eqn. [17]. This  $P$  accounts for the many-body ion-ion cross-correlations in the same way that  $P_{CR}$  accounts for the solvent-solvent cross-correlations in Eqn. [16].<sup>23</sup>

However, it was found by Hertz *et al.*<sup>20b</sup> that Eqn. [20] largely overestimates the ion-ion contribution when compared with experimental results. Therefore, a correction to Eqn. [20] was introduced based on the concept that the local field gradient contribution of an ion  $j$  may have already vanished due to the shielding effects of the surrounding ion cloud when the ions have diffused from a distance  $a$  to  $(a + \alpha)$ , with  $\alpha < a$ . In order to account for this effect, Eqn. [20] was modified to the following:<sup>20b,23</sup>

$$\Delta = \frac{4\pi\nu_j(P)^2(z_j e)^2 c' \tau_c f(a/\alpha)}{27a^3} \quad [21]$$

Here,  $f(a/\alpha)$  is a function of the ratio  $(a/\alpha)$ , and for the range  $x = (a/\alpha) \geq 1$ ,  $f(x)$  may be approximated by the analytic function:<sup>20b</sup>

$$f(x) = 1 - \frac{x}{2} + \frac{x^2}{2} \left[ 1 - \frac{x^2 + 2.335x + 0.251}{x^2 + 3.331x + 1.682} \right] \quad [22]$$

Now,  $\tau_c$  in Eqn. [21] is the effective correlation time resulting from the translational diffusion between the two ions and the rotational diffusion of ion  $j$  around the relaxing nucleus in ion  $i$ .<sup>23</sup>

A recent experimental finding concerns the functional concentration dependence for quadrupolar relaxation behavior of ionic nuclei in very dilute electrolyte solutions.<sup>27</sup> It was reported that at concentrations  $\leq 10^{-2}$  molal the concentration dependence of  $1/T_1$  for  $^{23}\text{Na}^+$ ,  $^7\text{Li}^+$ , and  $^{87}\text{Rb}^+$  in aqueous solution, and  $^{23}\text{Na}^+$  in HMPT, followed a  $c^{1/2}$  dependence. The new results have the consequence that, in the extrapolation of  $1/T_1$  to zero concentration for the determination of the ion-solvent contribution, a  $c^{1/2}$  dependence might be followed. Therefore, many of the previously reported relaxation rates at infinite dilution may be as much as 10% too high.<sup>18</sup>

#### II.3.4 $^{33}\text{S}$ Relaxation of Inorganic Ions In Aqueous Solution

The relaxation of quadrupolar nuclei in polyatomic ions has been briefly reviewed.<sup>18</sup> However, only a short presentation of the few studies of  $^{33}\text{S}$  relaxation in inorganic ions is given here. The effects of cation, concentration, and temperature on the  $^{33}\text{S}$  spin-lattice relaxation time,  $T_1$ , of  $\text{SO}_4^{2-}$  in aqueous and  $\text{D}_2\text{O}$  solutions have been studied using the inversion-recovery technique.<sup>28,29,30</sup> The model developed by Hertz<sup>20b</sup> for quadrupolar relaxation of ionic nuclei in electrolyte solutions at finite ion concentrations predicts that  $T_1$  should decrease with increasing concentration. The probability of increasing ion-ion interactions which produce the electric field gradient at the  $^{33}\text{S}$  nucleus increases with increasing salt concentration; hence,  $T_1$  should be sensitive to concentration changes. The faster  $^{33}\text{S}$  relaxation in the presence of  $\text{Cs}^+$  ions relative to that in the presence of an equal concentration of  $\text{NH}_4^+$  was reported to result from greater ion pairing of  $\text{Cs}^+$  with  $\text{SO}_4^{2-}$ .<sup>29</sup>



Belton *et al.*<sup>31</sup> studied the effects of counterion and pH on the linewidth, chemical shift, and relaxation times for  $^{33}\text{S}$  in aqueous sulfate ion. Even weak ion pairing interactions with the sulfate anion were reported to have significant effects upon the  $^{33}\text{S}$  chemical shift and linewidth. Interactions with  $\text{Al}^{3+}$  and  $\text{Mg}^{2+}$  were found to produce the largest effects. Since the  $^{33}\text{S}$  chemical shift and linewidth of aqueous  $(\text{NH}_4)_2\text{SO}_4$  appear to be the least sensitive to changes in pH and concentration, aqueous ammonium sulfate has gained wide acceptance as the  $^{33}\text{S}$  chemical-shift reference of choice.<sup>1</sup>

Hinton and Shungu<sup>29</sup> state that the change in the  $^{33}\text{S}$   $T_1$  of aqueous sulfate with changing electrolyte concentration is determined primarily in three ways: (1) a change in the correlation time describing the modulation of the electric field gradient about the  $^{33}\text{S}$  nucleus due to the water molecules; (2) ions affecting the relative orientation of water molecules around the relaxing ion and therefore the water-water correlation; and (3) the production of an electric field gradient due to ion-ion interactions.

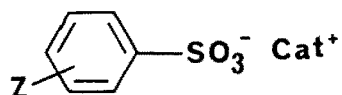
Hinton and Buster<sup>32</sup> investigated the effects of temperature and concentration on the  $T_1$  of  $^{33}\text{S}$  in solutions of  $\text{SO}_4^{2-}$  and  $\text{S}_2\text{O}_3^{2-}$  in  $\text{D}_2\text{O}$ . The counterion was  $\text{Na}^+$  in both cases. In a  $^{33}\text{S}$  enrichment experiment, it was shown conclusively that the single resonance observed for  $\text{S}_2\text{O}_3^{2-}$  was from the internal sulfur atom. The  $^{33}\text{S}$   $T_1$ 's for both species showed temperature and concentration dependence. At a given concentration and temperature, the relaxation time was less for  $\text{S}_2\text{O}_3^{2-}$  than for  $\text{SO}_4^{2-}$  because of the decreased charge symmetry about the internal sulfur atom in  $\text{S}_2\text{O}_3^{2-}$ .

## CHAPTER III

### RESULTS AND DISCUSSION

#### III.1 Use of $^{33}\text{S}$ NMR For the Determination of $\text{pK}_a$ 's of Arenesulfonic Acids

Figure 1.



1, Z = H	6, Z = <i>p</i> -N(CH <sub>3</sub> ) <sub>2</sub>	11, Z = <i>p</i> -Cl
2, Z = <i>m</i> -CH <sub>3</sub>	7, Z = <i>p</i> -NH <sub>2</sub>	12, Z = <i>p</i> -COCH <sub>3</sub>
3, Z = <i>m</i> -SO <sub>3</sub> <sup>-</sup>	8, Z = <i>p</i> -CH <sub>3</sub>	13, Z = <i>p</i> -SO <sub>3</sub> <sup>-</sup>
4, Z = <i>m</i> -CF <sub>3</sub>	9, Z = <i>p</i> -NH <sub>3</sub> <sup>+</sup>	14, Z = <i>p</i> -NH(CH <sub>3</sub> ) <sub>2</sub> <sup>+</sup>
5, Z = <i>m</i> -NO <sub>2</sub>	10, Z = <i>p</i> -Br	15, Z = <i>p</i> -NO <sub>2</sub>

The  $^{33}\text{S}$  NMR spectra of arenosulfonates ( $\text{ZC}_6\text{H}_4\text{SO}_3^- \text{ Cat}^+$ ) 1-15 were recorded using 0.046 M to 0.13 M aqueous solutions, where the sulfonates are almost completely ionized.<sup>10</sup> Consequently, the  $^{33}\text{S}$  chemical shifts were not affected by the

counterion.<sup>13</sup> Table 2 shows the  $^{33}\text{S}$  chemical shifts and linewidths of the arenesulfonates ( $\text{ZC}_6\text{H}_4\text{SO}_3^- \text{Cat}^+$ ) at  $20^\circ\text{C}$  and  $39^\circ\text{C}$ . Errors in the chemical-shift values are ca.  $\pm 0.3$  ppm for narrow lines and  $\pm 0.5$  ppm for broad lines. The temperature effect on the  $^{33}\text{S}$  chemical shifts of these compounds is negligible. The  $^{33}\text{S}$  chemical shifts for *m*-nitrobenzenesulfonic acid (5) and sodium *p*-nitrobenzenesulfonate (15) are substantially different from those previously recorded at 6.104 MHz (1.879 T) and  $39^\circ\text{C}$  in ca. 2 M aqueous solution.<sup>16</sup> Since the respective linewidths for acids 5 and 15 were 91 Hz and 125 Hz there was considerable error in the earlier chemical-shift measurements.

A substantial change in the  $^{33}\text{S}$  chemical shift was observed for both potassium *p*-aminobenzenesulfonate (7) and sodium *p*-dimethylaminobenzenesulfonate (6) upon HCl titration to the pH values in Table 2, thereby furnishing  $^{33}\text{S}$  chemical shifts for the corresponding zwitterions (9 and 14).<sup>33</sup> The  $^{33}\text{S}$  chemical shifts of these compounds fit the previously observed trend that  $^{33}\text{S}$  resonances of benzenesulfonates with electron-withdrawing substituents are found upfield from those of benzenesulfonates with electron-donating substituents.<sup>16</sup>

Table 2.  $^{33}\text{S}$  Chemical Shifts And Linewidths of Arenesulfonates ( $\text{ZC}_6\text{H}_4\text{SO}_3^- \text{Cat}^+$ )

Z	Cat <sup>+</sup>	Temp. °C	pH (20° C)	$\delta$ (ppm)	$\Delta\nu_{\frac{1}{2}}$ (Hz)
H	H <sup>+</sup>	20	2	-11.3	8.8
<i>m</i> -CH <sub>3</sub>	H <sup>+</sup>	20	2	-10.9	18.8
<i>m</i> -SO <sub>3</sub> <sup>-</sup>	2 Na <sup>+</sup>	20	4	-13.9	21.5
<i>m</i> -CF <sub>3</sub>	H <sup>+</sup>	20	2	-14.2	19.5
<i>m</i> -NO <sub>2</sub>	H <sup>+</sup>	20	2	-15.9	49.0
<i>p</i> -N(CH <sub>3</sub> ) <sub>2</sub>	Na <sup>+</sup>	20	8	-9.6	75.6
<i>p</i> -NH <sub>2</sub>	K <sup>+</sup>	20	11	-9.8	51.5
<i>p</i> -CH <sub>3</sub>	H <sup>+</sup>	20	2	-10.6	21.2
<i>p</i> -NH <sub>3</sub> <sup>+</sup>	K <sup>+</sup>	20	1	-14.2	18.1
<i>p</i> -Br	H <sup>+</sup>	20	2	-12.8	9.0
<i>p</i> -Cl	H <sup>+</sup>	20	2	-13.0	9.0
<i>p</i> -COCH <sub>3</sub>	Na <sup>+</sup>	20	4	-13.6	13.8
<i>p</i> -SO <sub>3</sub> <sup>-</sup>	2 K <sup>+</sup>	20	8	-13.8	18.8
<i>p</i> -NH(CH <sub>3</sub> ) <sub>2</sub> <sup>+</sup>	Na <sup>+</sup>	20	2	-15.3	55.0
<i>p</i> -NO <sub>2</sub>	Na <sup>+</sup>	20	5	-15.7	58.8
H	H <sup>+</sup>	39	2	-11.7	6.5
<i>m</i> -CH <sub>3</sub>	H <sup>+</sup>	39	2	-11.2	8.8
<i>m</i> -SO <sub>3</sub> <sup>-</sup>	2 Na <sup>+</sup>	39	4	-14.2	16.0
<i>m</i> -CF <sub>3</sub>	H <sup>+</sup>	39	2	-14.4	18.2
<i>m</i> -NO <sub>2</sub>	Na <sup>+</sup>	39	2	-16.2	42.5
<i>p</i> -N(CH <sub>3</sub> ) <sub>2</sub>	Na <sup>+</sup>	39	8	-9.6	45.0
<i>p</i> -NH <sub>2</sub>	K <sup>+</sup>	39	11	-10.0	23.8
<i>p</i> -CH <sub>3</sub>	H <sup>+</sup>	39	2	-11.1	11.5
<i>p</i> -NH <sub>3</sub> <sup>+</sup>	K <sup>+</sup>	39	1	-14.4	15.6
<i>p</i> -Br	H <sup>+</sup>	39	2	-13.2	7.5
<i>p</i> -Cl	H <sup>+</sup>	39	2	-13.3	6.2
<i>p</i> -COCH <sub>3</sub>	Na <sup>+</sup>	39	4	-13.9	12.5
<i>p</i> -SO <sub>3</sub> <sup>-</sup>	2 K <sup>+</sup>	39	8	-14.1	14.2
<i>p</i> -NH(CH <sub>3</sub> ) <sub>2</sub> <sup>+</sup>	Na <sup>+</sup>	39	2	-15.2	34.5
<i>p</i> -NO <sub>2</sub>	Na <sup>+</sup>	39	5	-15.7	47.5

The data yielded Taft dual substituent plots of  $\delta(^{33}\text{S})$  vs  $\sigma_{\text{I}}$  and  $\sigma_{\text{R}}$  following the relationships in Eqns. [23]-[26]; the substituent constants used, and calculated  $^{33}\text{S}$  chemical shifts appear in Table 3.<sup>34</sup> The correlation coefficients for experiments carried out at both temperatures are good (  $r = 0.993$  *meta*,  $r = 0.994$  *para* at 20° C;  $r = 0.994$  *meta*,  $r = 0.990$  *para* at 39° C ), and all calculated  $^{33}\text{S}$  chemical shifts are within experimental error of the measured values (Table 3). When experimental versus calculated chemical shifts are plotted, all slopes obtained are within experimental error of the theoretical value of 1.00.

$$\delta(^{33}\text{S}) = -6.38\sigma_{\text{I}} - 6.69\sigma_{\text{R}} - 11.69 \quad \textit{meta} \text{ at } 20^\circ \text{ C} \quad [23]$$

$$\delta(^{33}\text{S}) = -6.57\sigma_{\text{I}} - 5.32\sigma_{\text{R}} - 11.42 \quad \textit{para} \text{ at } 20^\circ \text{ C} \quad [24]$$

$$\delta(^{33}\text{S}) = -6.31\sigma_{\text{I}} - 6.40\sigma_{\text{R}} - 11.99 \quad \textit{meta} \text{ at } 39^\circ \text{ C} \quad [25]$$

$$\delta(^{33}\text{S}) = -6.10\sigma_{\text{I}} - 5.47\sigma_{\text{R}} - 11.81 \quad \textit{para} \text{ at } 39^\circ \text{ C} \quad [26]$$

The  $\text{pK}_{\text{a}}$ 's of arenesulfonic acids 1, 2, 8-10 previously determined by UV techniques<sup>11</sup> (Table 4) were employed to calculate  $\text{pK}_{\text{a}}$ 's of arenesulfonic acids 1-15. Linear regression analysis of  $\text{pK}_{\text{a}}$  vs  $\delta(^{33}\text{S})$  yielded the relationships in Eqns. [27] and [28], and results appear in Table 4.

$$\text{pK}_{\text{a}} = 0.130\delta(^{33}\text{S}) - 5.19 \quad r = 0.982 \quad \text{at } 20^\circ \text{ C} \quad [27]$$

$$\text{pK}_{\text{a}} = 0.139\delta(^{33}\text{S}) - 5.03 \quad r = 0.988 \quad \text{at } 39^\circ \text{ C} \quad [28]$$

**Table 3.** Taft Substituent Constants Used And Calculated  $^{33}\text{S}$  Chemical Shifts of Arenesulfonates ( $\text{ZC}_6\text{H}_4\text{SO}_3^-$ ) In Aqueous Solution At 20° And 39° C.

Z	$\sigma_I$	$\sigma_R$	$\delta(^{33}\text{S})$ Calcd (20° C)	$\delta(^{33}\text{S})$ Calcd (39° C)
H	0.00	0.00	-11.7	-12.0
<i>m</i> -CH <sub>3</sub>	-0.01	-0.13	-10.8	-11.1
<i>m</i> -SO <sub>3</sub> <sup>-</sup>	0.23	0.07	-13.6	-13.9
<i>m</i> -CF <sub>3</sub>	0.40	0.00	-14.2	-14.5
<i>m</i> -NO <sub>2</sub>	0.67	0.00	-16.0	-16.2
H	0.00	0.00	-11.4	-11.8
<i>p</i> -N(CH <sub>3</sub> ) <sub>2</sub>	0.17	-0.53	-9.7	-10.0
<i>p</i> -NH <sub>2</sub>	0.17	-0.51	-9.8	-10.1
<i>p</i> -CH <sub>3</sub>	-0.01	-0.13	-10.7	-11.0
<i>p</i> -NH <sub>3</sub> <sup>+</sup>	0.60	-0.18	-14.4	-14.5
<i>p</i> -Br	0.47	-0.33	-12.8	-12.9
<i>p</i> -Cl	0.47	-0.35	-12.6	-12.8
<i>p</i> -COCH <sub>3</sub>	0.30	0.09	-13.9	-14.1
<i>p</i> -SO <sub>3</sub> <sup>-</sup>	0.23	0.07	-13.3	-13.6
<i>p</i> -NH(CH <sub>3</sub> ) <sub>2</sub> <sup>+</sup>	0.70	-0.14	-15.3	-15.3
<i>p</i> -NO <sub>2</sub>	0.67	0.00	-15.8	-15.9

Table 4.  $pK_a$ 's of Arenesulfonic Acids ( $ZC_6H_4SO_3H$ ) Determined By Three Methods.

Method: Z	UV Spectroscopy <sup>a</sup>	Hammett Plot <sup>b</sup>		<sup>33</sup> S NMR <sup>c</sup>	
	$pK_a$	$\sigma$	$pK_a$	$pK_a$ (20°)	$pK_a$ (39°)
H	-6.65 ± 0.05	0.0	-6.66	-6.66	-6.66
<i>m</i> -CH <sub>3</sub>	-6.56 ± 0.05	-0.06	-6.62	-6.61	-6.60
<i>m</i> -SO <sub>3</sub> <sup>-</sup>	-5.1 > x > -7	0.05	-6.69	-7.00	-7.01
<i>m</i> -CF <sub>3</sub>		0.46	-6.96	-7.04	-7.04
<i>m</i> -NO <sub>2</sub>		0.71	-7.12	-7.25	-7.28
<i>p</i> -N(CH <sub>3</sub> ) <sub>2</sub>		-0.32	-6.45	-6.43	-6.37
<i>p</i> -NH <sub>2</sub>		-0.30	-6.47	-6.47	-6.42
<i>p</i> -CH <sub>3</sub>	-6.62 ± 0.05	-0.14	-6.57	-6.57	-6.57
<i>p</i> -NH <sub>3</sub> <sup>+</sup>	-7.04 ± 0.05	0.60	-7.05	-7.03	-7.03
<i>p</i> -Br	-6.86 ± 0.05	0.26	-6.83	-6.86	-6.87
<i>p</i> -Cl		0.24	-6.82	-6.88	-6.88
<i>p</i> -COCH <sub>3</sub>		0.47	-6.96	-6.96	-6.97
<i>p</i> -SO <sub>3</sub> <sup>-</sup>		0.09	-6.72	-6.99	-6.99
<i>p</i> -NH(CH <sub>3</sub> ) <sub>2</sub> <sup>+</sup>				-7.18	-7.14
<i>p</i> -NO <sub>2</sub>		0.81	-7.18	-7.23	-7.21

<sup>a</sup> Values taken from reference 11.

<sup>b</sup>  $\sigma$  values taken from reference 34. All  $pK_a$  values are  $\pm 0.05$ .

<sup>c</sup> All  $pK_a$  values are  $\pm 0.04$ .

The  $pK_a$  for the second ionization of *m*-benzenedisulfonic acid (3) was previously estimated to lie between -5.1 and -7 by UV spectroscopy.<sup>11a</sup> When the  $pK_a$ 's of *m*-benzenedisulfonic acid (3) and *p*-benzenedisulfonic acid (13) were previously determined by  $^1H$  NMR, only  $pK_a$ 's for the first ionization could be obtained because the solvent was sulfuric acid.<sup>11c</sup> The  $^{33}S$  NMR method produced a  $pK_a$  of  $-7.00 \pm 0.04$  for *m*-benzenedisulfonic acid (Table 4). Thus,  $^{33}S$  NMR provides a method of determining the second ionizations of 3 and 13. Further,  $^{33}S$  NMR furnishes  $pK_a$ 's for *m*-nitrobenzenesulfonic acid (5) and *p*-nitrobenzenesulfonic acid (15) which cannot be determined by UV techniques due to unresolved B bands, and which were not determined by  $^1H$  NMR in sulfuric acid.<sup>11</sup>

A Hammett plot of  $pK_a$  vs  $\sigma$  using UV determined  $pK_a$ 's of arenesulfonic acids 1, 2, 8-10 gave  $\rho = -0.646$  ( $r = 0.976$ ).<sup>35</sup> Linear regression analysis produced the calculated  $pK_a$ 's shown in Table 4 for comparison with experimental values. The  $pK_a$  for 14 could not be calculated from the Hammett plot because  $\sigma$  for this compound was unavailable. Good agreement is demonstrated between the  $pK_a$ 's determined by UV and  $^{33}S$  NMR. The  $pK_a$ 's determined by  $^{33}S$  NMR are plotted in Figures 2 and 3, as well as those determined by UV and calculated values from the Hammett plot shown for comparison. Therefore, we conclude that  $^{33}S$  NMR is an accurate and facile method for determining  $pK_a$ 's of arenesulfonic acids, which is free of the experimental difficulties of previous methods.



Figure 2.

# pKa's of Arenesulfonic Acids vs.

<sup>33</sup>S Chemical Shifts of Arenesulfonates

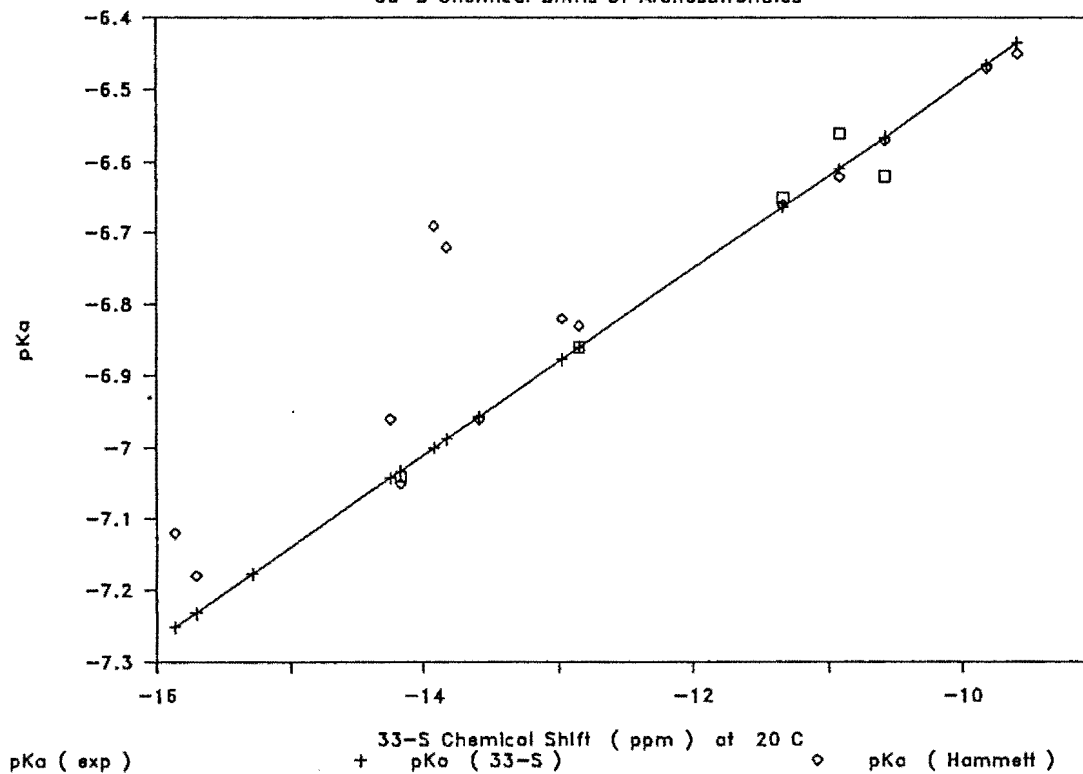
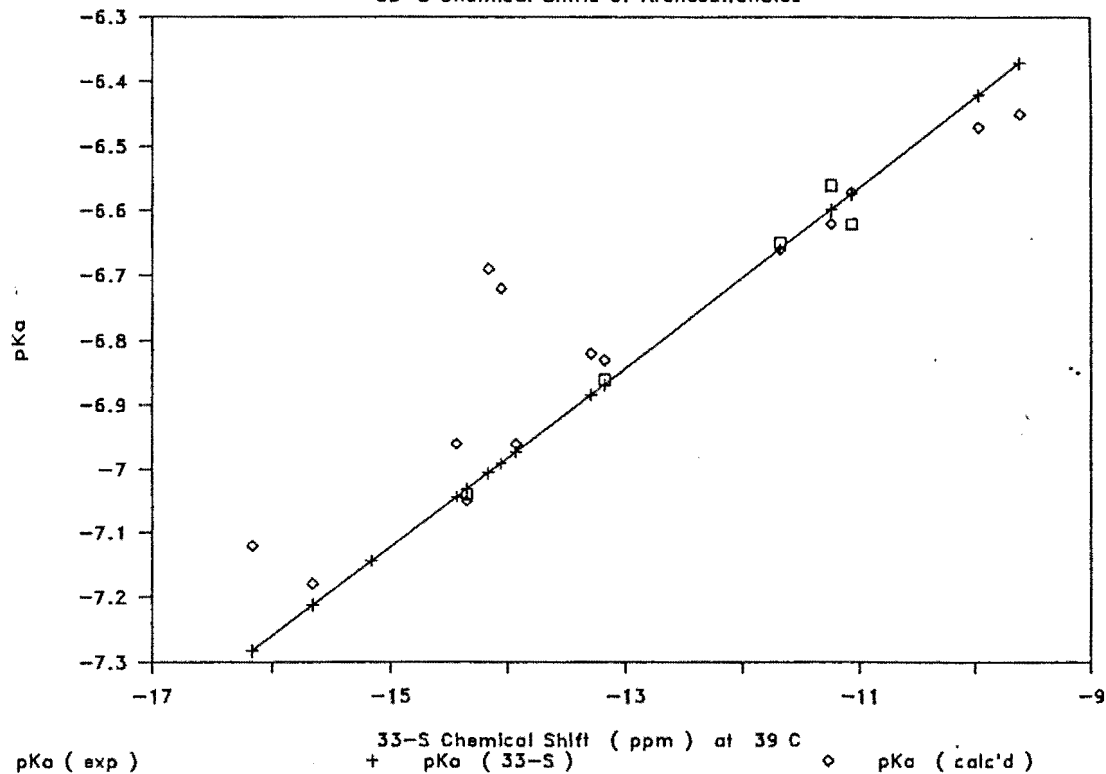


Figure 3.

### pKa's of Arenesulfonic Acids vs.

<sup>33</sup>S Chemical Shifts of Arenesulfonates



### III.2 Concentration And Counterion Dependence of $^{33}\text{S}$ Quadrupolar Relaxation In Aqueous Benzenesulfonates

The  $^{33}\text{S}$  NMR data obtained for benzenesulfonates in aqueous solution as a function of cation concentration, and counterion at 20° C appear in Tables 5-9. The counterions were  $\text{Li}^+$ ,  $\text{Na}^+$ ,  $\text{K}^+$ ,  $\text{Mg}^{2+}$ , and  $\text{H}^+$ . It was found that  $^{33}\text{S}$  chemical shifts of the benzenesulfonates in water were, within experimental error, independent of concentration and counterion. The  $^{33}\text{S}$  chemical shifts were  $\delta = -11.3 \pm 0.2$  ppm.

Values for the quadrupolar relaxation rate,  $R_Q = 1/T_{Q,2}$ , were obtained from  $^{33}\text{S}$  linewidths using Eqn. [1] for benzenesulfonates dissolved in water and are also listed in Tables 5-9. These data are plotted as a function of concentration at 20° C in Figures 4-9. The straight lines in Figures 4-8 were obtained from linear regression analysis of the data  $\leq 1$  molar concentration.<sup>36</sup> Extrapolation to zero solute concentration yielded estimates of the quadrupolar relaxation rates at infinite dilution,  $R_Q^0$ , which appear in Table 10. The resulting values of  $R_Q^0$  are all within 6% of the mean value ( $33.9 \text{ s}^{-1}$ ), which is close to the estimated 5% experimental error in the linewidth measurements. When only values for metal counterions are considered, for which there are a greater number of data points and particularly at low concentrations, the resulting  $R_Q^0$ 's are within experimental error of the mean value ( $33.4 \text{ s}^{-1}$ ).

The electrostatic model assumes implicitly that Eqn. [21], for the ion-ion contribution, and hence Eqn. [13] for the observed relaxation rate are only applicable when exchange of ions from the free state to the bound state is very slow compared to the relaxation rate of the nucleus studied.<sup>20a</sup> Since proton exchange is rapid in aqueous benzenesulfonate at all concentrations studied here, the high value of the  $^{33}\text{S}$  relaxation rate at infinite dilution,  $R_Q^0$ , obtained for benzenesulfonic acid results from the equilibrium between the protonated and ionized acid. Therefore, the  $^{33}\text{S}$

relaxation behavior when  $H^+$  is the counterion should be considered separately from the relaxation behavior observed for the metal counterions.

**Table 5.**  $^{33}\text{S}$  NMR Data For Lithium Benzenesulfonate In Aqueous Solution.

Concentration (mol / L)	$\delta$ (ppm)	$\Delta\nu_{\frac{1}{2}}$ (Hz)	$R_Q$ ( $\text{s}^{-1}$ )
2.000	-11.4	26.0	81.7
1.800	-11.4	23.1	72.6
1.600	-11.4	20.2	63.6
1.440	-11.4	17.9	56.2
1.280	-11.3	17.8	55.8
1.152	-11.3	16.1	50.6
1.000	-11.4	14.8	46.3
0.8998	-11.3	14.4	45.2
0.8000	-11.3	14.4	45.2
0.6400	-11.3	13.6	42.8
0.5000	-11.3	12.6	39.6
0.4000	-11.3	12.0	37.7
0.3200	-11.3	11.9	37.3
0.2500	-11.4	12.0	37.7
0.2000	-11.3	11.6	36.5
0.1600	-11.3	11.2	35.3
0.1000	-11.3	10.9	34.2
0.0500	-11.3	11.5	36.1
0.0250	-11.3	10.2	32.2

**Table 6.**  $^{33}\text{S}$  NMR Data For Sodium Benzenesulfonate In Aqueous Solution.

Concentration (mol / L)	$\delta$ (ppm)	$\Delta\nu_{\frac{1}{2}}$ (Hz)	$R_Q$ ( $\text{s}^{-1}$ )
1.796	-11.4	17.5	55.0
1.436	-11.4	16.9	53.0
1.149	-11.4	14.0	44.0
0.8984	-11.5	13.8	43.2
0.7187	-11.5	13.1	41.2
0.4492	-11.4	11.9	37.3
0.2246	-11.4	11.4	35.8
0.1123	-11.3	10.8	33.8
0.0562	-11.5	10.6	33.4
0.0281	-11.4	10.2	32.2

Table 7.  $^{33}\text{S}$  NMR Data For Potassium Benzenesulfonate In Aqueous Solution.

Concentration (mol / L)	$\delta$ (ppm)	$\Delta\nu_{\frac{1}{2}}$ (Hz)	$R_Q$ ( $\text{s}^{-1}$ )
2.009	-11.4	15.0	47.1
1.607	-11.4	13.6	45.6
1.286	-11.4	13.2	42.4
1.005	-11.4	12.7	41.2
0.8037	-11.3	12.4	37.3
0.6430	-11.2	12.2	37.3
0.4018	-11.4	11.8	38.5
0.2010	-11.3	11.5	36.1
0.1005	-11.3	11.3	35.3
0.0402	-11.4	11.2	36.1
0.0201	-11.4	11.2	34.2

**Table 8.**  $^{33}\text{S}$  NMR Data For Benzenesulfonic Acid In Aqueous Solution.

Concentration (mol / L)	$\delta$ (ppm)	$\Delta\nu_{\frac{1}{2}}$ (Hz)	$R_Q$ ( $\text{s}^{-1}$ )
1.780	-11.2	21.2	66.6
0.892	-11.3	14.0	44.0
0.446	-11.4	12.5	39.3
0.223	-11.3	12.5	39.3
0.112	-11.2	11.5	36.1

**Table 9.**  $^{33}\text{S}$  NMR Data For Magnesium Benzenesulfonate In Aqueous Solution.

$\text{Mg}^{2+}$ Concentration (mol / L)	$\delta$ (ppm)	$\Delta\nu_{\frac{1}{2}}$ (Hz)	$R_Q$ ( $\text{s}^{-1}$ )
0.2014	-11.3	13.5	42.4
0.1611	-11.3	13.2	41.6
0.1290	-11.3	12.5	39.3
0.1007	-11.3	12.5	39.3
0.0644	-11.3	11.9	37.3
0.0504	-11.3	11.0	34.6
0.0201	-11.3	10.9	34.2
0.0101	-11.4	10.1	31.8



**Table 10. Linear Regression Results For  $^{33}\text{S}$   $R_Q$  vs Counterion Concentration:  
Five Benzenesulfonates In Aqueous Solution At 20°C.**

Counter-Ion	$R_Q^0$ ( $\text{s}^{-1}$ )	Std. Err. of $R_Q$ Estimate	Slope	Std. Err. of Slope	r
$\text{Li}^+$	33.4	1.0	13.4	0.9	0.97648
$\text{Na}^+$	32.4	0.5	12.0	0.6	0.99492
$\text{K}^+$	35.1	1.2	4.9	1.2	0.84979
$\text{Mg}^{2+}$	32.6	1.1	53.4	6.0	0.96418
$\text{H}^+$	35.9	1.2	9.0	2.0	0.95309

Figure 4.

$^{33}\text{S}$  RQ vs Conc. For  $\text{PhSO}_3\text{Li}$

In  $\text{H}_2\text{O}$  At  $20^\circ\text{C}$

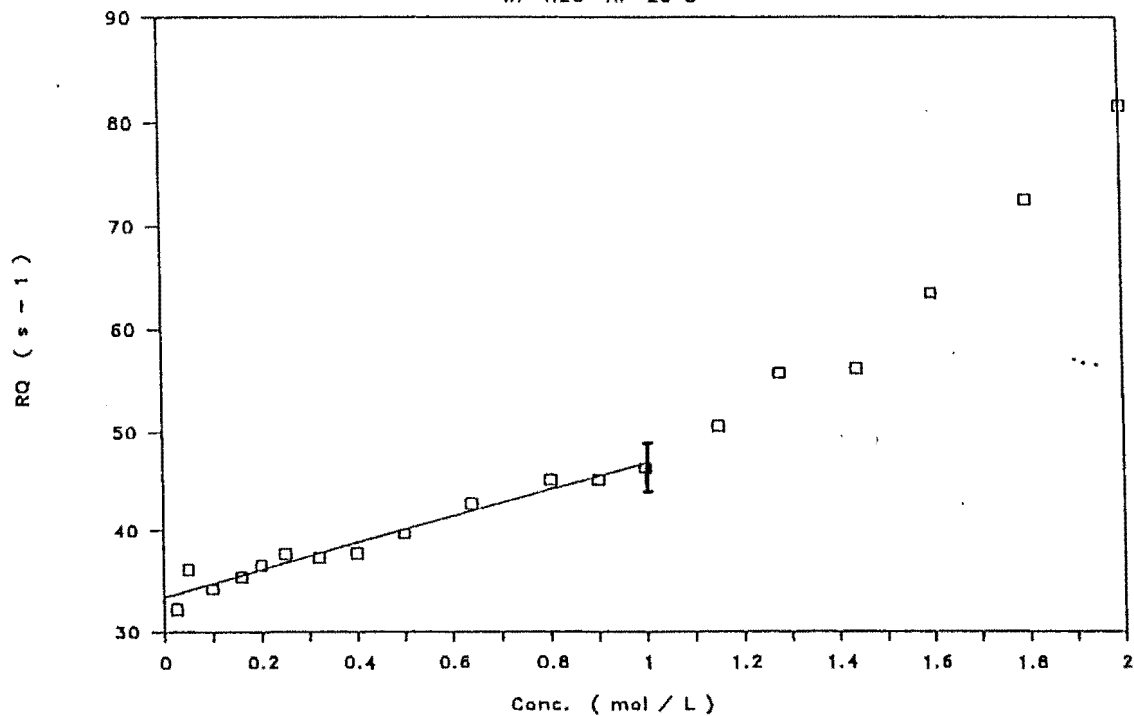


Figure 5.

### $^{33}\text{S}$ RQ vs Conc. For $\text{PhSO}_3\text{Na}$

In  $\text{H}_2\text{O}$  At  $20^\circ\text{C}$

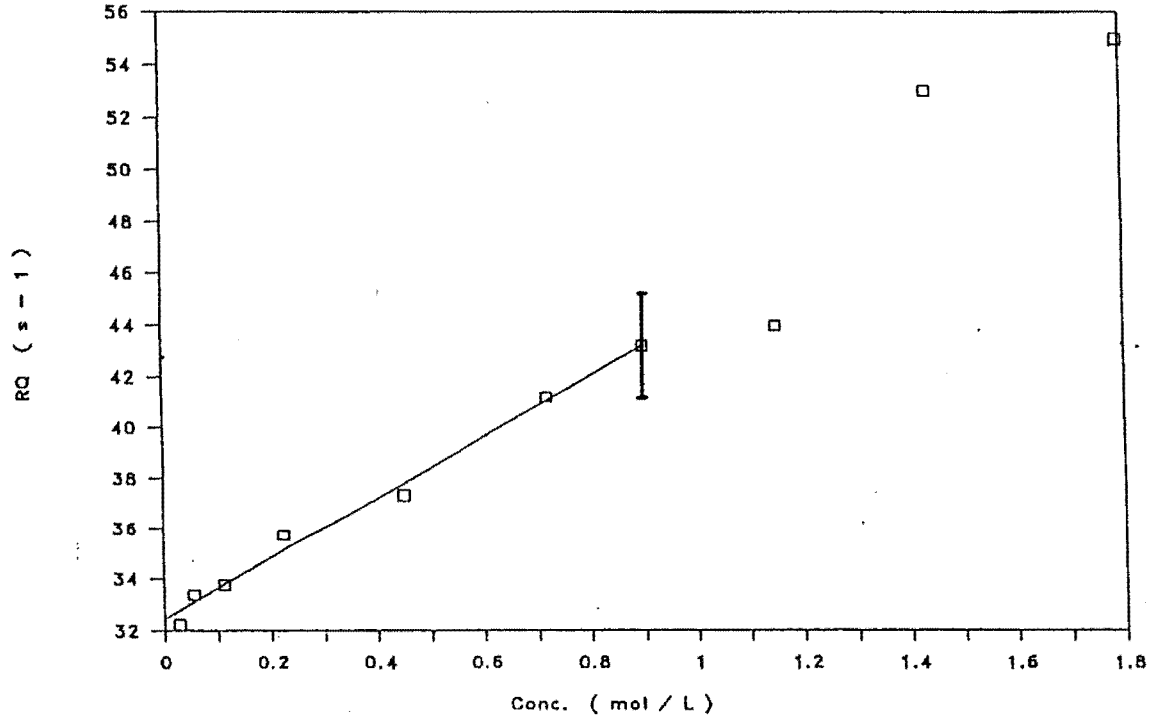


Figure 6.

33 S RQ vs Conc. For PhSO3K

In H2O At 20 C

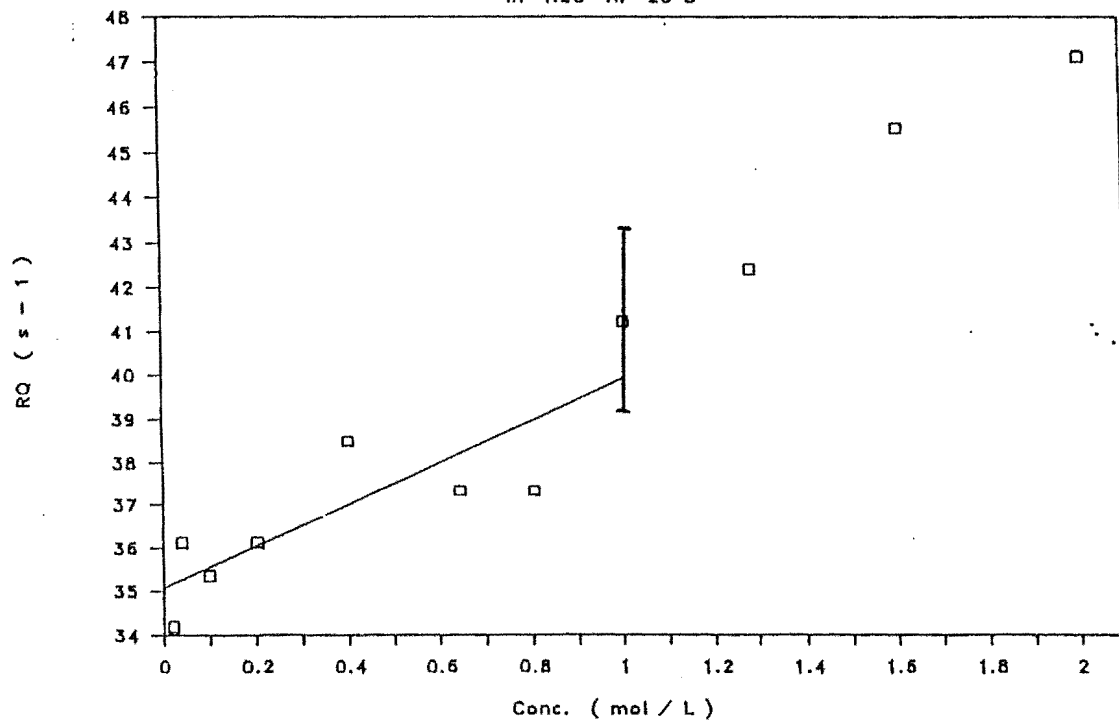


Figure 7.

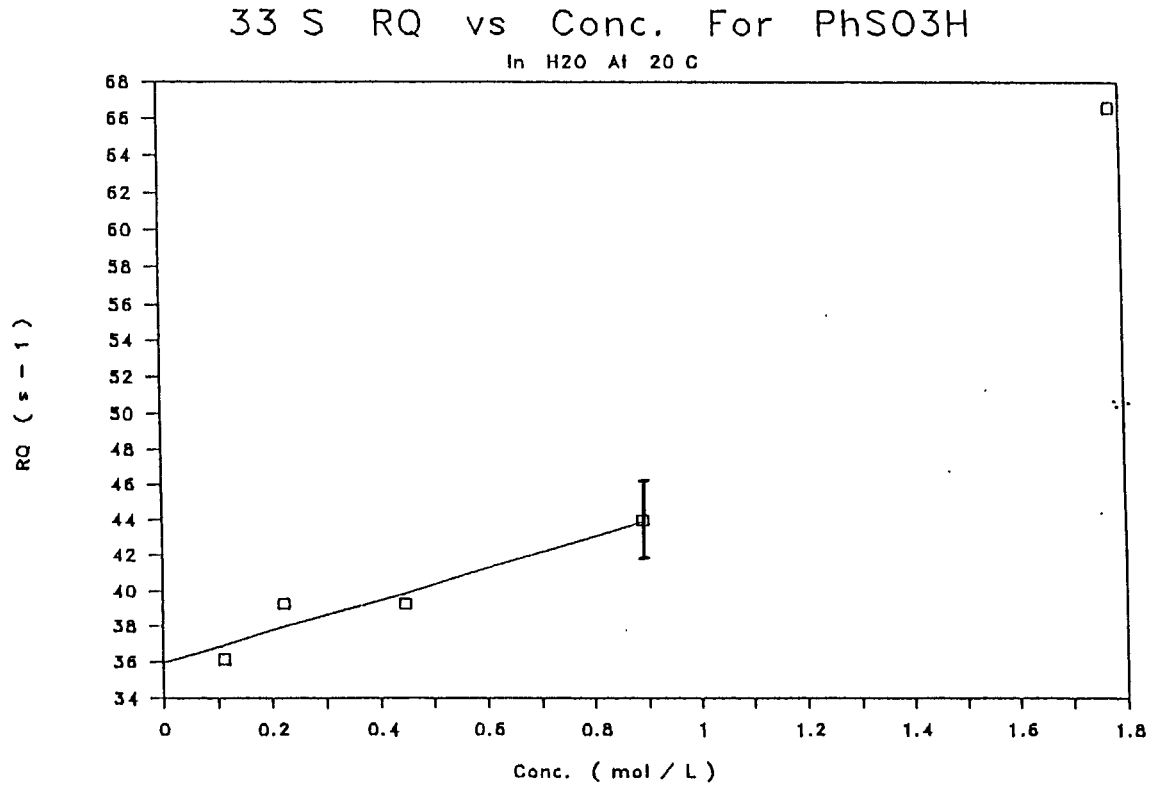


Figure 8.

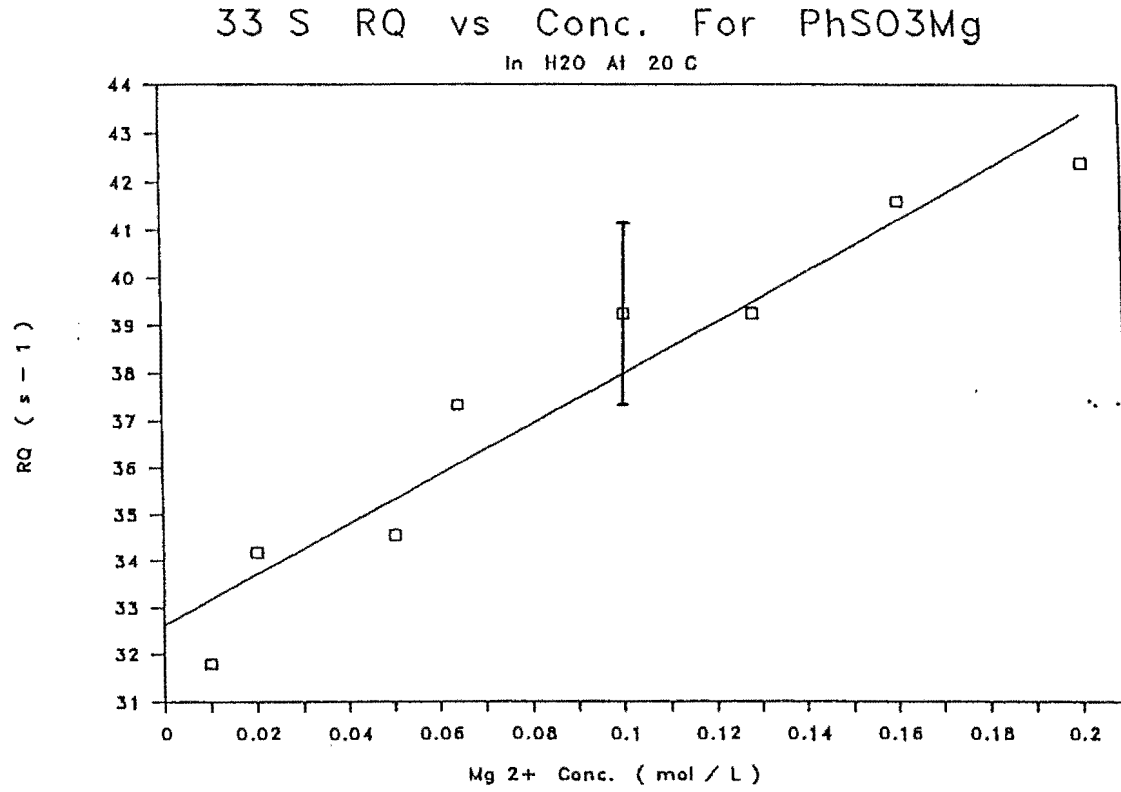


Figure 9.

33 S RQ vs Conc. For ( PhSO3 ) n M

In H2O At 20 C

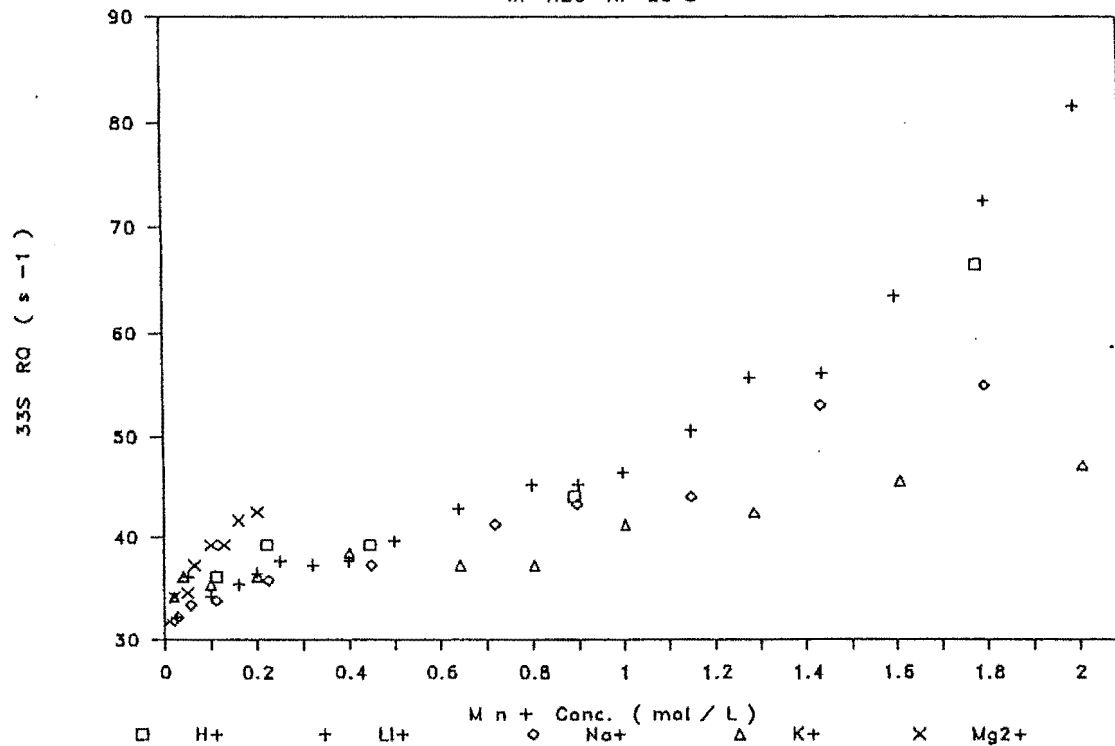
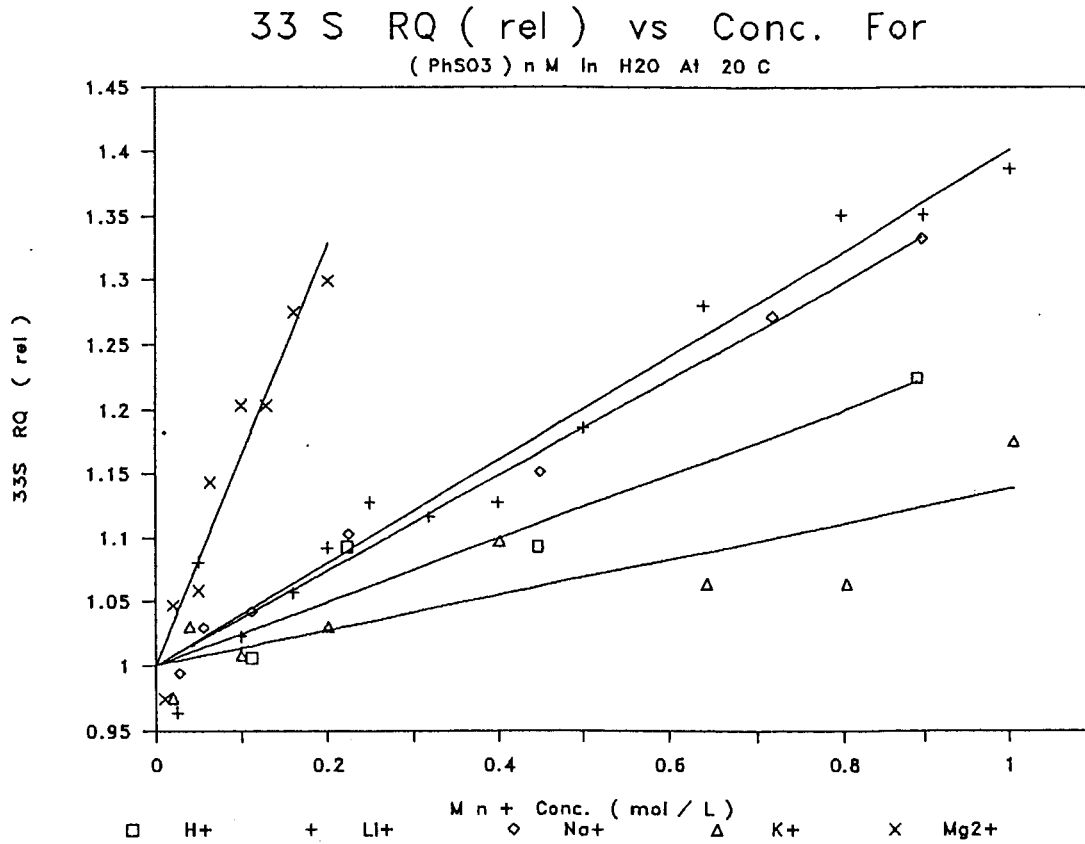


Figure 10.





The data in Figure 9 show that there is a definite specific counterion effect on the rate of  $^{33}\text{S}$  relaxation in aqueous benzenesulfonates, especially at concentrations above 1 M. When  $\text{H}^+$  is the counterion,  $^{33}\text{S}$  relaxation is rapid because of the equilibrium between the protonated and ionized benzenesulfonic acid. For the metal ions, the order of counterion induced relaxation is  $\text{Mg}^{2+} > \text{Li}^+ > \text{Na}^+ > \text{K}^+$ ; in the presence of  $\text{Mg}^{2+}$ ,  $^{33}\text{S}$  relaxation is especially rapid even at low concentrations. A good way to compare the relative effects of counterions on the  $^{33}\text{S}$  relaxation rate is to consider values of  $R_{Q,\text{rel}}$  which are obtained by dividing the observed relaxation rates by the corresponding relaxation rates at infinite dilution. Hence,  $R_{Q,\text{rel}} = R_Q^{\text{obsd}} / R_Q^0$ , and these values are plotted in Figure 10 as a function of concentration ( $\leq 1 \text{ M}$ ) at  $20^\circ \text{ C}$ .

The relative magnitudes of counterion effects can be explained in terms of a few of the physical constants of these ions in aqueous solution. A list of the relevant physical constants of the counterions used appears in Table 11. The effective ionic radii,  $r_{\text{ION}}$ , and correlation times of water molecules in the first hydration sphere,  $\tau_c(\text{H}_2\text{O})$ , are given for the hydrated ions of coordination number 4 and 6.

The counterion contribution to  $^{33}\text{S}$  relaxation is given by Eqn. [21]. Recently, it has been shown by  $^{25}\text{Mg}^{2+}$  and  $^{35}\text{Cl}^-$  relaxation measurements in aqueous  $\text{MgCl}_2$  that the polarization factor  $P$  is constant over a wide concentration range.<sup>23</sup> Therefore,  $P$  is assumed constant here for the aqueous benzenesulfonates. Then, the counterion contribution to the  $^{33}\text{S}$  relaxation rate is proportional to the following counterion properties:

- i. square of the charge
- ii. concentration
- iii. correlation time

iv. inverse cube of the distance of closest approach between the counterion and the relaxing nucleus

v. shielding effects of the surrounding ion cloud

Thus, if the correlation time of water molecules in the first hydration sphere of the counterion,  $\tau_c(\text{H}_2\text{O})$ , is assumed constant and water-water cross-correlations are neglected, then the slopes in Table 10 are proportional to the coefficients of concentration in Eqn. [21].

---

Table 11. Physical Constants of the Metal Counterions Used.

---

Counterion	$(1+\gamma_\infty)$	Coordi- nation No.	$r_{\text{ion}}^c$ Å	$\tau_c(\text{H}_2\text{O})$ ps at 25° C
Li <sup>+</sup>	0.74 <sup>a</sup>	4	0.73	5 <sup>d</sup>
Na <sup>+</sup>	5.1 <sup>a</sup>	6	1.16	3.75 <sup>d</sup>
K <sup>+</sup>	18.3 <sup>a</sup>	6	1.52	2.5 <sup>d</sup>
Mg <sup>2+</sup>	4.32 <sup>b</sup>	6	0.86	4 <sup>e</sup>

---

<sup>a</sup> reference 20a.

<sup>b</sup> reference 37.

<sup>c</sup> reference 38.

<sup>d</sup> reference 20a.

<sup>e</sup> reference 23.

The exact distance of closest approach between the center of the counterion and  $^{33}\text{S}$  in the benzenesulfonate ion, and the rates of diffusion of the counterions in the solutions studied here, are not known. However, differences in the degree of counterion effect on the  $^{33}\text{S}$  relaxation rate may be discussed in terms of the diffusion rate of the counterion, here compared on the basis of  $\tau_c(\text{H}_2\text{O})$ ,  $r_{\text{ion}}$ , and the charge of the counterion. The slopes (Table 10) obtained when  $\text{Li}^+$  and  $\text{Na}^+$  are the counterions are not significantly different, so that a difference in the influence of these two counterions on  $^{33}\text{S}$  relaxation at concentrations below 1 M is negligible; although, at higher concentrations the observed  $^{33}\text{S}$  relaxation rates are distinctly higher in the presence of  $\text{Li}^+$ . Higher relaxation rates in the presence of  $\text{Li}^+$  were expected even at moderate concentrations due to the large  $\tau_c(\text{H}_2\text{O})$  and small  $r_{\text{ion}}$  for this species. Perhaps the smaller than expected slope was a result of more effective screening of the counterion contribution to the local field gradient at  $^{33}\text{S}$  by the  $\text{Li}^+$  ion cloud (Eqns. [21] and [22]).

The  $^{33}\text{S}$  relaxation rates for potassium benzenesulfonate are the lowest, even at high concentrations, and the slope of  $^{33}\text{S}$   $R_Q$  vs concentration below 1 M is also the smallest. Also,  $\text{K}^+$  has the smallest  $\tau_c(\text{H}_2\text{O})$  and largest  $r_{\text{ion}}$  of the monovalent metal ions. Thus,  $\text{K}^+$  makes the smallest ion-ion contribution to the local field gradient inducing  $^{33}\text{S}$  relaxation in aqueous benzenesulfonate.

The effective ionic radius and  $\tau_c(\text{H}_2\text{O})$  of  $\text{Mg}^{2+}$  are comparable to those of  $\text{Li}^+$ , and the ratio of the  $^{33}\text{S}$  relaxation slopes is roughly 4:1, which is the ratio of the square of the charges on the respective ions. Given this, it might be concluded that strongly hydrated, divalent  $\text{Mg}^{2+}$  also produces more effective screening of the counterion contribution to the local field gradient at  $^{33}\text{S}$  by ion cloud formation. Also, the highest level of magnesium benzenesulfonate concentration used in this study

was very near the point of saturation in water at 20° C. Therefore, the data strongly suggest that faster  $^{33}\text{S}$  relaxation in the presence of  $\text{Mg}^{2+}$  at low concentrations is largely a result of the larger charge to size ratio of this ion, and rapid  $^{33}\text{S}$  relaxation induced by ion-pairing is not indicated.

### III.2.1 Concentration Dependence of $^{23}\text{Na}$ Quadrupolar Relaxation In Dilute Aqueous Sodium Benzenesulfonate

Due to the low natural abundance of  $^{33}\text{S}$ , its relaxation behavior in aqueous benzenesulfonate could not be studied below 20 mM concentration. Therefore, the quadrupolar relaxation of  $^{23}\text{Na}^+$  was investigated in aqueous sodium benzenesulfonate. Due to the 100% natural abundance of  $^{23}\text{Na}^+$ , the spin-lattice relaxation time,  $T_1$ , could be measured by the inversion-recovery technique down to millimolar levels. Also, the substantial anti-shielding factor,  $(1+\gamma_\infty)$ , (Table 11) and large quadrupole moment cause  $^{23}\text{Na}^+$  relaxation to be quite sensitive to the ion-ion contribution to quadrupolar relaxation. The resulting  $^{23}\text{Na}^+$  relaxation data are shown in Table 12 as a function of concentration at 20° C. The estimated experimental error in the data is 5%.

Since it has been reported that the relaxation behavior of  $^{23}\text{Na}^+$  shows a square-root-concentration dependence in some systems at low concentrations,<sup>27</sup> extrapolation to zero solute concentration to obtain estimates of the spin-lattice relaxation rate at infinite dilution,  $1/T_1^0$ , was done in three ways to test this behavior in aqueous sodium benzenesulfonate. First, the relaxation data were extrapolated using rates obtained at concentrations below 1 M and a first order dependence. Second, extrapolation was performed using data below 0.2 M and a first order dependence. Third, extrapolation was performed using data below 0.2 M and a  $c^{1/2}$  dependence. The results obtained by the three data treatments are shown in

Table 13 and are labeled Methods 1-3, respectively. The data are also plotted in Figures 11-13, and the lines were generated either from  $1/T_1$  vs concentration,  $c$ , for Figures 11 and 12, or from  $1/T_1$  vs the square root of concentration,  $c^{1/2}$ , for Figure 13.

Table 12.  $^{23}\text{Na}$  Relaxation Data For Sodium Benzenesulfonate In Aqueous Solution.

Concentration (mol / L)	$T_1$ (ms)	$1/T_1$ ( $\text{s}^{-1}$ )
1.796	26.9	37.2
1.436	31.3	31.9
1.149	36.3	27.5
0.898	37.5	26.7
0.7187	40.7	24.6
0.4492	45.6	21.9
0.2246	48.0	20.8
0.1123	50.8	19.7
0.0562	52.8	18.9
0.0281	53.7	18.6
0.0140	53.6	18.7
0.0070	53.2	18.8
0.0035	54.3	18.4
0.0018	54.2	18.4
0.0009	55.0	18.2

Figure 11.

$^{23}\text{Na}$   $1/T_1$  vs Conc. For  $\text{PhSO}_3\text{Na}$  In  $\text{H}_2\text{O}$

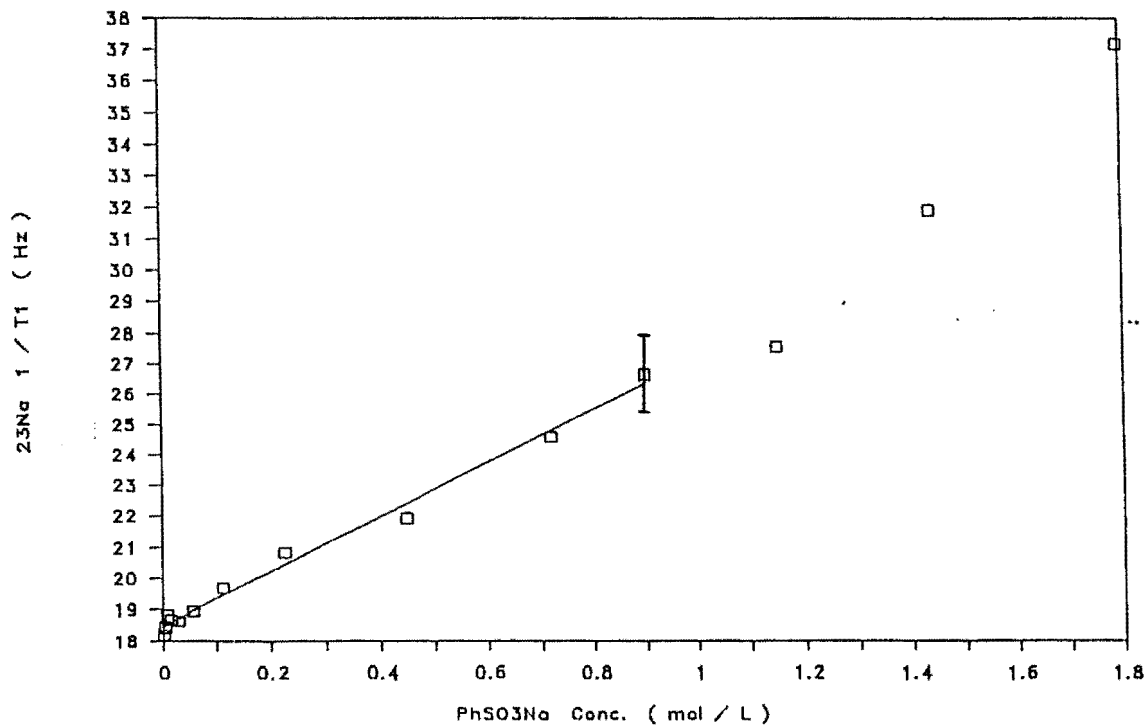


Figure 12.

$^{23}\text{Na}$   $1/T_1$  vs Conc. For  $\text{PhSO}_3\text{Na}$  In  $\text{H}_2\text{O}$

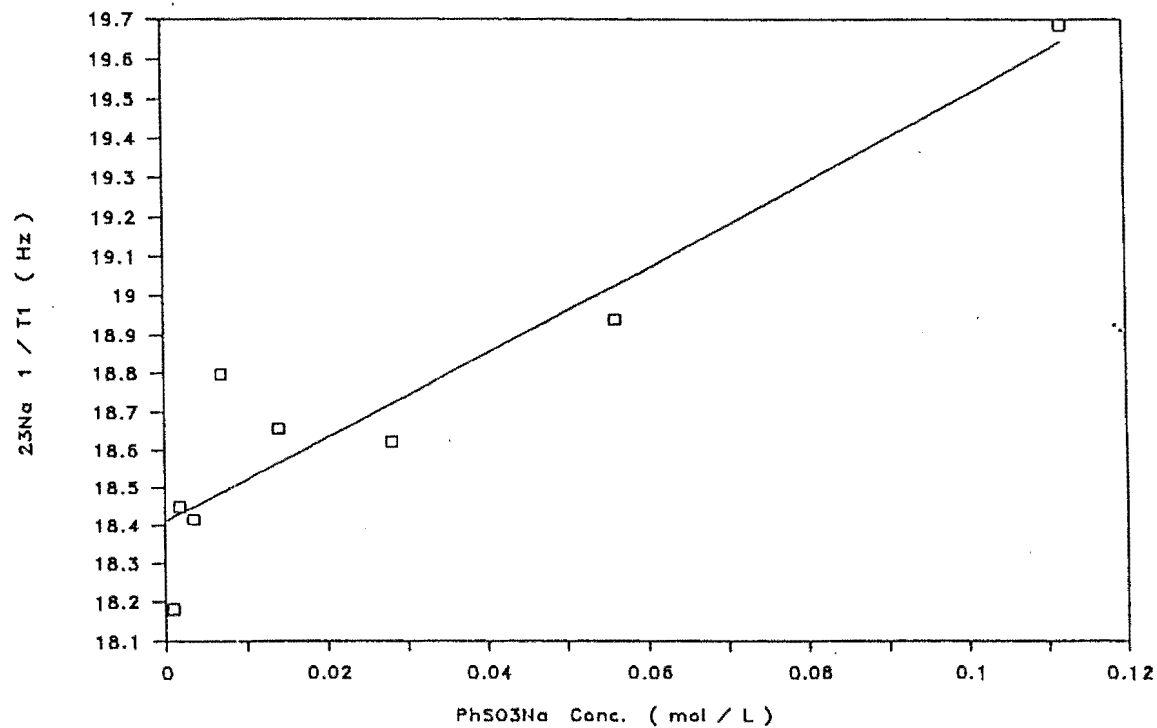




Figure 13.

### $^{23}\text{Na}$ $1/T_1$ vs SQRT Conc.

For  $\text{PhSO}_3\text{Na}$  In  $\text{H}_2\text{O}$  At  $20^\circ\text{C}$

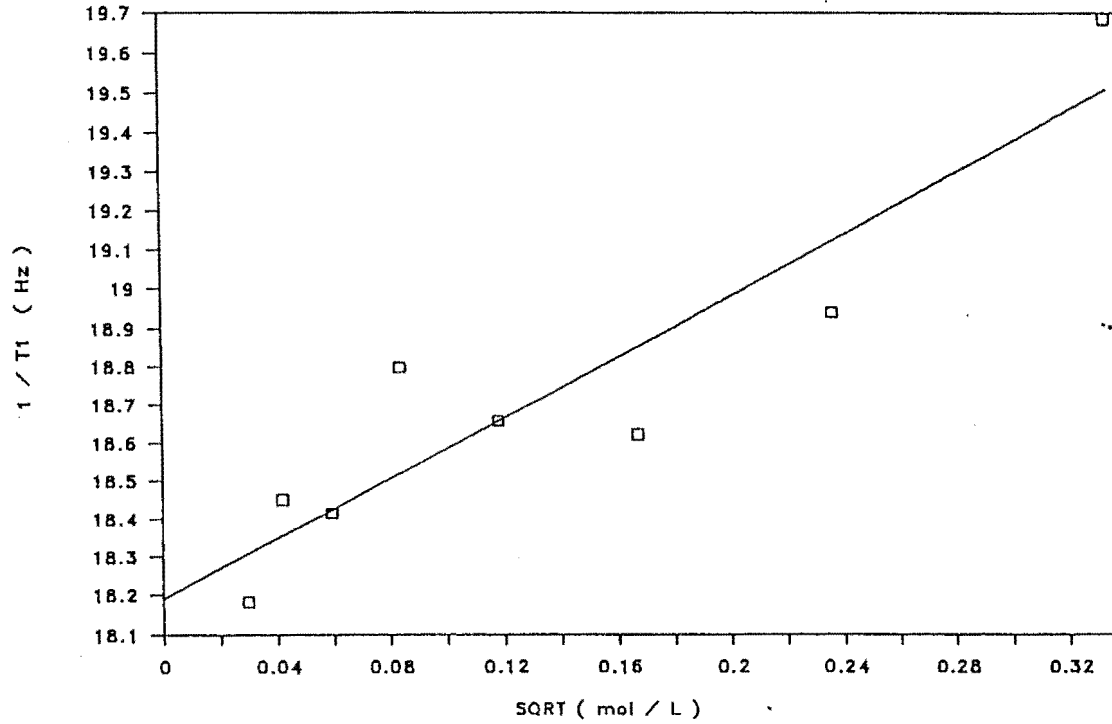


Table 13. Linear Regression Results For  $^{23}\text{Na}$   $1/T_1^0$  vs Concentration of Sodium Benzenesulfonate In Aqueous Solution At  $20^\circ\text{C}$ .

Method	$1/T_1^0$ ( $\text{s}^{-1}$ )	Std. Err. of $1/T_1$ Estimate	Slope	Std. Err. of Slope	r
1	18.47	0.28	8.79	0.27	0.99543
2	18.41	0.17	10.98	1.69	0.93557
3	18.19	0.19	3.93	0.67	0.92200

The relaxation rates at infinite dilution,  $1/T_1^0$ , obtained by the three methods all agree well within the limit of the estimated experimental error (i. e. 5%). In light of the better fit with Methods 1 and 2, the  $c^{1/2}$  dependence expected from the results of Sacco *et al.*<sup>27</sup> was not detected here. This may be due to the error in  $T_1$  measurements, and the high degree of scatter in the data at low concentrations. Similarly, Struis *et al.*<sup>23</sup> could not detect a  $c^{1/2}$  dependence of  $^{25}\text{Mg}^{2+}$  relaxation in dilute aqueous  $\text{MgCl}_2$  solutions down to 0.024 M. It could be argued on the basis of the difference in the slopes obtained by Methods 1 and 2 that there is a substantial change in  $^{23}\text{Na}^+$  quadrupolar relaxation behavior at low concentration. However, the slopes obtained from the two linear regressions are not significantly different, and the data are less reliable at very low concentrations. Therefore, the linear extrapolation approach obtained with moderately concentrated solutions (i. e.  $\leq 1$  M) seems valid for both  $^{23}\text{Na}^+$  and  $^{33}\text{S}$  relaxation rates in benzenesulfonate.

### III.2.3 Concentration And Counterion Dependence of $^{33}\text{S}$ Relaxation In Concentrated Aqueous Benzenesulfonates

The limit of solubility of sodium benzenesulfonate in water is approximately 2.4 M at 25° C. Therefore, aqueous solutions of benzenesulfonates above 1 M discussed here will be referred to as concentrated. The  $^{33}\text{S}$  relaxation data in Figure 9 for benzenesulfonates with monovalent counterions all show definite curvature above approximately 1.2 M.

Clearly,  $\text{Li}^+$  induces the fastest  $^{33}\text{S}$  relaxation in benzenesulfonate at a given level in concentrated solution. The order of counterion contribution of monovalent metal ions to the rate of  $^{33}\text{S}$  relaxation was found to be  $\text{Li}^+ > \text{Na}^+ > \text{K}^+$ . The relative magnitude of this effect below 1 M has already been discussed in terms of  $\tau_{\text{c}}(\text{H}_2\text{O})$ ,  $r_{\text{ion}}$ , and screening effects for these counterions in aqueous solution. However, it was assumed that  $\tau_{\text{c}}(\text{H}_2\text{O})$  for a given counterion was fairly constant at concentrations below 1 M so that water-water cross-correlations were neglected.

The Debye-Stokes-Einstein model predicts that the reorientational correlation time

$$\tau_{\text{c}} = f_{\text{r}} \frac{V\eta}{kT} \quad [23]$$

for solute or solvent molecules will increase linearly with the ratio of the shear viscosity  $\eta$  to temperature  $T$ ;  $f_{\text{r}}$  is the microviscosity factor,  $V$  is the molecular volume, and  $k$  is the Boltzmann constant.<sup>39</sup> Therefore, in early investigations the concentration dependence of quadrupolar relaxation of ions in solution was tentatively related to the concentration dependence of the viscosity of electrolyte solutions.<sup>40</sup> However, it has recently been shown that the variations of  $^{25}\text{Mg}^+$  and  $^{35}\text{Cl}^+$  relaxation rates in aqueous  $\text{MgCl}_2$  cannot be accounted for simply on the basis of changing viscosity.<sup>23</sup>

Since the  $^{33}\text{S}$  relaxation data for lithium benzenesulfonate showed the most curvature at high concentrations, the  $^7\text{Li}^+$  spin-lattice relaxation time,  $T_1$ , in this system was studied as a function of concentration at  $20^\circ\text{C}$ . The results are presented in Table 14, and plotted in Figure 14. The straight line in Figure 14 was obtained from linear regression using relaxation data recorded below 1 M. The results of the linear extrapolation are presented in Table 15.

---

Table 14.  $^7\text{Li}^+$  Relaxation Data For Lithium Benzenesulfonate In Aqueous Solution.

---

Concentration (mol / L)	$T_1$ (s)	$1/T_1$ ( $10^{-2}\text{ s}^{-1}$ )
1.800	6.2	16.1
1.600	6.5	15.3
1.440	7.3	13.7
1.152	9.4	10.7
0.900	10.3	9.7
0.640	11.9	8.4
0.400	14.6	6.8
0.200	14.3	7.0
0.100	16.9	5.9
0.050	17.0	5.9

---

Figure 14.

${}^7\text{Li } 1/T_1$  vs Conc. For  $\text{PhSO}_3\text{Li}$  In  $\text{H}_2\text{O}$

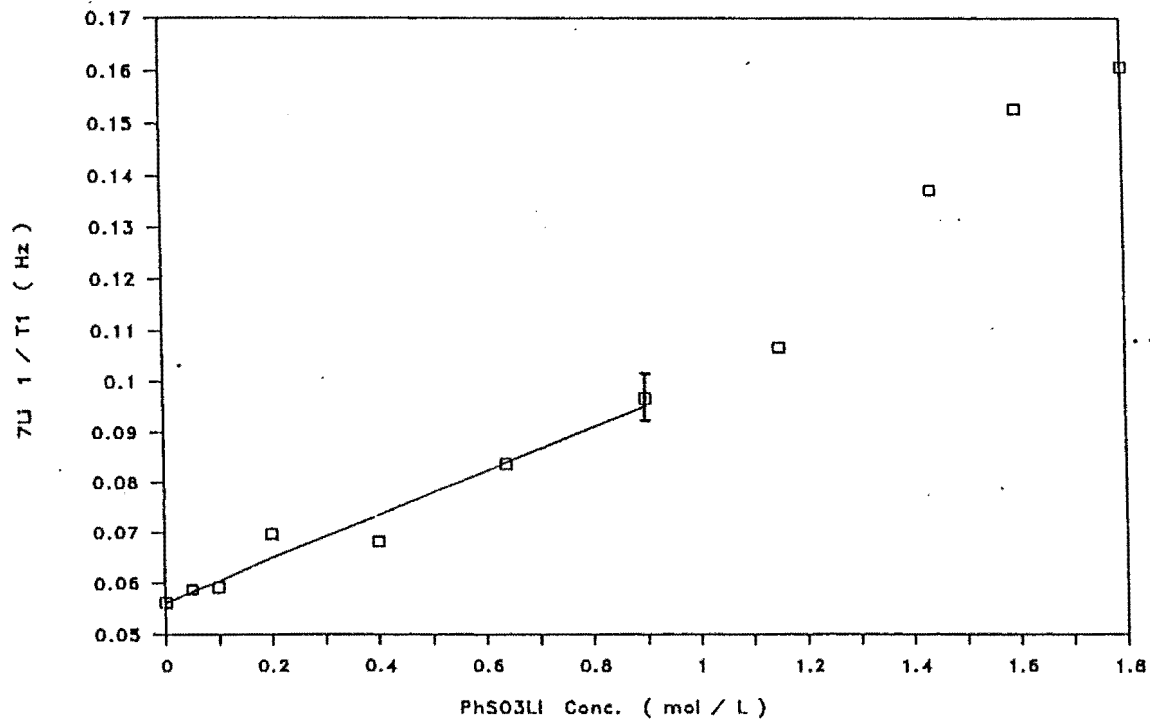


**Table 15.** Linear Regression Results For  ${}^7\text{Li}^+$   $1/T_1$  vs Concentration For Aqueous Lithium Benzenesulfonate At 20° C.

$1/T_1^0$	$(10^{-2} \text{ s}^{-1})$	5.6
Std. Err. of $1/T_1$		0.4
Estimate	$(10^{-2})$	
Slope	$(10^{-2})$	43.5
Std. Err. of		
Slope	$(10^{-2})$	0.5

Hertz<sup>20b,22</sup> has shown that the ion-solvent and ion-ion contributions to the quadrupolar relaxation rate of  ${}^7\text{Li}^+$  and  ${}^{23}\text{Na}^+$  in aqueous solution are given by Eqns. [19] and [21], respectively. Substantial curvature is observed in the relaxation rate of  ${}^7\text{Li}^+$  with increasing lithium benzenesulfonate concentration above 1 M (Figure 14). The same relaxation behavior is observed for  ${}^{23}\text{Na}^+$  relaxation (Figure 11), as well as for  ${}^{33}\text{S}$  relaxation in the benzenesulfonates (Figure 9). This suggests that the correlation time of water molecules in the first hydration sphere of the cation,  $\tau_c(\text{H}_2\text{O})$ , may be changing with increasing concentration; the correlation time,  $\tau_c$ , of the benzenesulfonate ion may also be changing with increasing concentration.

In order to separate the two possible effects,  ${}^{13}\text{C}$  spin-lattice relaxation times,  $T_1$ , were measured as a function of lithium benzenesulfonate concentration at 20° C.

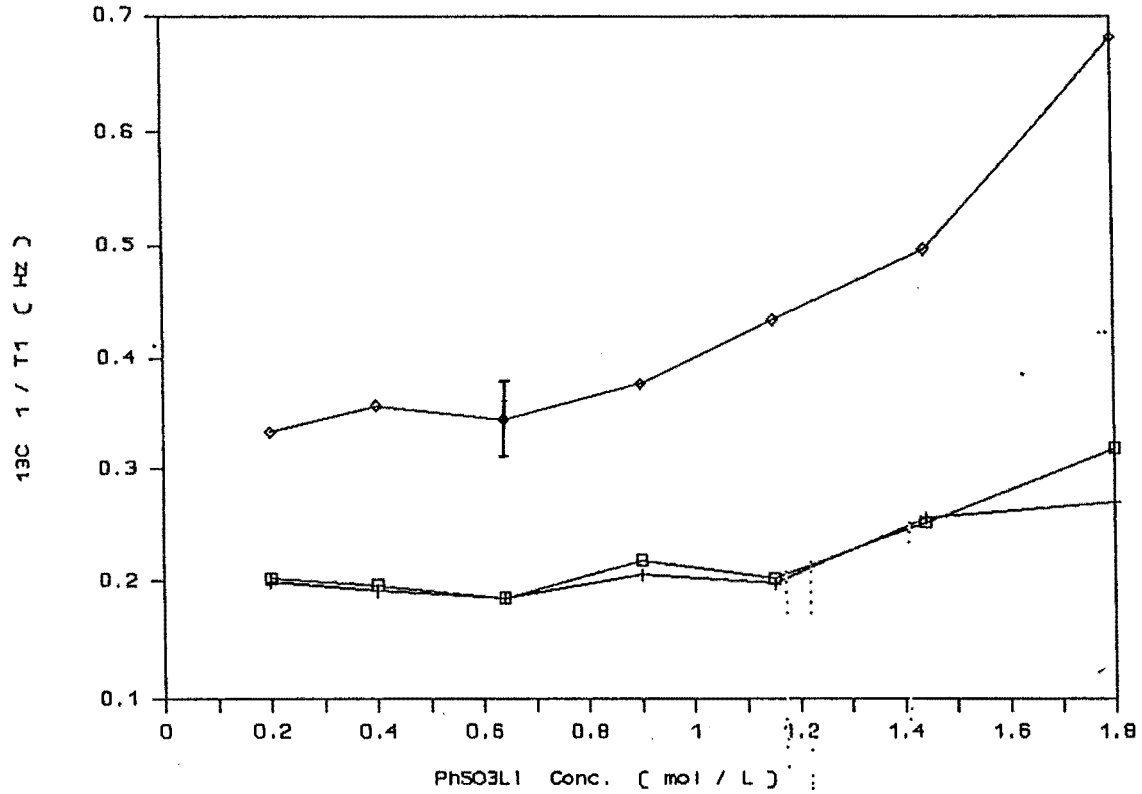
The data presented in Table 16 and plotted in Figure 15 show that the relaxation rates,  $1/T_1$ , of protonated carbons on the phenyl ring are constant, within the experimental error of 5%, below 1 M. However, above 1 M  $1/T_1$  increases with increasing concentration.

Table 16.  $^{13}\text{C}$  Relaxation Data For Lithium Benzenesulfonate In Aqueous Solution.

Concentration (mol / L)	$T_1$ (s)		
	C 2,6	C 3,5	C 4
1.800	3.7	3.1	1.5
1.440	4.0	4.0	2.0
1.152	5.1	4.9	2.3
0.900	4.9	4.6	2.7
0.640	5.4	5.4	2.9
0.400	5.2	5.1	2.8
0.200	5.0	4.9	3.0

Figure 15.

$^{13}\text{C}$   $1/T_1$  vs Conc. For  $\text{PhSO}_3\text{Li}$  In  $\text{H}_2\text{O}$





The  $^{13}\text{C}$  relaxation rates of protonated carbons on the phenyl ring are related to the correlation time through:<sup>41</sup>

$$1 / T_1 = N\hbar^2\gamma_C^2\gamma_H^2 r_{\text{CH}}^{-6}\tau_{\text{eff}} \quad [24]$$

Here  $\gamma_C$  and  $\gamma_H$  are the respective magnetogyric ratios of  $^{13}\text{C}$  and  $^1\text{H}$ ,  $N$  is the number of directly bonded hydrogens,  $r_{\text{CH}}$  is the CH distance, and  $\tau_{\text{eff}}$  is the effective reorientational correlation time. In order for Eqn. [24] to be applicable, the extreme narrowing limit must obtain and scalar coupling must be eliminated by proton decoupling. The data in Table 16 clearly show that the phenyl ring is reorienting anisotropically. As expected, the correlation time for reorientation parallel to the principle symmetry axis,  $\tau_{\parallel}$ , is shorter than the reorientation time perpendicular to this axis,  $\tau_{\perp}$ .

The  $^{13}\text{C}$  data suggest that the rate of rotational diffusion of the benzenesulfonate ion decreases with increasing concentration. Also, a marked increase in  $\tau_c(\text{H}_2\text{O})$  of the cation is indicated from the  $\text{Li}^+$  relaxation data. The conclusion, then, is that the  $^{33}\text{S}$  relaxation rate in concentrated aqueous benzenesulfonates (i. e.  $>1 \text{ M}$ ) increases non-linearly with concentration due to an additional sulfonate-cation hydration water contribution. This water-water cross-correlation effect appears not to make a substantial contribution to quadrupolar relaxation of the nuclei studied in aqueous benzenesulfonates at concentrations  $\leq 1 \text{ M}$ . Struis *et al.*<sup>23</sup> observed the same behavior for  $^{35}\text{Cl}^-$  relaxation in aqueous  $\text{MgCl}_2$ , and concluded that at 5.49 molal the magnesium hydration water molecule contribution was responsible for *ca.* 75% of the total chloride-water contribution to  $^{35}\text{Cl}^-$  relaxation.

### III.3 Concentration, Counterion, And Solvent Dependence of $^{33}\text{S}$ Quadrupolar Relaxation In Benzenesulfonates

The  $^{33}\text{S}$  NMR data obtained for benzenesulfonates solution as a function of concentration, counterion, and solvent at 20° C appear in Tables 17-19. The counterions were  $\text{Li}^+$ ,  $\text{Na}^+$ ,  $\text{K}^+$ , and  $\text{H}^+$ . The solvents used were formamide (FA), formamide plus 18 mole% water (FA/ $\text{H}_2\text{O}$ ), and N-methylformamide (NMF). It was found that the  $^{33}\text{S}$  chemical shifts of the benzenesulfonates in a given solvent were, within experimental error, independent of concentration and counterion. Aqueous ammonium sulfate was the chemical-shift reference. The  $^{33}\text{S}$  chemical shifts were  $\delta = -12.2 \pm 0.2$  ppm in formamide,  $\delta = -12.1 \pm 0.4$  ppm in formamide plus 18 mole% water, and  $\delta = -12.9 \pm 0.7$  ppm in N-methylformamide. Uncertainties in the  $^{33}\text{S}$  chemical-shift measurements were a consequence of the wide spectral lines observed. The chemical shifts were not corrected for bulk magnetic susceptibility.

However, a concentration, counterion, and solvent dependence of  $^{33}\text{S}$  linewidths was observed. Values of  $^{33}\text{S}$  relaxation rates,  $R_Q$ , were obtained from linewidth measurements and appear in Tables 17-19. The relaxation rates are also plotted as a function of concentration at 20° C in Figures 16-18. The straight lines in Figures 16-18 were obtained from linear regression analysis of the data  $\leq 1$  molar concentration. Extrapolation to zero solute concentration yielded estimates of the quadrupolar relaxation rate at infinite dilution,  $R_Q^0$ , which appear in Table 20. The resulting values of  $R_Q^0$  in a given solvent all agree within 12%, which is close to the estimated 10% experimental error in the linewidth measurements. Once again, when only values for metal counterions are considered, the resulting  $R_Q^0$ 's in a given solvent agree within experimental error.

Table 17.  $^{33}\text{S}$  NMR Data For Benzenesulfonates In Formamide Solution.

Counterion	Concentration (mol / L)	$\delta$ (ppm)	$\Delta\nu_{\frac{1}{2}}$ (Hz)	$R_Q$ ( $s^{-1}$ )
$\text{H}^+$	1.816	-12.1	135.0	424
$\text{H}^+$	0.908	-12.1	70.0	220
$\text{H}^+$	0.454	-12.1	56.2	177
$\text{H}^+$	0.227	-12.0	55.8	175
$\text{H}^+$	0.114	-12.0	51.2	161
$\text{Li}^+$	0.922	-12.2	68.8	216
$\text{Li}^+$	0.461	-12.1	60.2	189
$\text{Li}^+$	0.230	-12.1	43.1	135
$\text{Li}^+$	0.115	-12.1	43.6	137
$\text{Na}^+$	0.811	-12.4	73.2	230
$\text{Na}^+$	0.406	-12.1	55.6	175
$\text{Na}^+$	0.203	-12.2	48.8	153
$\text{Na}^+$	0.101	-12.2	42.0	132
$\text{K}^+$	0.997	-12.2	83.0	261
$\text{K}^+$	0.499	-12.1	57.5	181
$\text{K}^+$	0.249	-12.2	51.2	161
$\text{K}^+$	0.125	-12.1	44.9	141

**Table 18.**  $^{33}\text{S}$  NMR Data For Benzenesulfonates In Formamide Plus 18 Mole%  
Water Solution.

Counterion	Concentration (mol / L)	$\delta$ (ppm)	$\Delta\nu_{\frac{1}{2}}$ (Hz)	$R_Q$ ( $s^{-1}$ )
H <sup>+</sup>	2.020	-12.5	89.7	282
H <sup>+</sup>	1.010	-12.2	64.5	203
H <sup>+</sup>	0.505	-12.0	53.5	168
H <sup>+</sup>	0.252	-12.3	51.5	162
H <sup>+</sup>	0.126	-12.3	44.0	138
Li <sup>+</sup>	0.893	-12.3	49.6	156
Li <sup>+</sup>	0.447	-12.2	40.6	128
Li <sup>+</sup>	0.223	-12.2	36.2	114
Li <sup>+</sup>	0.112	-11.7	33.8	106
Na <sup>+</sup>	0.721	-11.9	49.4	155
Na <sup>+</sup>	0.360	-12.0	43.8	138
Na <sup>+</sup>	0.180	-12.0	39.4	124
Na <sup>+</sup>	0.090	-12.0	35.6	112
K <sup>+</sup>	2.030	-12.3	98.5	309
K <sup>+</sup>	1.015	-12.4	58.5	184
K <sup>+</sup>	0.508	-12.2	45.0	141
K <sup>+</sup>	0.254	-12.2	43.8	138
K <sup>+</sup>	0.127	-12.1	42.5	134

Table 19.  $^{33}\text{S}$  NMR Data For Benzenesulfonates In N-Methylformamide Solution.

Counterion	Concentration (mol / L)	$\delta$ (ppm)	$\Delta\nu_{\frac{1}{2}}$ (Hz)	$R_Q$ (s $^{-1}$ )
H $^+$	2.250	-13.2	223	701
H $^+$	1.125	-12.4	132	416
H $^+$	0.562	-13.5	121	381
H $^+$	0.281	-13.6	119	373
H $^+$	0.141	-13.5	110	346
Li $^+$	0.897	-13.2	139	437
Li $^+$	0.488	-13.1	112	352
Li $^+$	0.244	-13.2	101	317
Li $^+$	0.122	-13.0	104	327
Na $^+$	0.719	-12.7	131	412
Na $^+$	0.359	-12.7	114	358
Na $^+$	0.180	-13.0	109	342
Na $^+$	0.090	-13.3	104	327
K $^+$	2.020	-13.2	430	1351
K $^+$	1.010	-12.2	191	600
K $^+$	0.505	-13.0	142	446
K $^+$	0.252	-13.2	124	390
K $^+$	0.126		115	361

Figure 16.

S33 RQ vs Conc. For PhSO<sub>3</sub>M  
In Formamide At 20 C

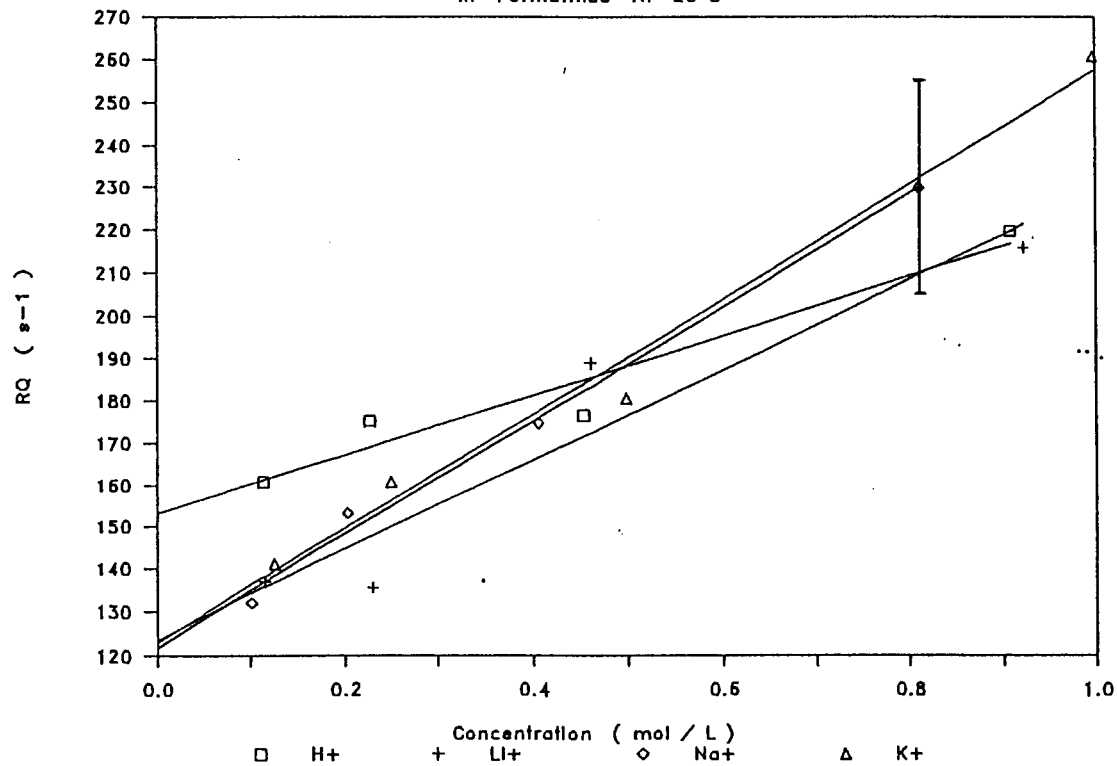


Figure 17.

### S33 RQ vs Conc. For PhSO<sub>3</sub>M

In Formamide / H<sub>2</sub>O At 20 C

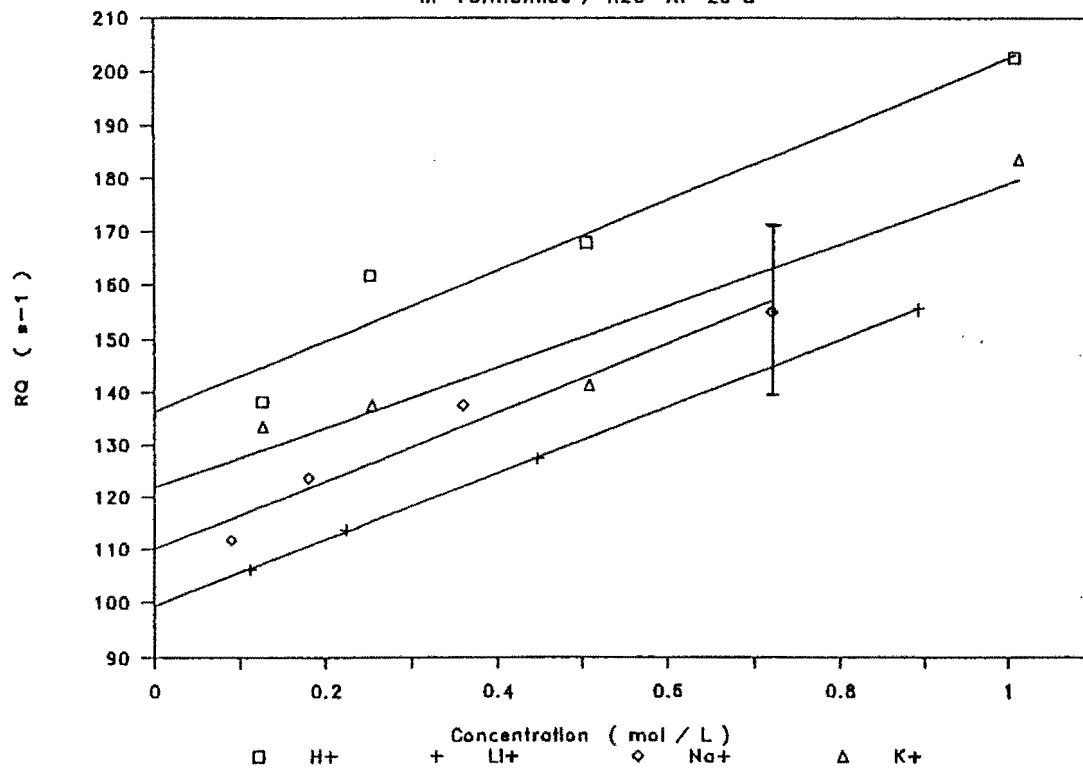
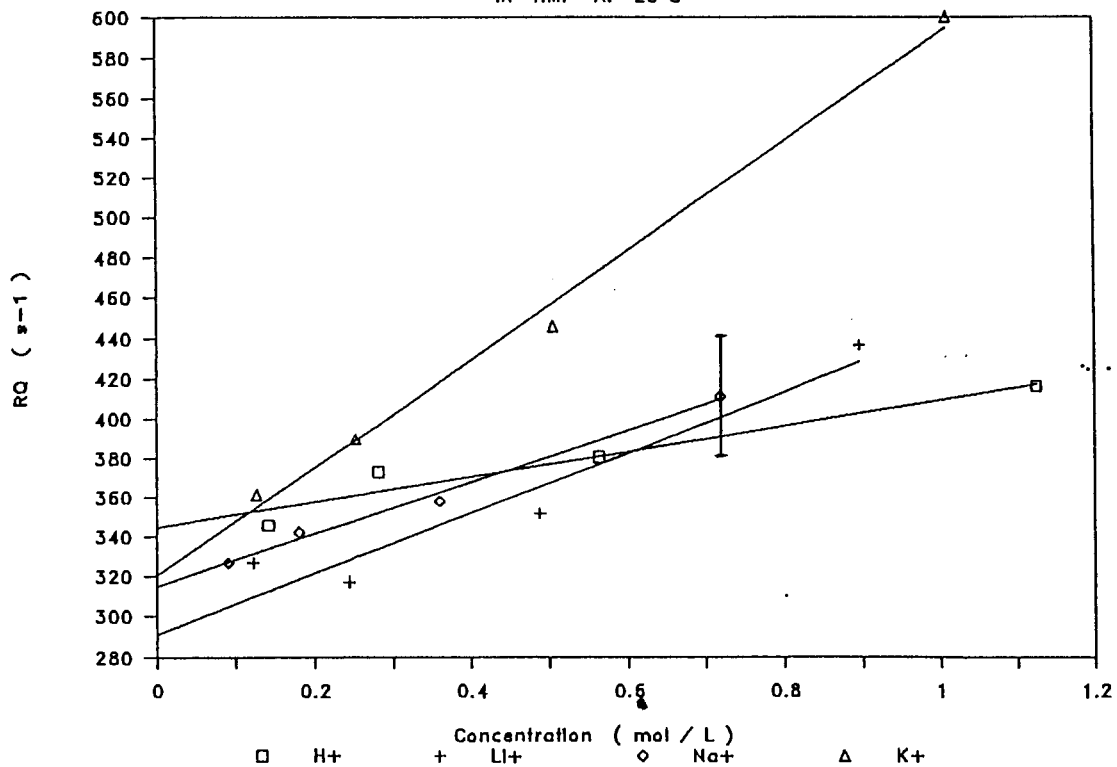


Figure 18.

### S33 RQ vs Conc. for PhSO<sub>3</sub>M

In NMF At 20 C





**Table 20. Linear Regression Results For  $^{33}\text{S}$   $R_Q$  vs Concentration: Four Benzenesulfonates In Formamide, Formamide Plus 18 Mole % Water, And N-Methylformamide At 20° C.**

	$R_Q^0$ ( $\text{s}^{-1}$ )	Std. Err. of $R_Q$ Estimate	Slope	Std. Err. of Slope	r
<b>HCONH<sub>2</sub></b>					
H <sup>+</sup>	153	8	70.4	13	0.96919
Li <sup>+</sup>	124	15	106	25	0.95019
Na <sup>+</sup>	122	4	134	7	0.99695
K <sup>+</sup>	123	8	135	12	0.99256
<b>HCONH<sub>2</sub>/H<sub>2</sub>O</b>					
H <sup>+</sup>	136	8	66.1	12	0.97080
Li <sup>+</sup>	99.3	0.3	63.3	0.4	0.99996
Na <sup>+</sup>	110	8	65.6	9	0.98012
K <sup>+</sup>	122	8	57.2	12	0.96071
<b>HCONHCH<sub>3</sub></b>					
H <sup>+</sup>	345	9	64.6	12	0.96489
Li <sup>+</sup>	291	18	153	31	0.96132
Na <sup>+</sup>	315	4	132	9	0.99581
K <sup>+</sup>	321	10	272	15	0.99700

Figures 16-18 clearly show that  $^{33}\text{S}$  relaxation in benzenesulfonates is faster in the amides than in water (Figure 9) across the entire concentration range studied. These organic solvents were chosen because the high dipole moments and dielectric constants led to favorable solubility of all of the benzenesulfonates used. Some of the physical properties of the solvents used are shown in Table 21.

Table 21. Some Physical Properties of the Pure Solvents Used (at 25° C).<sup>a</sup>

Solvent	Mol. Wt.	Density (g/cm <sup>3</sup> )	Viscosity (cP)	Dipole Moment (Debye)	Dielectr. Constant	Reorient. Correlation Time (ps)
Water	18.02	0.99	0.89	1.84	78.3	2.5
FA	45.04	1.13	3.30	3.73	109.5	5 <sup>b</sup>
NMF	59.07	0.99	1.65	3.83	182.4	5 <sup>b</sup>

<sup>a</sup> Reference 22. <sup>b</sup> Reference 42.

The lack of  $^{33}\text{S}$  chemical-shift dependence on benzenesulfonic acid concentration indicates that proton exchange is rapid at all concentrations and in all solvents studied here. Therefore, the high value of the  $^{33}\text{S}$  relaxation rate at infinite dilution,  $R_Q^0$ , obtained for benzenesulfonic acid in the amide solutions results from the equilibrium between the protonated and ionized acid. Thus, the  $^{33}\text{S}$  relaxation behavior when  $\text{H}^+$  is the counterion should be considered separately from the

relaxation behavior observed for the metal counterions.

Examination of the linear regression results in Table 20 shows that the slopes obtained for the metal counterions were not significantly different, for a given solvent, in either formamide or the formamide plus 18 mole% water solutions. Therefore, a specific counterion effect on  $^{33}\text{S}$  relaxation rates was not observed in these solvents. However, the  $^{33}\text{S}$  relaxation rates of benzenesulfonate in formamide are slightly higher than in formamide-water (Figures 16 and 17). Holz *et al.*<sup>42</sup> found from  $^{23}\text{Na}^+$  spin-lattice relaxation measurements, that  $\text{Na}^+$  is not preferentially solvated in formamide-water mixtures. That is, the local mole fractions of the two solvents in the solvation sphere of  $\text{Na}^+$  do not differ from the macroscopic mole fractions in the mixture. It was also found from  $^2\text{H}$  and  $^{14}\text{N}$  nuclear magnetic relaxation measurements, that the reorientational correlation times of water and formamide molecules in a 20 mole% water mixture are both 4 picoseconds.<sup>42</sup> Therefore, assuming that all of the metal cations in the benzenesulfonate solutions are not preferentially solvated in the formamide-water mixture, the slightly lower  $^{33}\text{S}$  relaxation rates observed are a consequence of the shorter correlation times of the solvent molecules when compared to 100% formamide.

No significant difference in the slopes was observed for the  $^{33}\text{S}$  relaxation rates of lithium and sodium benzenesulfonates dissolved in N-methylformamide (Table 20). However, a much larger ion-ion contribution to the  $^{33}\text{S}$  relaxation rate was observed for potassium benzenesulfonate dissolved in NMF. Faster  $^{33}\text{S}$  relaxation for potassium benzenesulfonate dissolved in NMF due to ion pairing was not indicated because the  $R_Q^0$  was within experimental error of the values obtained for lithium and sodium benzenesulfonates in spite of the larger slope observed for the potassium salt. Also,  $^{33}\text{S}$  chemical shifts are within experimental error of those observed in the presence of the other counterions. A slope lower than that of the sodium salt was

expected on the basis of the  $r_{ion}$  dependence of the ion-ion contribution Eqn. [21]. Perhaps, screening of the counterion contribution to the local field gradient at  $^{33}\text{S}$  by the  $\text{K}^+$  ion cloud is less effective than that of  $\text{Li}^+$  and  $\text{Na}^+$  in NMF.

At zero solute concentration, the ion-ion contribution to the  $^{33}\text{S}$  relaxation rate may be neglected, and the ion-solvent contribution (Eqns. [16]-[19]) is due to the quadrupolar interaction with the local field gradient produced by the solvent dipoles. The field gradient is modulated in time by the reorientation of the solvent molecules. The observed trend in solvent induced  $^{33}\text{S}$  relaxation rates in benzenesulfonates at infinite dilution is water < formamide-water < formamide < NMF.

Hertz<sup>22</sup> observed the same trend in relaxation rates for the quadrupolar halides in water, formamide, and N-methylformamide, and offered only a qualitative discussion of the observed differences in the relaxation behavior of anions in the amides. According to the electrostatic interpretation, the observed trend in  $^{33}\text{S}$   $R_Q$ 's (Table 20) for the benzenesulfonates in water, formamide, and the formamide-water mixture is a consequence of the high dipole moment and the long reorientational correlation time of the formamide molecule (Table 21). In the formamide-water mixture, the reorientational correlation times of both water and formamide molecules are somewhat shorter than the correlation time of 100% formamide but longer than that of water.<sup>42</sup> However, formamide contributes 82% of the solvent electric dipole moment producing the local field gradient at  $^{33}\text{S}$  in the mixture. Despite the rapid  $^{33}\text{S}$  relaxation observed in the formamide and formamide-water mixture when compared to that observed in water, the electrostatic model suggests that large, polarizable anions such as benzenesulfonate in water and the formamide solutions are weakly solvated by a fully random distribution of solvent dipoles over the entire space of the solution up to the surface of the ion. In this case a primary solvation sphere in the usual sense is absent and the ion-solvent contribution to the  $^{33}\text{S}$  relaxation rate in

benzenesulfonate is best described by the "fully random distribution," FRD, model of Eqn. [16a]. The FRD model was used to calculate the relaxation rates at infinite dilution of  $^{35}\text{Cl}^-$ ,  $^{81}\text{Br}^-$ , and  $^{127}\text{I}^-$  dissolved in water or formamide which agreed within an order of magnitude with experimental results.<sup>22</sup>

The ratio of the dipole moments of formamide and NMF is not sufficient to produce the difference in  $^{33}\text{S}$  relaxation behavior observed for benzenesulfonate dissolved in these solvents. In fact, the reorientational correlation time of the NMF molecule implied an expected  $^{33}\text{S}$   $R_Q^0$  for benzenesulfonate in NMF similar to the formamide solution. The electrostatic model suggests that the change in expected relaxation behavior is a consequence of stronger solvation in NMF. Thus, a larger local field gradient experienced by relaxing  $^{33}\text{S}$  is produced by solvent dipoles which are more tightly packed about the benzenesulfonate ion, but randomly oriented in the first solvation sphere, and perhaps to a lesser extent by solvent dipoles beyond this sphere with a fully random distribution. Therein, the ion-solvent contribution to  $^{33}\text{S}$  relaxation behavior in benzenesulfonate dissolved in NMF is best described by the "Non-Oriented Solvation," NOS, model of Eqn. [17].

The trend in extrapolated  $^{33}\text{S}$  relaxation rates at infinite dilution follows the same trend as values of absolute ion standard entropies,  $S_{\text{ion}}^0$ , obtained for the larger halides in water, formamide, and NMF.<sup>43</sup> Absolute ion standard entropies can be regarded as a measure of order around the ion in solution, and the values of  $S_{\text{ion}}^0$  for the larger halides decrease in the order  $\text{H}_2\text{O} > \text{HCONH}_2 > \text{HCONHCH}_3$ . These thermodynamic data imply that solvent packing about these anions increases in this order. Absolute standard entropies for benzenesulfonate are unavailable. However, the  $^{33}\text{S}$  NMR data indicate that the rapid  $^{33}\text{S}$  relaxation for benzenesulfonate in NMF over the entire concentration range studied is predominantly due to stronger solvation of benzenesulfonate in this solvent compared to solvation in water or formamide.

## CHAPTER IV

### CONCLUSIONS

#### IV.1 Use of $^{33}\text{S}$ NMR For the Determination of $\text{pK}_a$ 's of Arenesulfonic Acids

An improved linear correlation was found between  $^{33}\text{S}$  chemical shifts and the  $\text{pK}_a$ 's of benzenesulfonic, *m*-methylbenzenesulfonic, *p*-methylbenzenesulfonic, *p*-ammoniobenzenesulfonic, and *p*-bromobenzenesulfonic acids, previously determined by UV spectroscopy. That linear correlation was used to determine the previously unreported  $\text{pK}_a$ 's ( $\pm 0.04$ ) from  $^{33}\text{S}$  chemical shifts of the following: *p*-aminobenzenesulfonic (-6.47), *p*-dimethylaminobenzenesulfonic (-6.43), *p*-dimethylammoniobenzenesulfonic (-7.18), *p*-chlorobenzenesulfonic (-6.88), *p*-acetylbenzenesulfonic (-6.96), *p*-nitrobenzenesulfonic (-7.23), *m*-(trifluoromethyl)benzenesulfonic (-7.04), and *m*-nitrobenzenesulfonic (-7.25) acids. Also,  $^{33}\text{S}$  chemical shifts provided an improved value for the second  $\text{pK}_a$  of *m*-benzenedisulfonic acid (-7.00), and the previously unreported second  $\text{pK}_a$  of *p*-benzenedisulfonic acid (-6.99).

Earlier, the  $\text{pK}_a$ 's of *m*-nitrobenzenesulfonic and *p*-nitrobenzenesulfonic acids could not be determined by UV techniques because of unresolved B bands in the spectra. Also,  $\text{pK}_a$ 's for the second ionizations of *m*-benzenedisulfonic and *p*-benzenedisulfonic acids could not be determined by  $^1\text{H}$  NMR because it is necessary to record spectra using sulfuric acid as the solvent. Therefore,  $^{33}\text{S}$  NMR was found to

be an accurate and facile method for determining  $pK_a$ 's of arenesulfonic acids, which is free from the experimental difficulties of previous methods.

#### IV.2 Concentration, Counterion, And Solvent Dependence of $^{33}\text{S}$ Quadrupolar Relaxation In Benzenesulfonates

A definite specific counterion effect on the rate of  $^{33}\text{S}$  quadrupolar relaxation in aqueous benzenesulfonates was observed, especially at concentrations above 1 M. When  $\text{H}^+$  was the counterion,  $^{33}\text{S}$  relaxation is rapid because of the equilibrium between the protonated and ionized benzenesulfonic acid. For the metal ions, the order of counterion induced  $^{33}\text{S}$  quadrupolar relaxation in aqueous benzenesulfonates is  $\text{Mg}^{2+} > \text{Li}^+ > \text{Na}^+ > \text{K}^+$ . In the presence of  $\text{Mg}^{2+}$ ,  $^{33}\text{S}$  relaxation is especially rapid even at low concentrations.

The solvent dependent rate of  $^{33}\text{S}$  quadrupolar relaxation in all benzenesulfonates studied was found to increase in the order  $\text{H}_2\text{O} < \text{HCONH}_2\text{-H}_2\text{O} < \text{HCONH}_2 < \text{HCONHCH}_3$  across the entire concentration range studied. A specific counterion effect on  $^{33}\text{S}$  quadrupolar relaxation rates in the alkali metal benzenesulfonates dissolved in formamide or formamide plus 18 mole% water was not evident. However, rapid  $^{33}\text{S}$  relaxation in the presence of  $\text{H}^+$  was observed for benzenesulfonic acid dissolved in these solvents due to proton exchange. A much larger ion-ion contribution to the  $^{33}\text{S}$  quadrupolar relaxation rate was observed for potassium benzenesulfonate dissolved in N-methylformamide than when  $\text{H}^+$ ,  $\text{Li}^+$ , or  $\text{Na}^+$  were the counterion.

Extrapolation of concentration dependent  $^{33}\text{S}$  relaxation rates to the limit of infinite dilution furnished estimates of the ion-solvent contribution to  $^{33}\text{S}$  quadrupolar relaxation. The solvent dependent  $^{33}\text{S}$  relaxation rates at infinite dilution were found to increase in the order  $\text{H}_2\text{O} < \text{HCONH}_2\text{-H}_2\text{O} < \text{HCONH}_2 < \text{HCONHCH}_3$ . The data

indicate that solvation of benzenesulfonate in water and formamide is similar, while solvation in N-methylformamide is different.



## CHAPTER V

### EXPERIMENTAL SECTION

#### V.1. Use of $^{33}\text{S}$ NMR For the Determination of $\text{pK}_a$ 's of Arenesulfonic Acids

Sulfonic acids 1, 2, 8, 11 and sodium sulfonates 3, 12, 6 were obtained from commercial sources and were used without further purification. Sulfonic acids 4, 5, 10, were prepared previously and completely identified.<sup>16</sup> Dipotassium *p*-benzenedisulfonate (13) was prepared and identified by literature methods.<sup>44</sup> Sodium *p*-nitrobenzenesulfonate (15) was prepared by dissolving *p*-nitrobenzenesulfonic acid<sup>16</sup> in deionized water and adding one equivalent of NaOH.

Potassium *p*-aminobenzenesulfonate (7) was prepared by stirring a suspension of *p*-aminobenzenesulfonic acid (Fisher) in deionized water and adding one molar equivalent of solid KOH. Complete dissolution of the potassium salt was achieved by continued stirring and gentle heating. The resulting solution was frozen and the water removed in vacuo.

Potassium *p*-ammoniobenzenesulfonate (9) and sodium *p*-dimethylammonio-benzenesulfonate (14) were prepared by incremental acidification of aqueous solutions of 7 and 6 with a minimum amount of 12 M HCl, with subsequent  $^{33}\text{S}$  chemical shift determinations. No further changes in the  $^{33}\text{S}$  spectra were observed when the pH values given in Table 2 were reached.

The natural abundance  $^{33}\text{S}$  spectra were recorded unlocked at 23.008 MHz (7.047 T) on a Varian VXR-300 NMR spectrometer, operating in the Fourier transform mode, using a high-resolution, broadband probe and 10 mm o. d. sample tubes. The concentrations of the aqueous arenesulfonates were 0.046 to 0.13 M. In all cases,  $^{33}\text{S}$  chemical shifts were referenced to 0.12 M aqueous ammonium sulfate contained in a coaxial 5 mm o. d. NMR sample tube. Broadband (square wave modulated) proton decoupling was employed throughout.

The  $^{33}\text{S}$  spectral width was 10,000 Hz, acquisition times were 0.147 s (2944 data points) for spectra recorded at  $20 \pm 1^\circ \text{C}$ , 0.198 s (3968 data points) for those recorded at  $39 \pm 1^\circ \text{C}$ , and FID's were transformed in 32 K data points. In most cases, acquisition of transients was continued until a signal to noise ratio of at least 20 was attained. In order to minimize "baseline roll" resulting from acquisition of ultrasonic acoustic ringing in the probe, a receiver dead time (Varian VXR parameter ROF2) of  $50 \mu\text{s}$  was employed.<sup>45</sup>

For spectra recorded at  $39 \pm 1^\circ \text{C}$ , the probe temperature was calibrated by recording the  $^1\text{H}$  NMR of degassed ethylene glycol (Aldrich, 99+% spectrophotometric grade) contained in a sealed 10 mm o. d. NMR sample tube.<sup>46</sup> The  $^1\text{H}$  NMR spectra were recorded without field-frequency lock, and the magnetic field was shimmed on the FID. All samples for spectra recorded at  $39 \pm 1^\circ \text{C}$  were thermostated for at least 30 minutes prior to insertion into the probe, and the sample temperature was allowed to equilibrate with the probe for approximately 30 minutes prior to acquisition of transients.

## V.2 Concentration, Counterion, And Solvent Dependence of $^{33}\text{S}$ Quadrupolar Relaxation In Benzenesulfonates

The  $^{33}\text{S}$  NMR measurements for benzenesulfonates were determined as a function of concentration at  $20 \pm 1^\circ \text{C}$  in the pure solvents water, formamide, N-methylformamide, and a binary mixture of formamide plus 18 mole% water. Benzenesulfonic acid and sodium benzenesulfonate were commercially available, and the other benzenesulfonates were prepared by neutralization of benzenesulfonic acid with one equivalent of the corresponding hydroxide in water. Lithium and potassium benzenesulfonates used in the amide solutions were obtained by freezing the respective aqueous sulfonate solution and removing the water in vacuo. Lithium hydroxide, potassium hydroxide, formamide, and N-methylformamide were of the highest purity commercially available, and were used without further purification.

The natural abundance spectra were recorded unlocked at  $20 \pm 1^\circ \text{C}$  and 23.008 MHz (7.047 T) on a Varian VXR-300 spectrometer, operating in the Fourier transform mode, using a high-resolution, solution-state, broadband probe and 10 mm o. d. sample tubes. The typical spectral width was 10,000 Hz, and acquisition times were 147 ms (2944 data points) for the solvents water and formamide, and 48 ms (960 data points) for the formamide-water mixture and N-methylformamide. Spectra were typically transformed in 32 K data points.

A 50  $\mu\text{s}$  pulse width was used. For all amide solutions, the pulse was followed by a 50  $\mu\text{s}$  receiver dead time (Varian VXR parameter ROF2) prior to acquisition of the FID. The use of this receiver delay time was sufficient to eliminate spectral artifacts<sup>47</sup> such as "baseline roll" caused by acoustic ringing in the probe. The ACOUSTIC pulse sequence<sup>47b</sup> was used for the aqueous benzenesulfonates with a receiver dead time of 10  $\mu\text{s}$ .

In all cases, chemical shifts were referenced to aqueous ammonium sulfate.

The reference was contained in a 5 mm o. d. sample tube coaxial with the 10 mm o. d. tube for the amide solutions and the aqueous benzenesulfonic acid solutions. The chemical shift of aqueous ammonium sulfate at  $\text{pH } 5.5 \pm 0.5$  was found to be independent of concentration from 0.1 to 4 M; therefore the concentration of the reference solution was chosen such that it would approximately match the concentration of the sample solution. For the aqueous sulfonate salts, the reference was 4 M aqueous ammonium sulfate contained in a 10 mm o. d. sample tube, and the "sample replacement" technique was used. Spectra of benzenesulfonates dissolved in the amides and benzenesulfonic acid in water were recorded in duplicate; reported  $^{33}\text{S}$  chemical shifts and linewidths are averages of the two measurements.

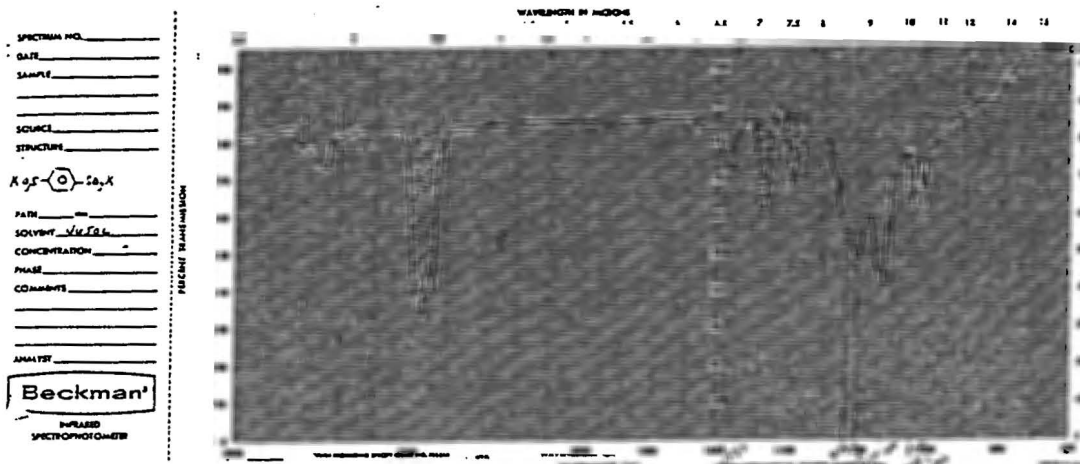
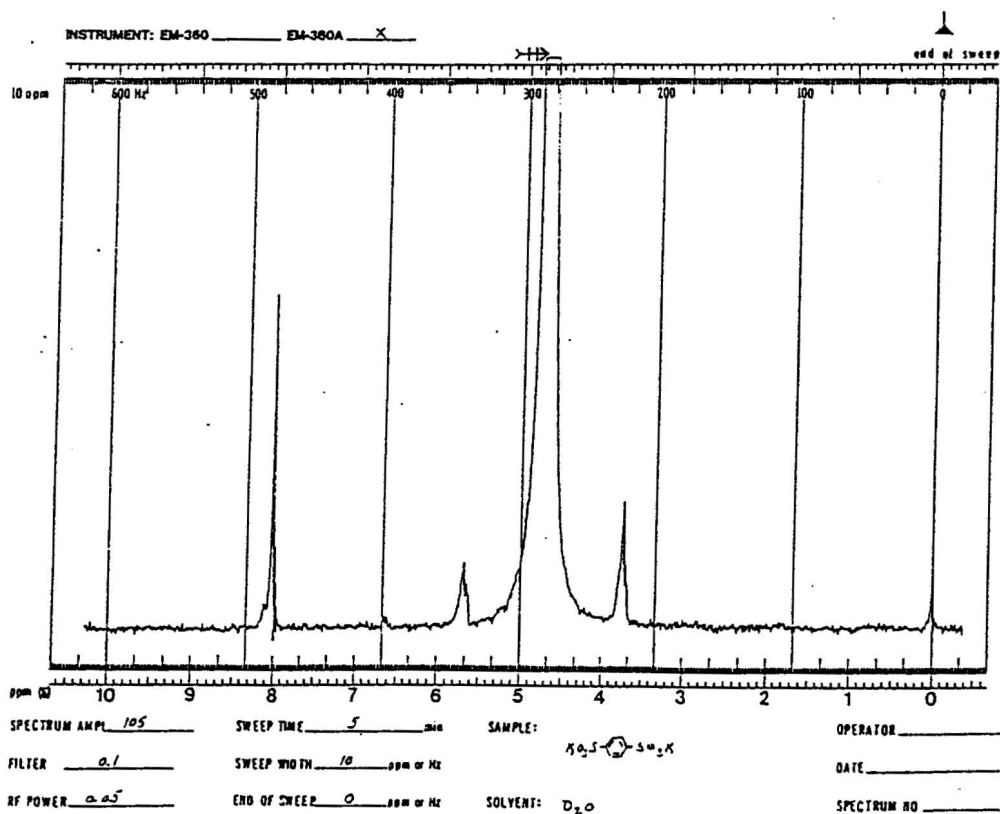
The  $^{23}\text{Na}^+$  spin-lattice relaxation measurements for aqueous sodium benzenesulfonate were determined as a function of concentration at  $20 \pm 1^\circ \text{C}$  by the inversion recovery technique (i.e.  $180^\circ$  pulse -  $\tau$  -  $90^\circ$  pulse - observe - long delay). The spectra were recorded unlocked at 79.348 MHz (7.047 T) on a Varian VXR-300 spectrometer, operating in the Fourier transform mode, using a high-resolution, solution-state, broadband probe and 10 mm o. d. sample tubes. The spectral width was 10,000 Hz, the acquisition time was 0.499 s (9984 data points), and spectra were transformed in 16 K data points. The  $90^\circ$  pulse width was 28  $\mu\text{s}$ , and the  $180^\circ$  pulse width was 56  $\mu\text{s}$ . Seven to eight  $\tau$  values were used, and the long relaxation delay was equal to four times  $T_1$ .

The  $^7\text{Li}^+$  spin-lattice relaxation measurements for aqueous lithium benzenesulfonate were determined as a function of concentration at  $20 \pm 1^\circ \text{C}$  by the inversion recovery technique. All samples were deoxygenated by "ultrasonication" and purging with argon. The spectra were recorded unlocked at 116.589 MHz (7.047 T) on a Varian VXR-300 spectrometer, operating in the Fourier transform mode, using a high-resolution, solution-state, broadband probe and 10 mm o. d. sample tubes. The

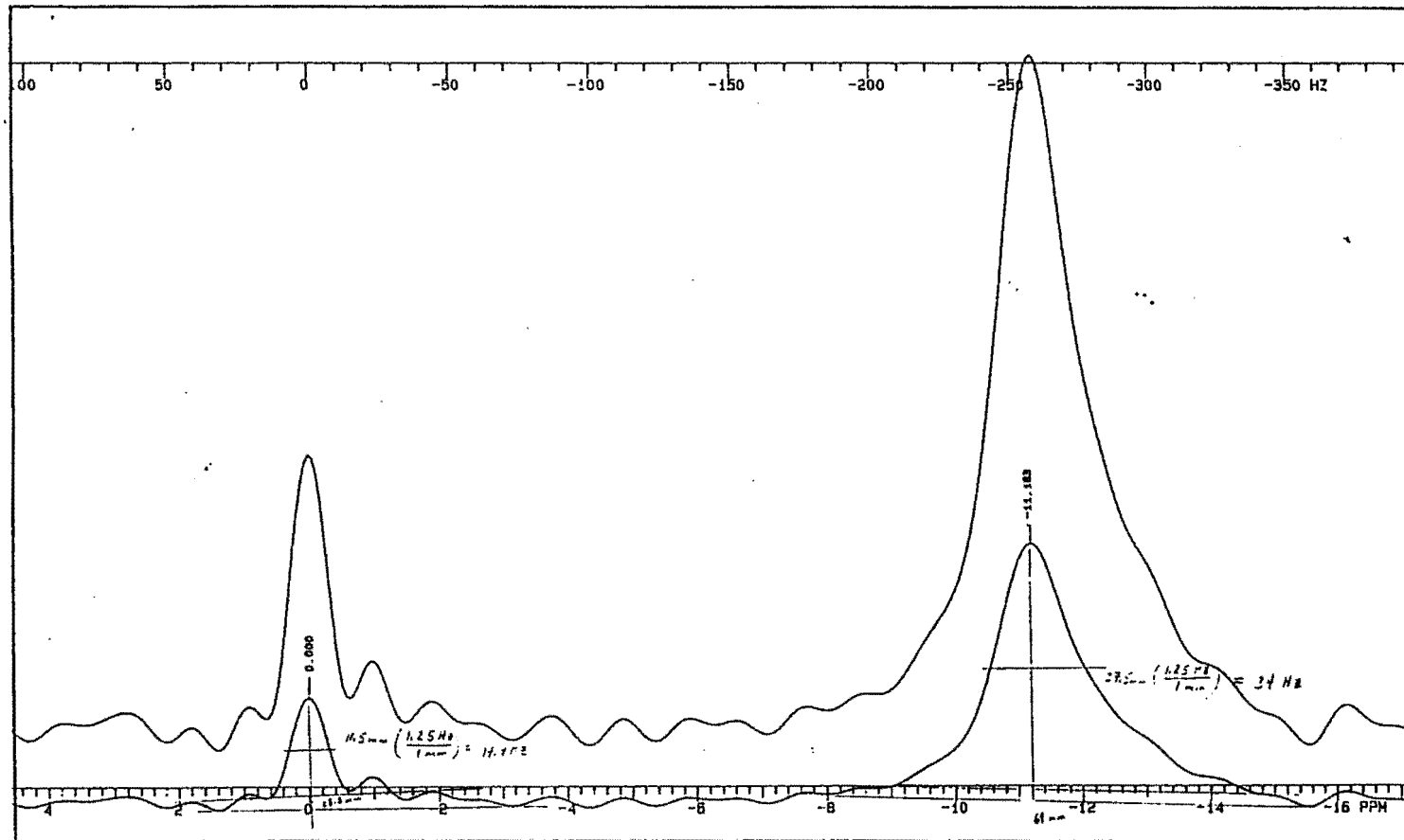
spectral width was 10,000 Hz, the acquisition time was 3.002 s (60,032 data points), and spectra were transformed in 64 K data points. The 90° pulse width was 42  $\mu$ s, and the 180° pulse width was 84  $\mu$ s. Seven to eight tau values were used, and the long relaxation delay was equal to four times  $T_1$ .

The  $^{13}\text{C}$  spin-lattice relaxation measurements for aqueous lithium benzenesulfonate were determined as a function of concentration at  $20 \pm 1^\circ \text{C}$  by the inversion recovery technique. All samples were deoxygenated by "ultrasonication" and purging with argon. The natural abundance spectra were recorded unlocked at 75.431 MHz (7.047 T) on a Varian VXR-300 spectrometer, operating in the Fourier transform mode, using a high-resolution, solution-state, broadband probe and 10 mm o. d. sample tubes. The spectral width was 5,000 Hz, the acquisition time was 1.638 s (16,384 data points), and spectra were transformed in 64 K data points. The 90° pulse width was 45  $\mu$ s, and the 180° pulse width was 90  $\mu$ s. Seven to eight tau values were used, and the long relaxation delay was equal to four times  $T_1$ .

**SELECTED SPECTRA**

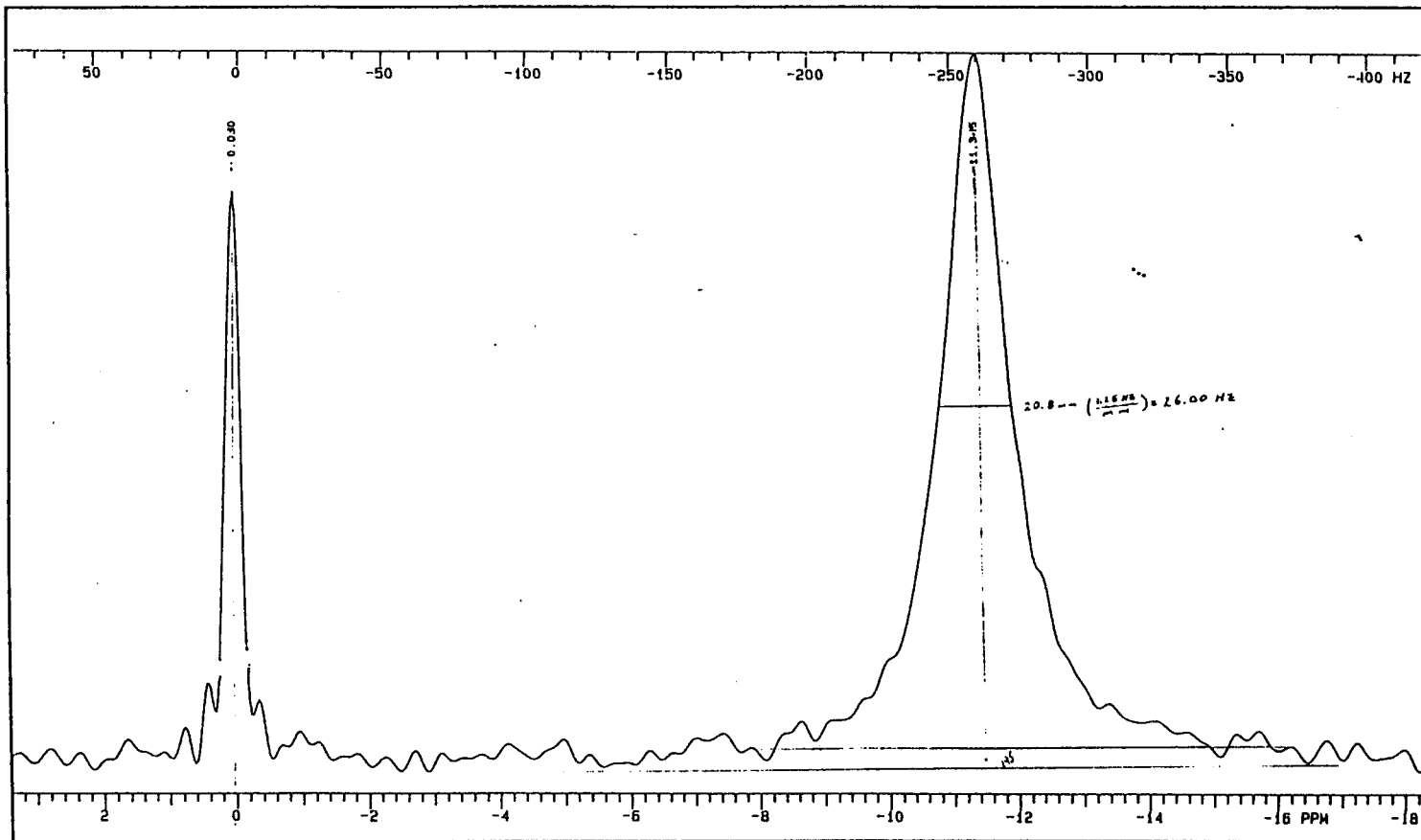
IR Spectrum of *para*-Benzenedisulfonic Acid Dipotassium Salt $^1\text{H}$  NMR Spectrum of *para*-Benzenedisulfonic Acid Dipotassium Salt

$^{33}\text{S}$  NMR Spectrum of 1.78 M Aqueous Benzenesulfonic Acid And Aqueous Ammonium Sulfate Reference At 20° C

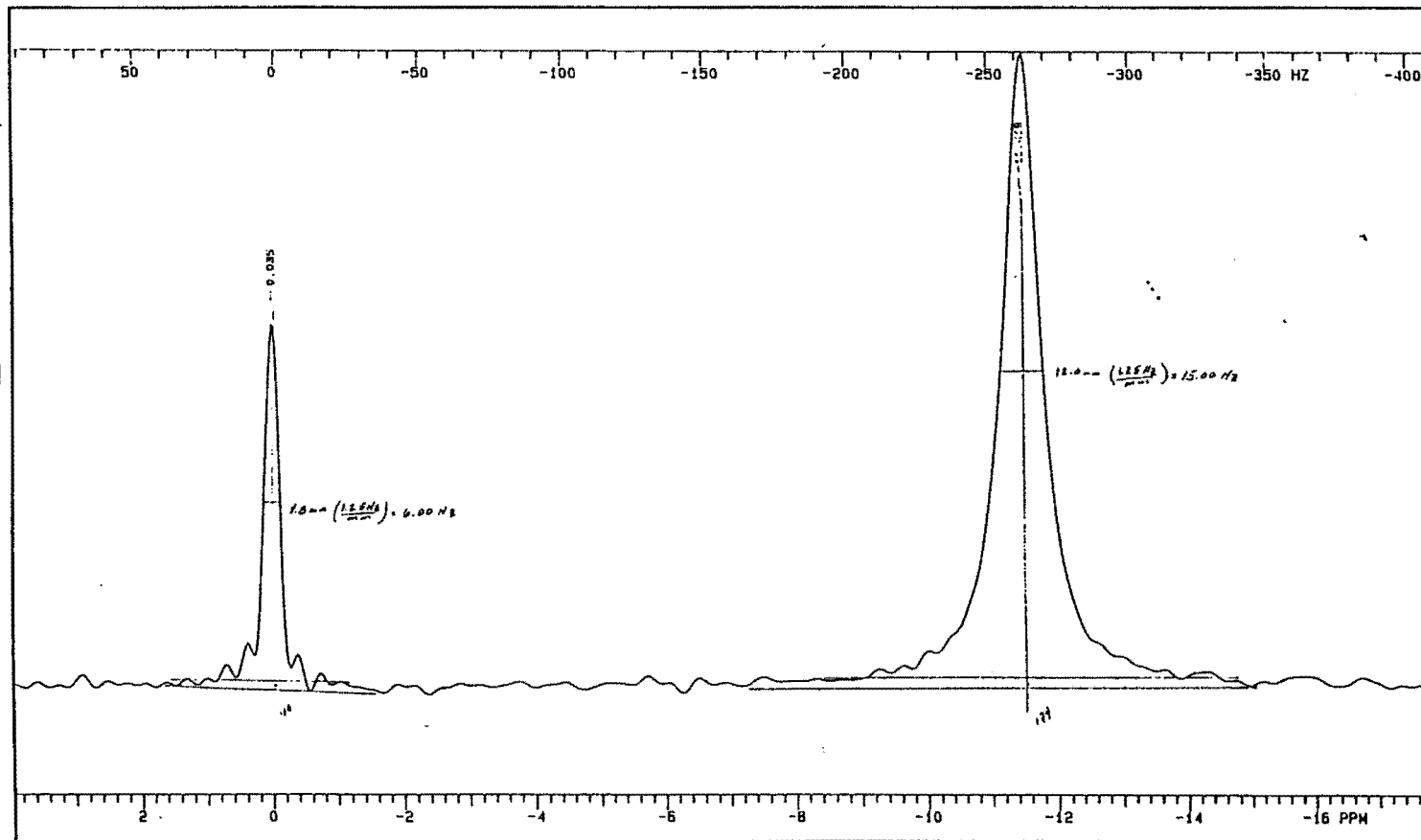




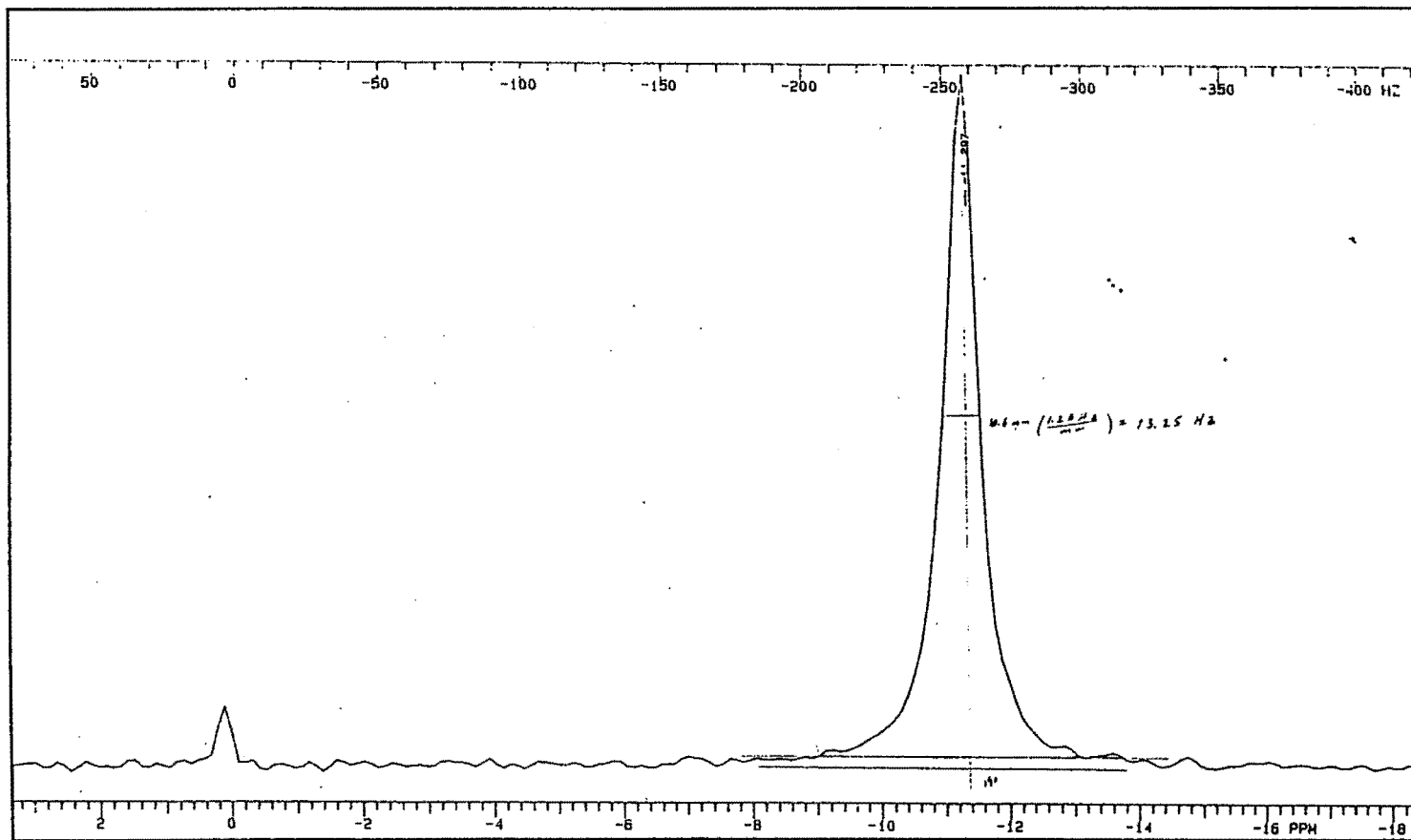
$^{33}\text{S}$  NMR Spectrum of 2.00 M Aqueous Lithium Benzenesulfonate And Aqueous Ammonium Sulfate Reference At 20° C



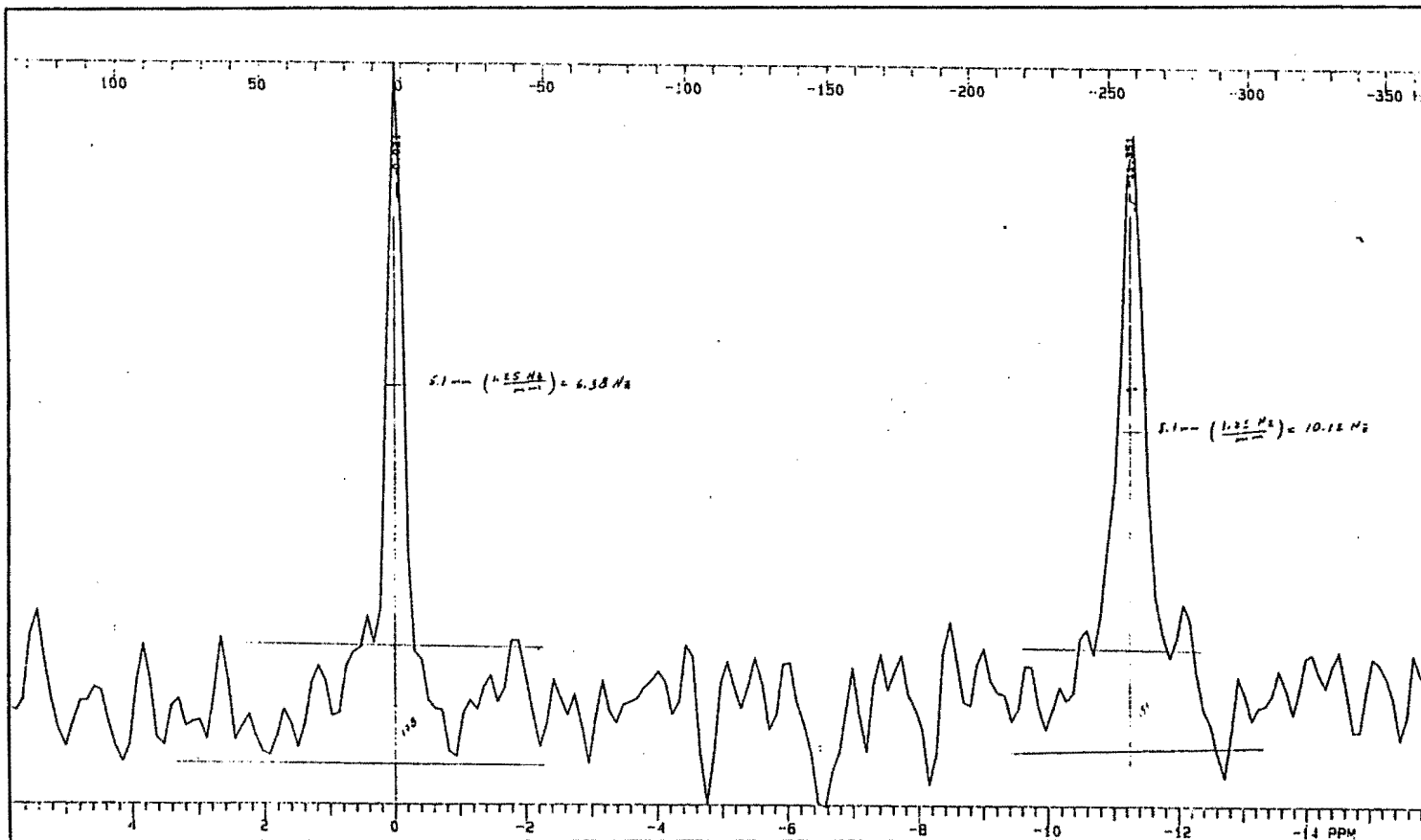
$^{33}\text{S}$  NMR Spectrum of 2.01 M Aqueous Potassium Benzenesulfonate And Aqueous Ammonium Sulfate Reference At 20° C



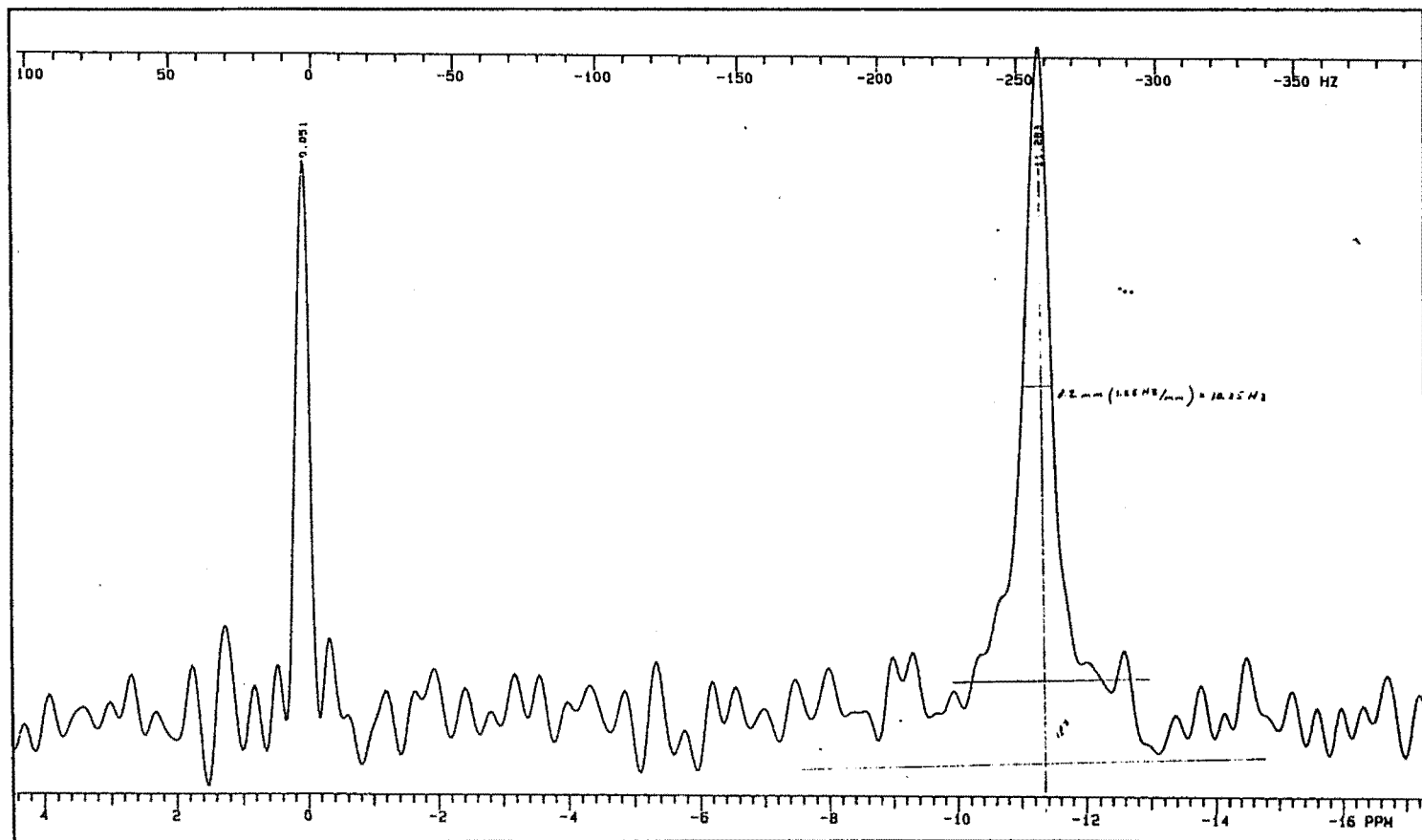
$^{33}\text{S}$  NMR Spectrum of 0.201 M Aqueous Magnesium Benzenesulfonate And Aqueous Ammonium Sulfate Reference At 20° C



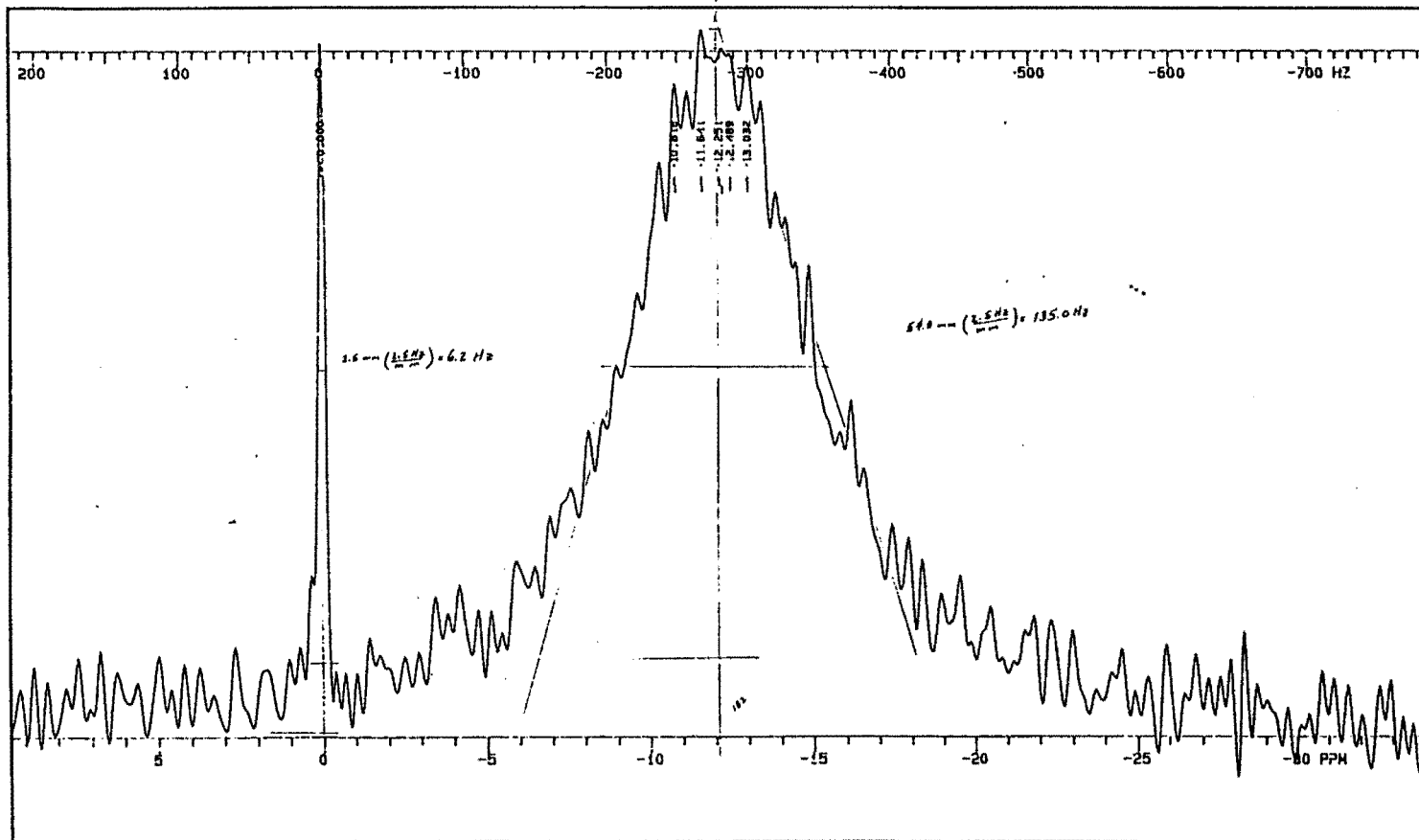
$^{33}\text{S}$  NMR spectrum of 0.010 M Aqueous Magnesium Benzenesulfonate And Aqueous Ammonium Sulfate Reference At 20° C



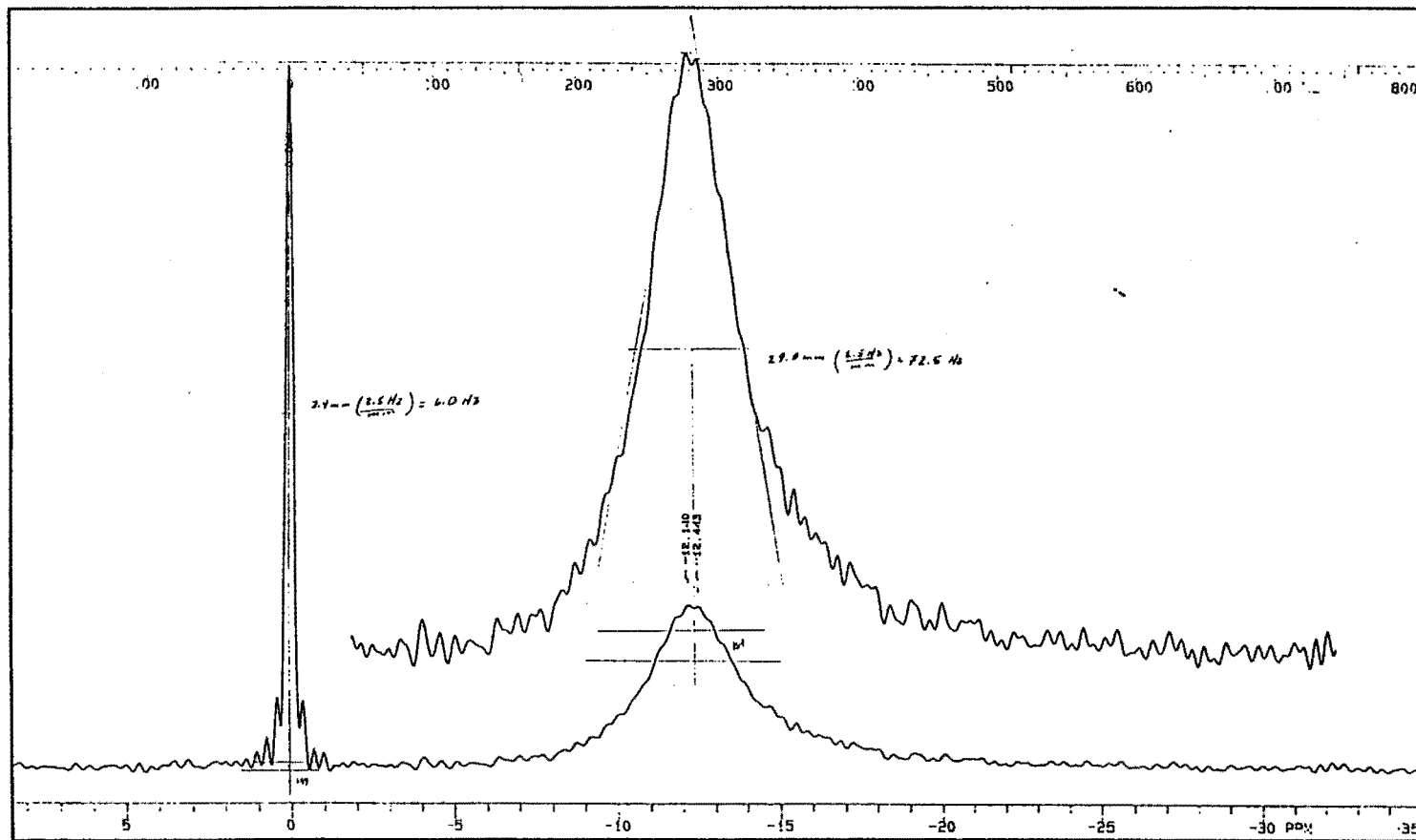
$^{33}\text{S}$  NMR Spectrum of 0.025 M Aqueous Lithium Benzenesulfonate And Aqueous Ammonium Sulfate Reference At 20° C



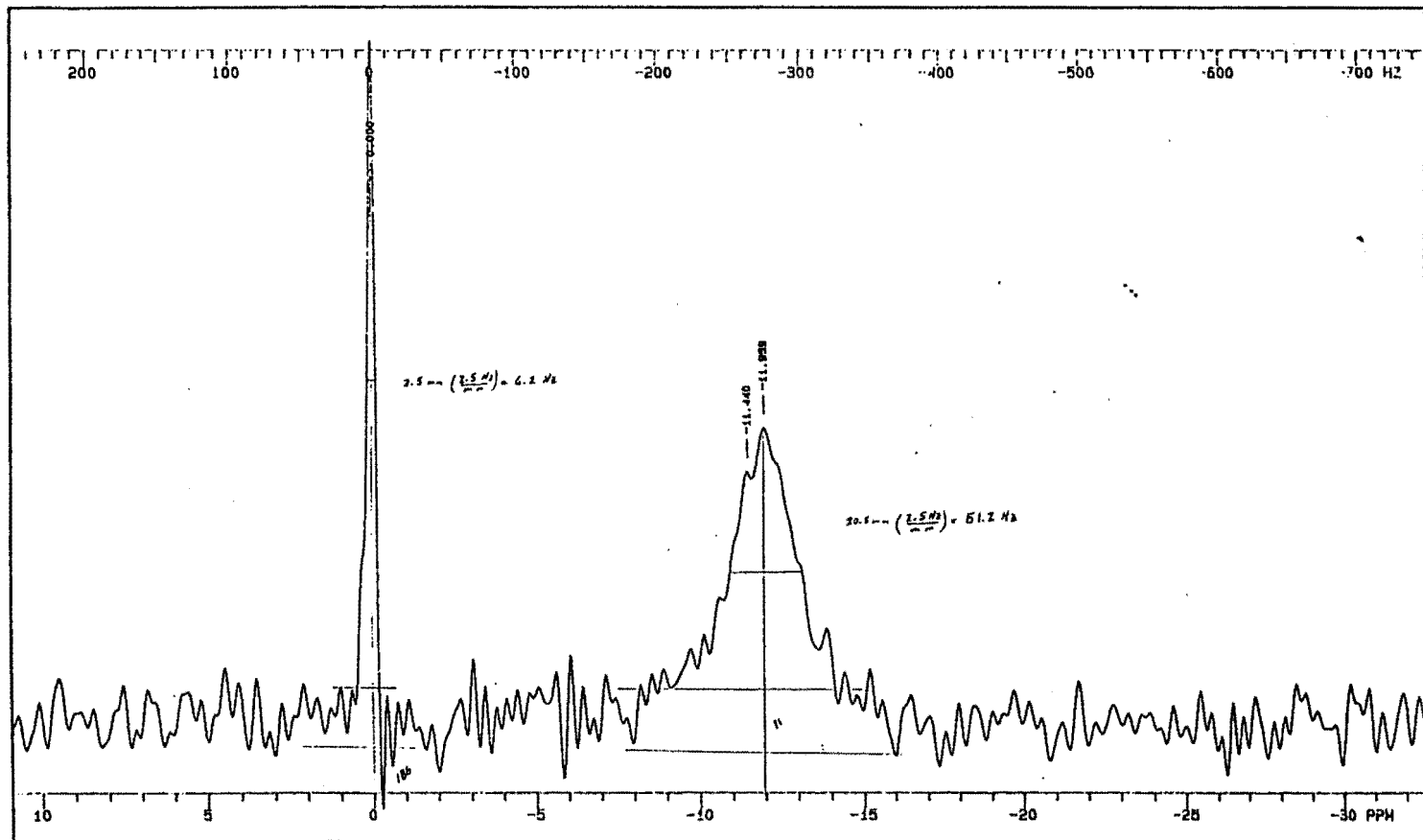
$^{33}\text{S}$  NMR Spectrum of 1.82 M Benzenesulfonic Acid In Formamide And Aqueous Ammonium Sulfate Reference At 20° C



$^{33}\text{S}$  NMR Spectrum of 0.81 M Sodium Benzenesulfonate In Formamide And Aqueous Ammonium Sulfate Reference At 20° C

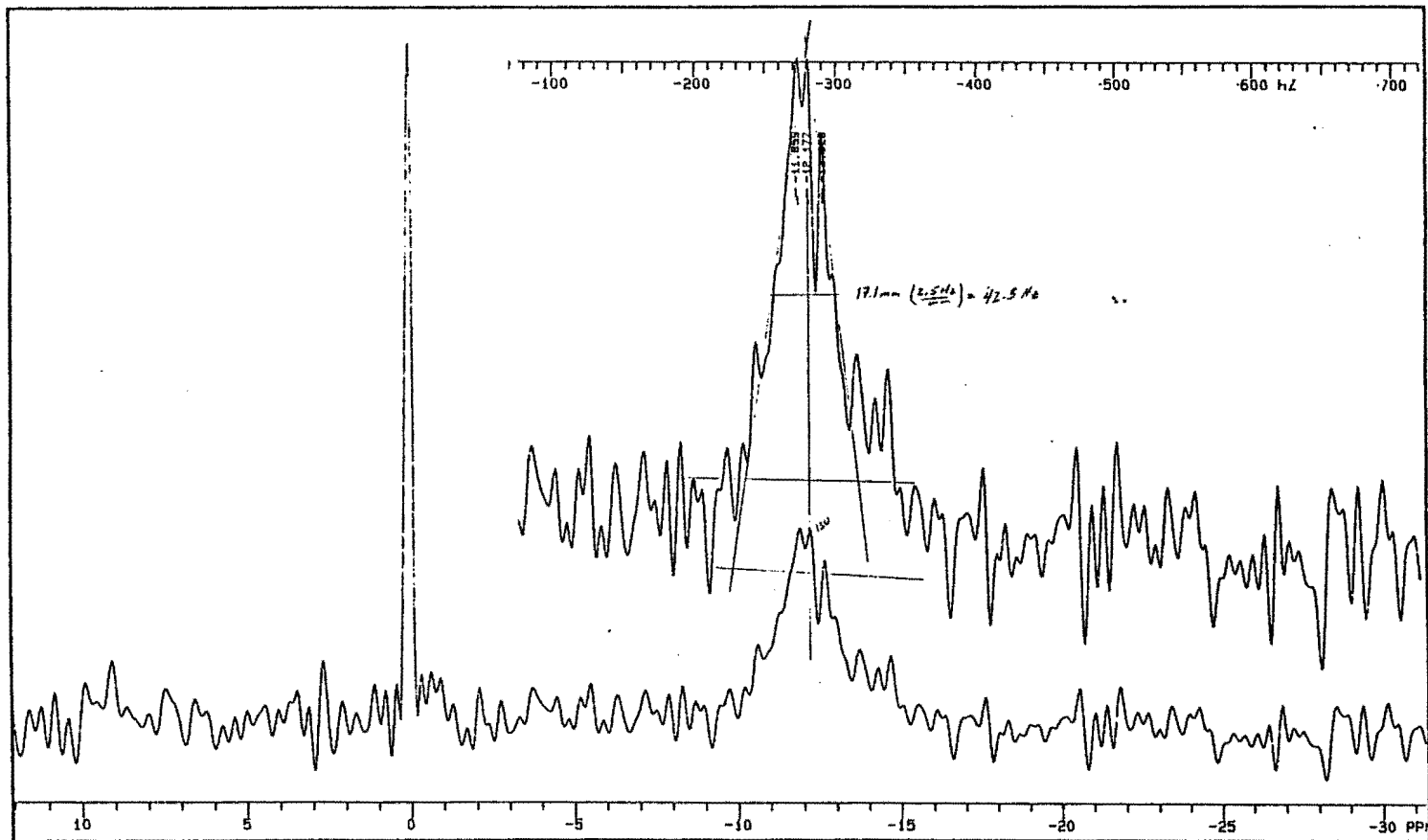


$^{33}\text{S}$  NMR Spectrum of 0.11 M Benzenesulfonic Acid In Formamide And Aqueous Ammonium Sulfate Reference At 20° C

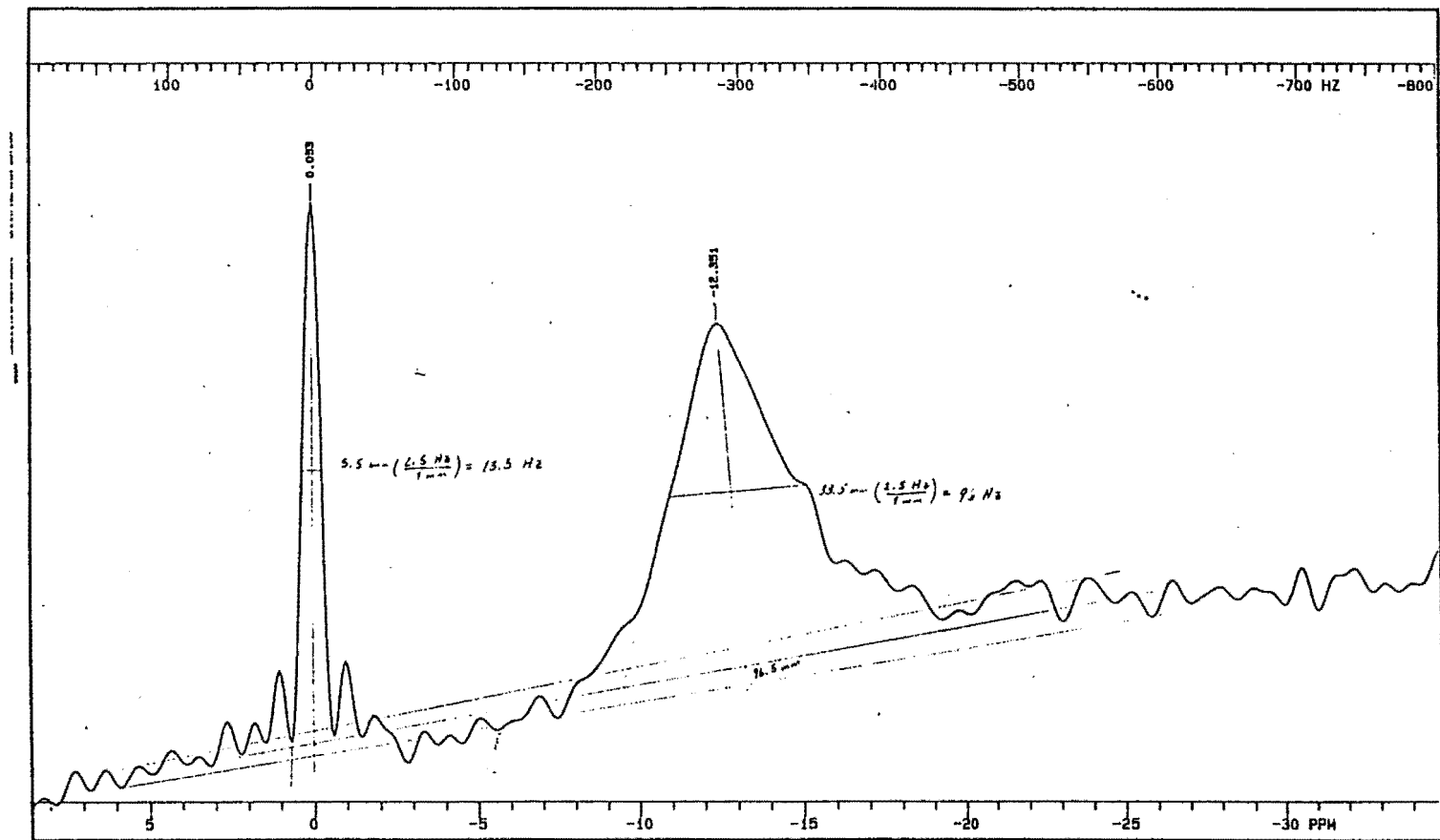




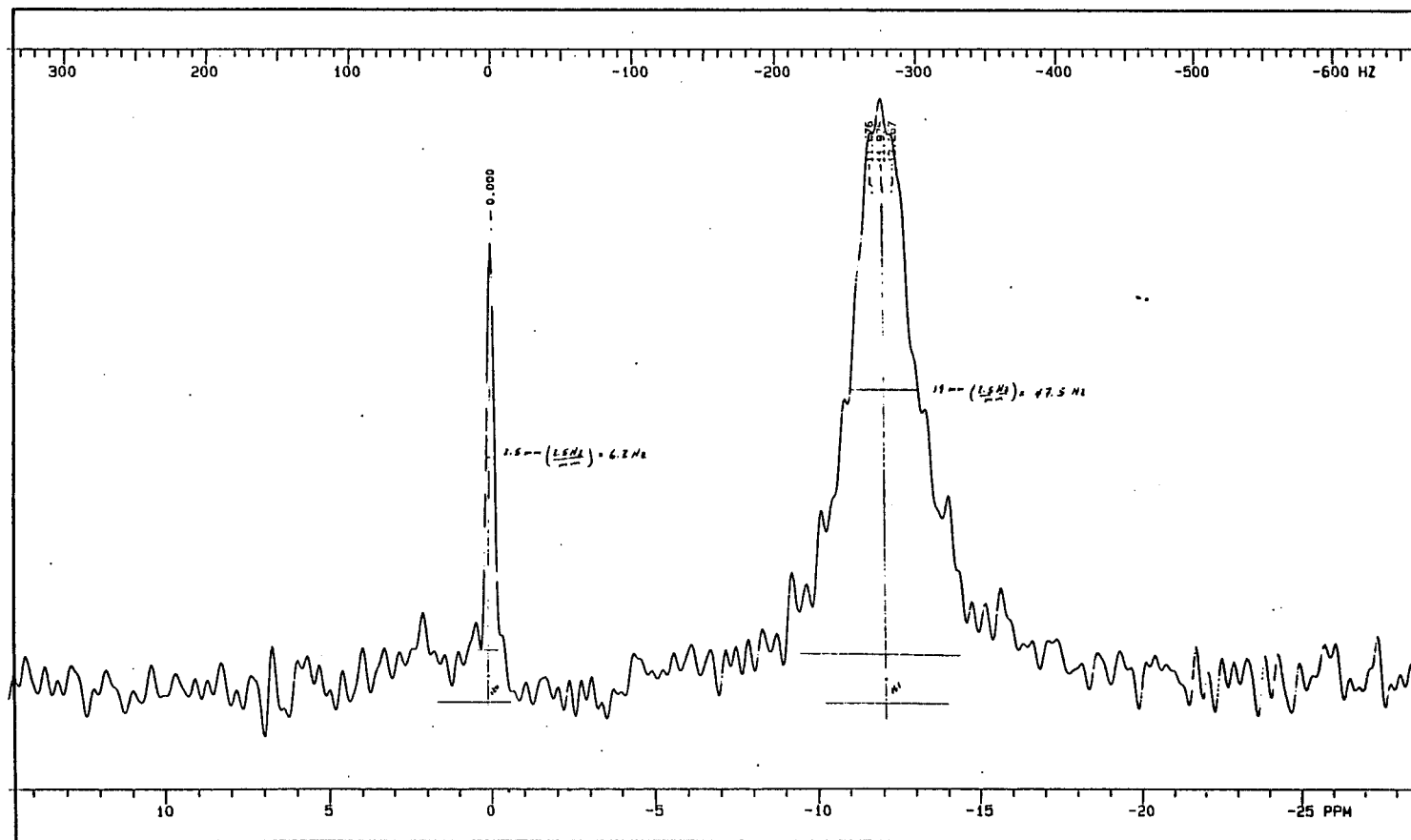
$^{33}\text{S}$  NMR Spectrum of 0.10 M Sodium Benzenesulfonate In Formamide And Aqueous Ammonium Sulfate Reference At 20° C



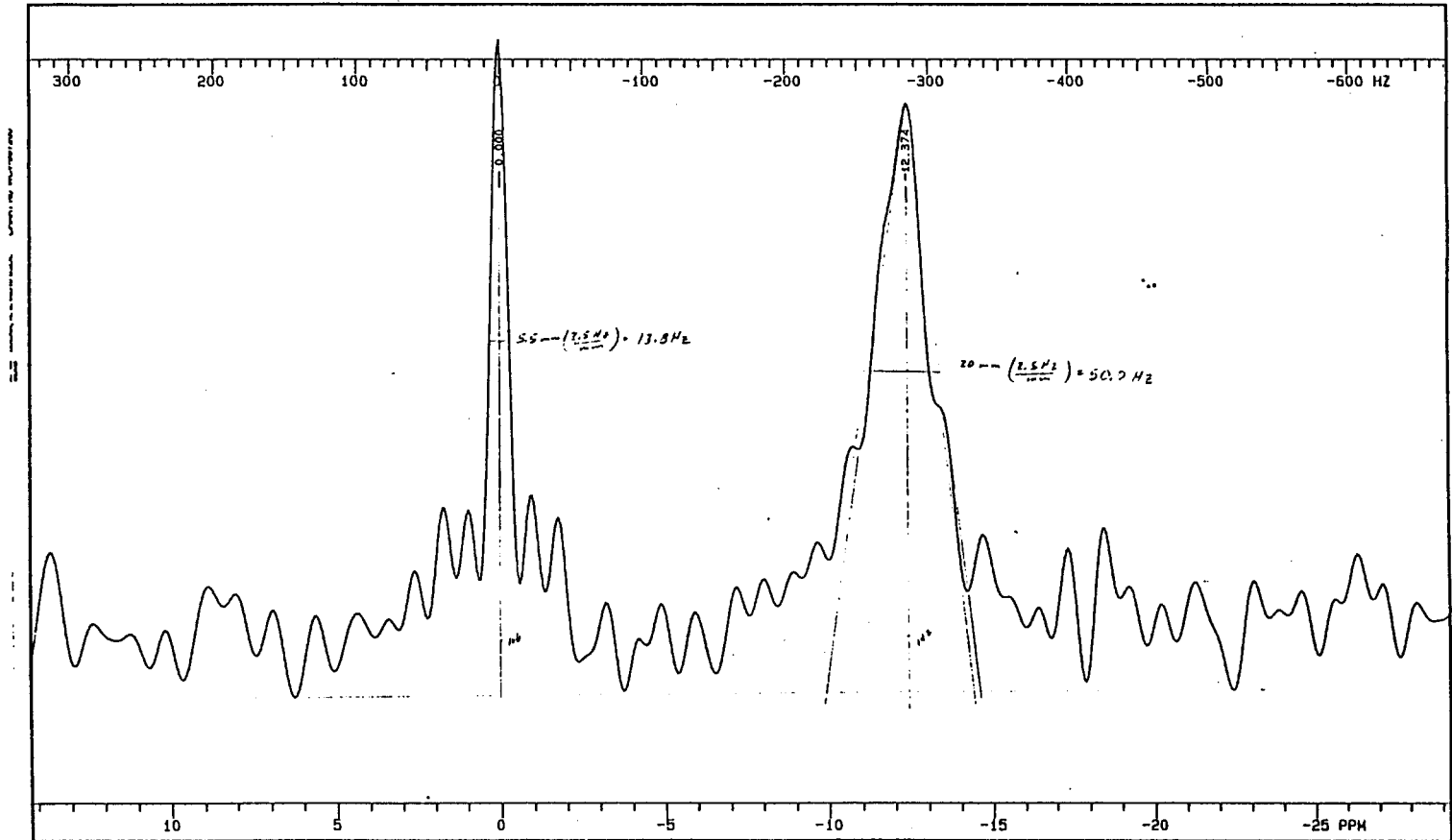
$^{33}\text{S}$  NMR Spectrum of 2.02 M Benzenesulfonic Acid In Formamide- $\text{H}_2\text{O}$  And Aqueous Ammonium Sulfate Reference At 20° C



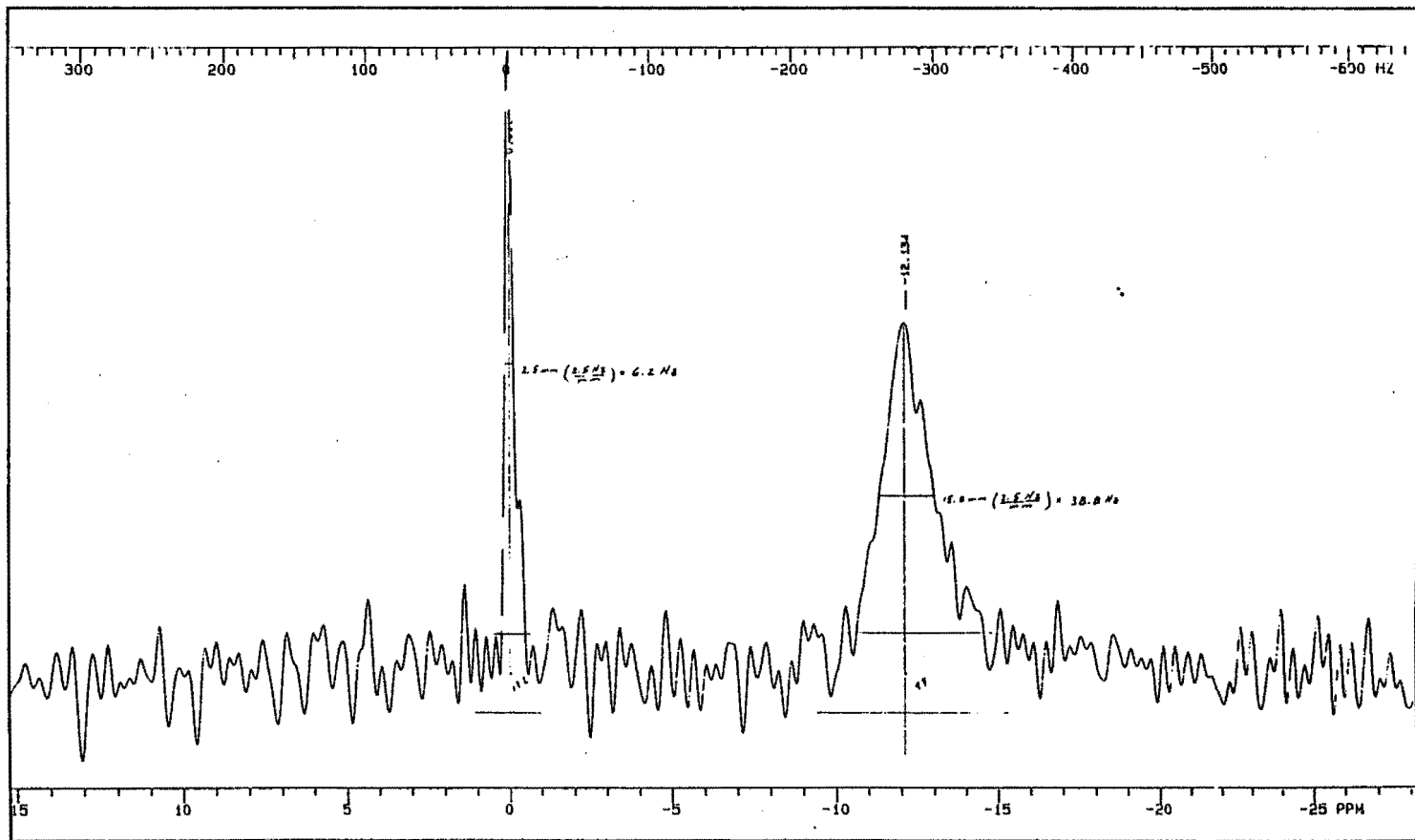
$^{33}\text{S}$  NMR Spectrum of 0.72 M Sodium Benzenesulfonate In Formamide- $\text{H}_2\text{O}$  And  
Aqueous Ammonium Sulfate Reference At  $20^\circ\text{C}$



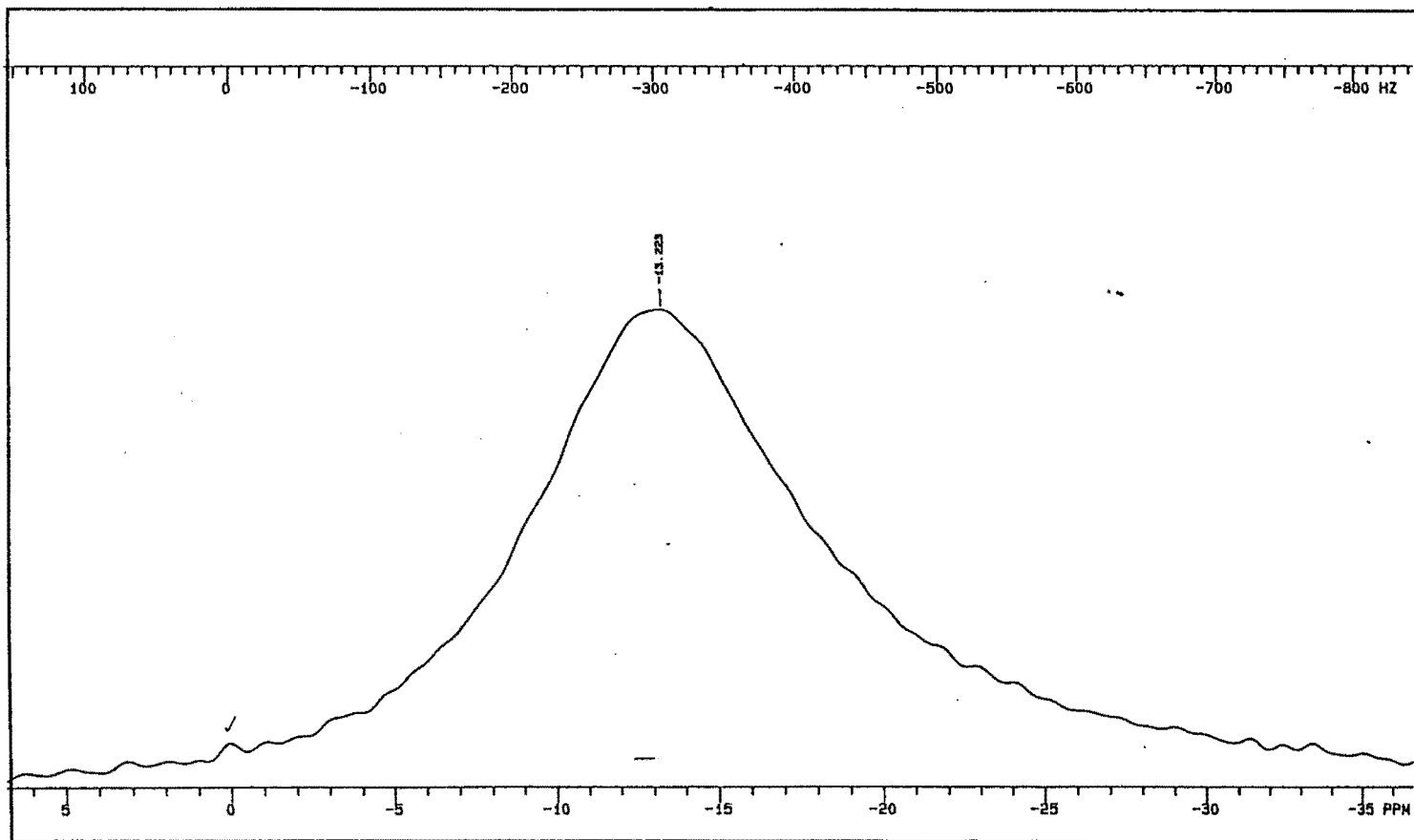
$^{33}\text{S}$  NMR Spectrum of 0.13 M Benzenesulfonic Acid In Formamide- $\text{H}_2\text{O}$  And  
Aqueous Ammonium Sulfate Reference At  $20^\circ\text{C}$



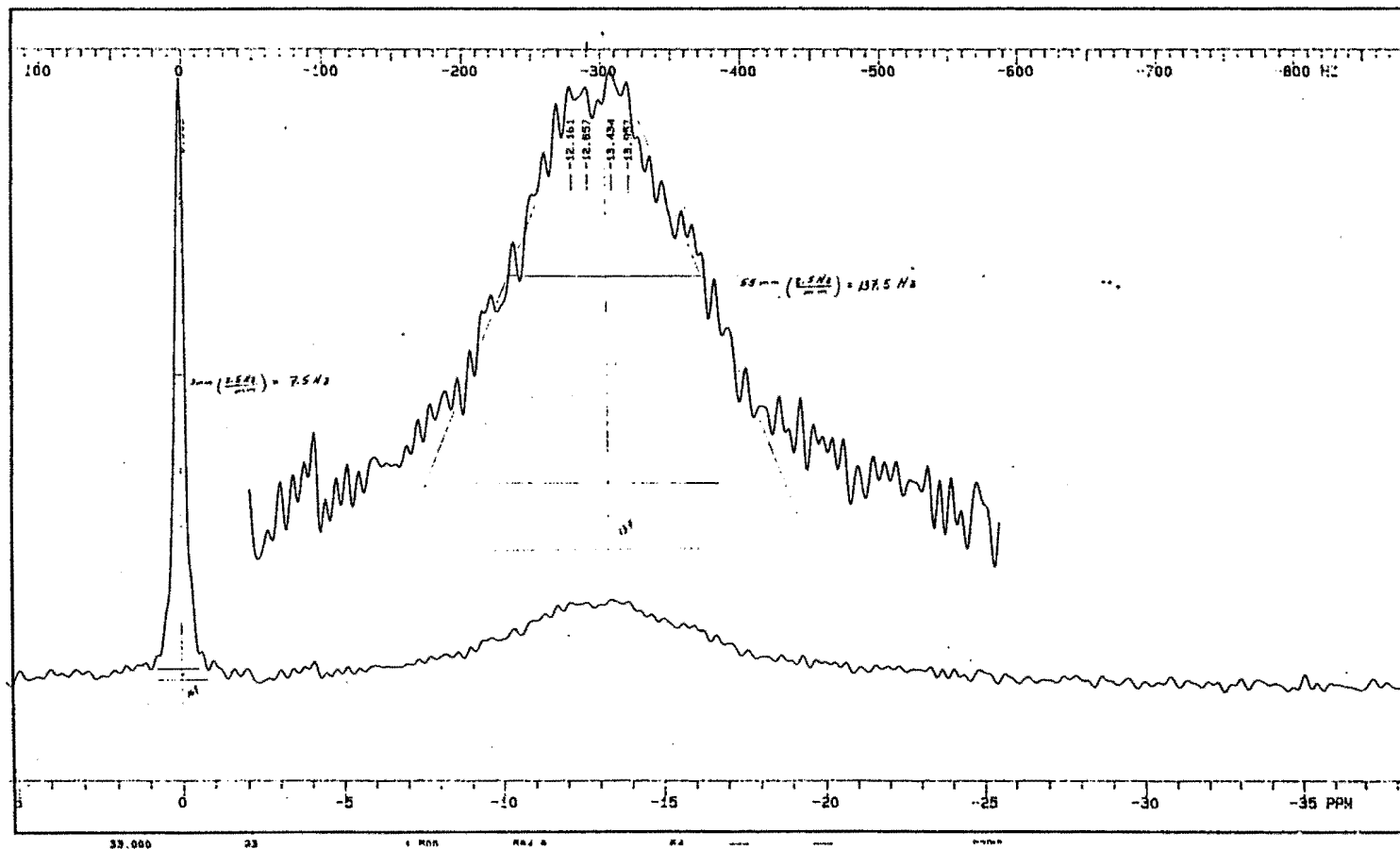
$^{33}\text{S}$  NMR Spectrum of 0.090 M Sodium Benzenesulfonate In Formamide- $\text{H}_2\text{O}$  And  
Aqueous Ammonium Sulfate Reference At  $20^\circ\text{C}$



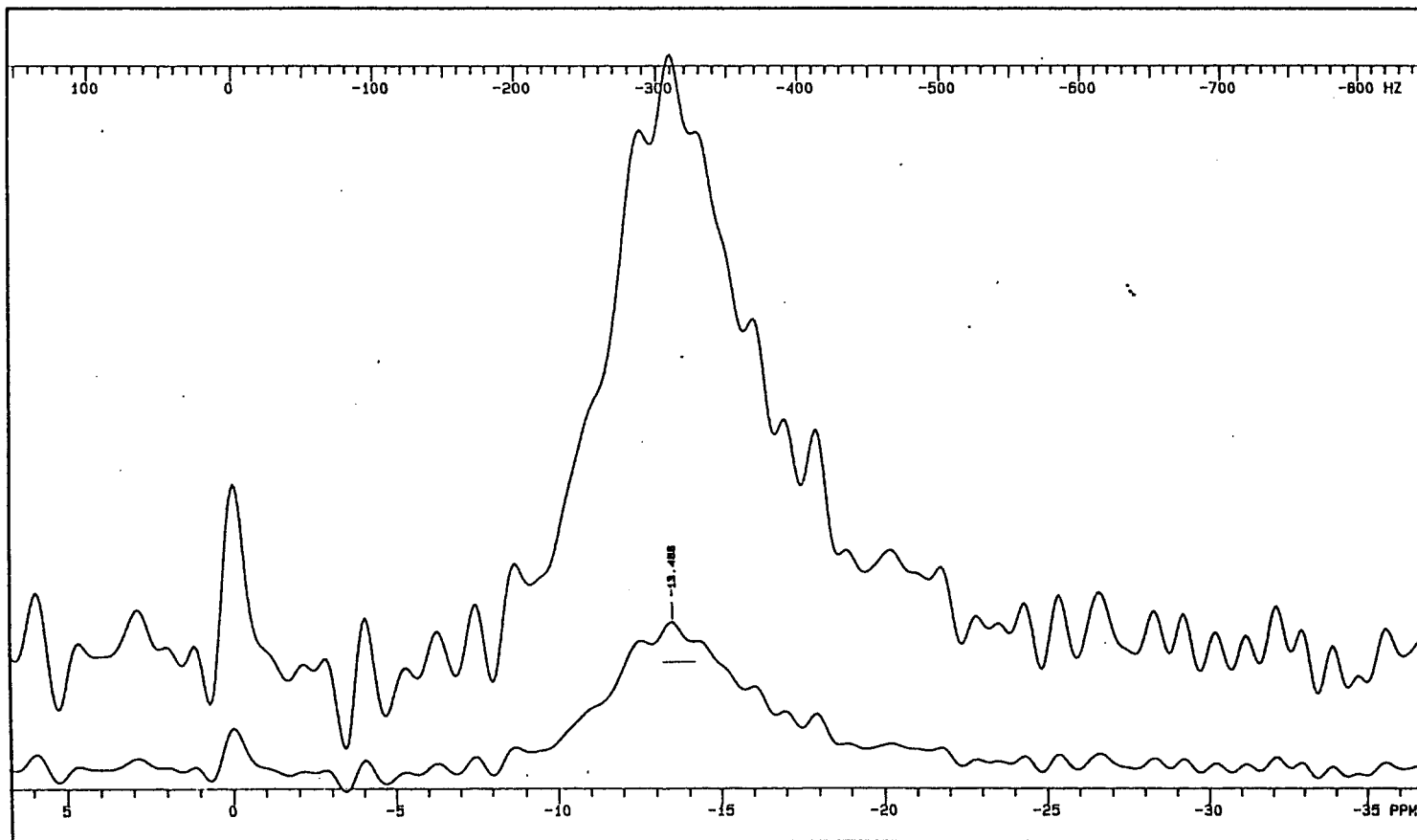
$^{33}\text{S}$  NMR Spectrum of 2.25 M Benzenesulfonic Acid In N-Methylformamide And  
Aqueous Ammonium Sulfate Reference At 20° C



$^{33}\text{S}$  NMR Spectrum of 0.90 M Lithium Benzenesulfonate In N-Methylformamide And  
Aqueous Ammonium Sulfate Reference At 20° C

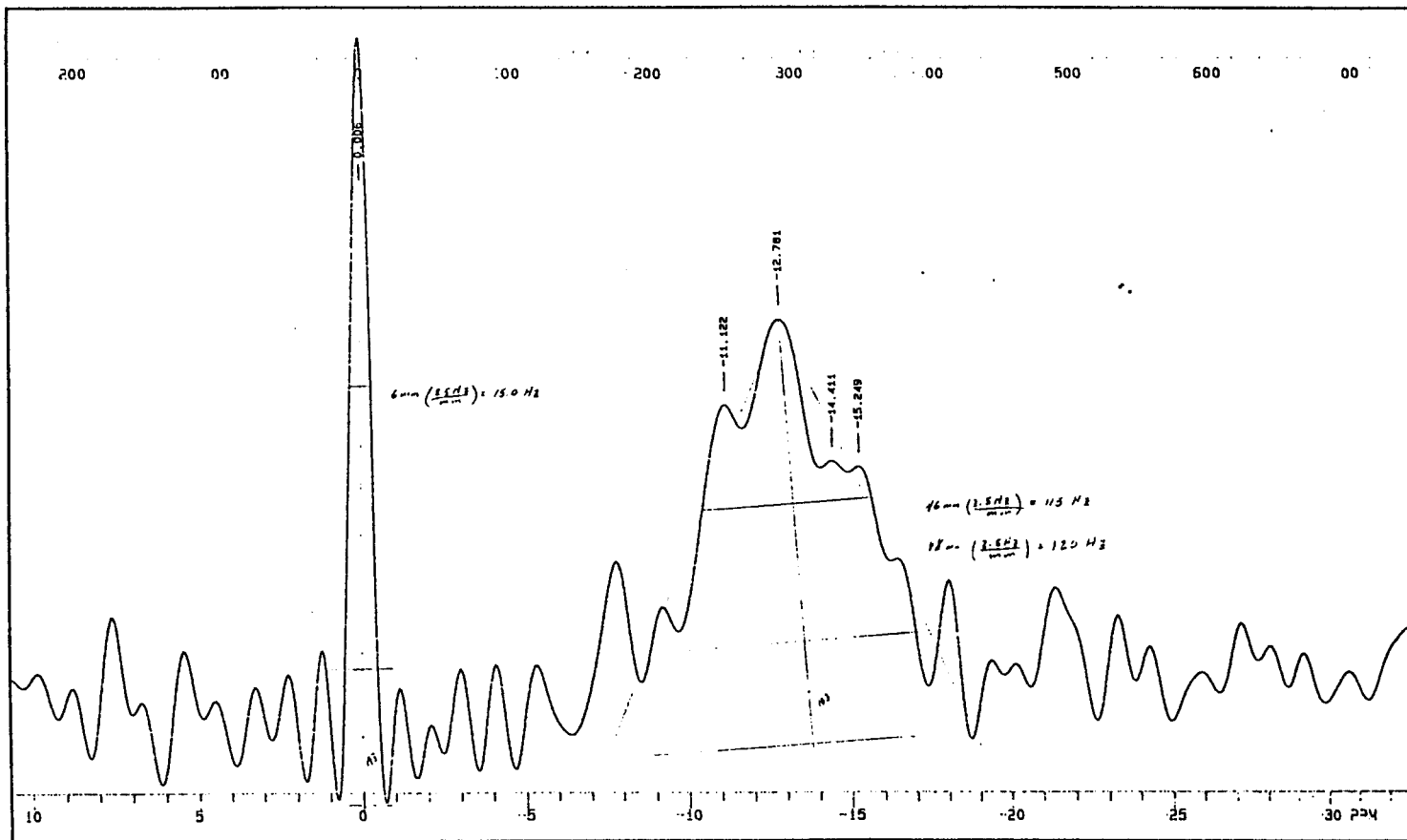


$^{33}\text{S}$  NMR Spectrum of 0.14 M Benzenesulfonic Acid In N-Methylformamide And  
Aqueous Ammonium Sulfate Reference At 20° C

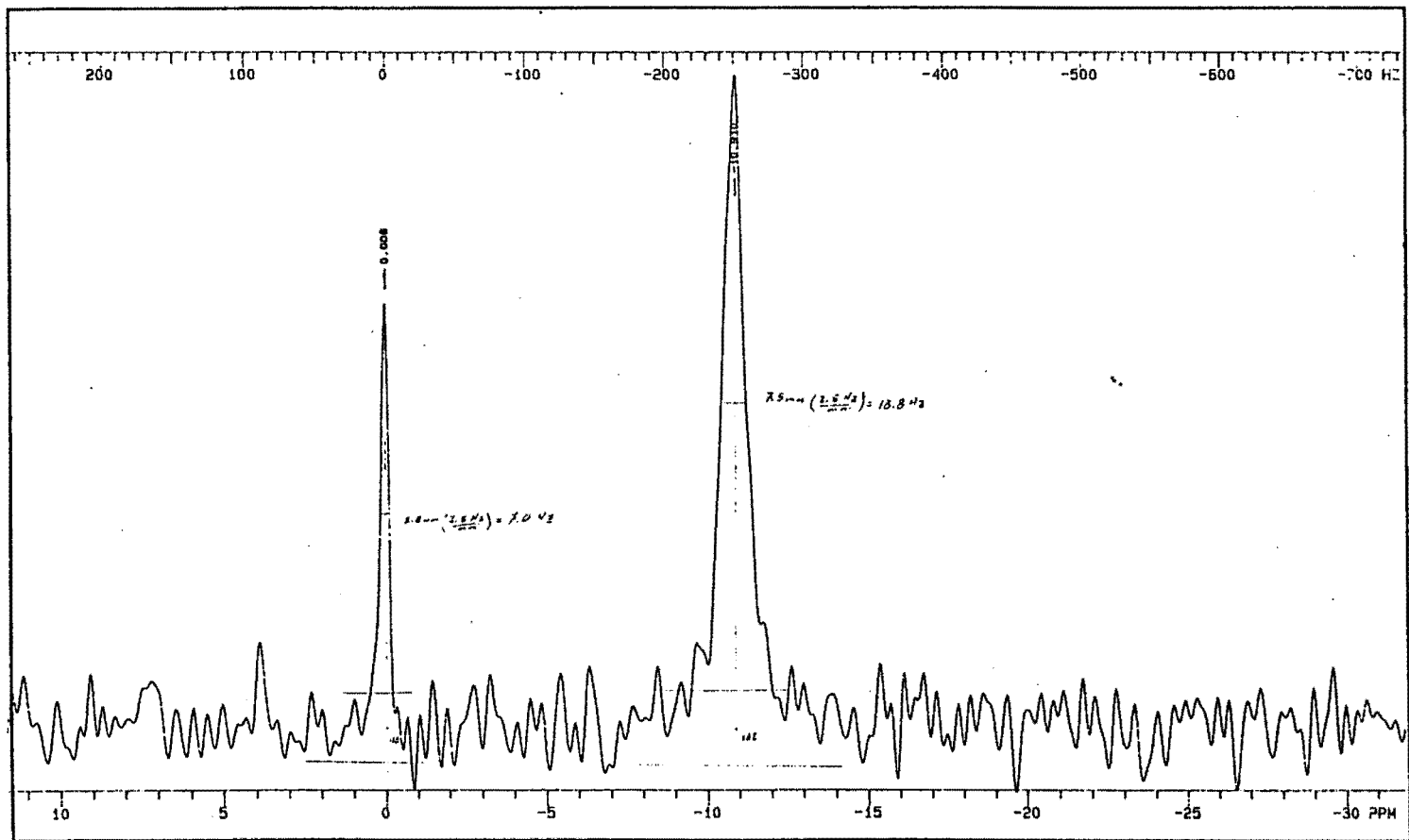




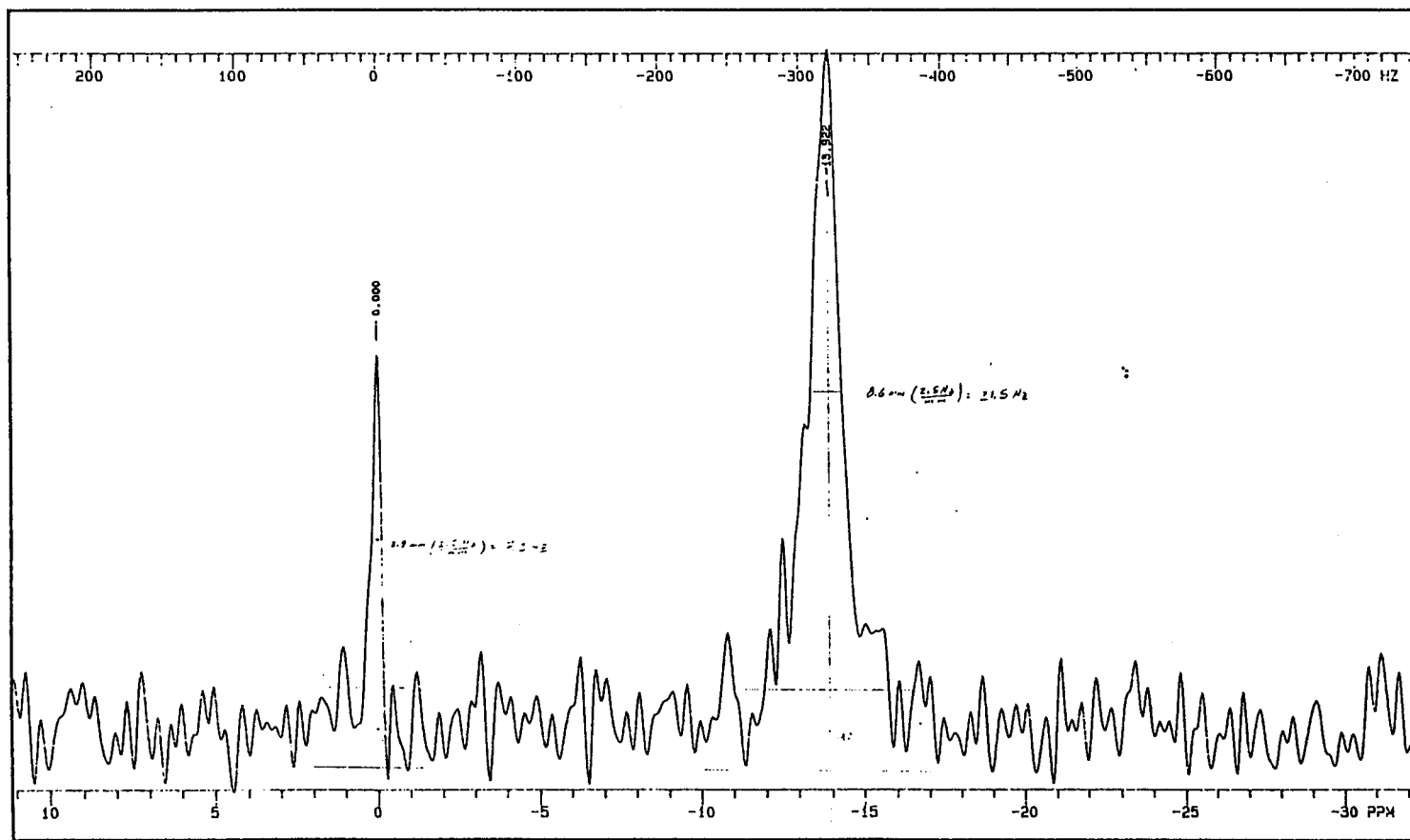
$^{33}\text{S}$  NMR Spectrum of 0.12 M Lithium Benzenesulfonate In N-Methylformamide And  
Aqueous Ammonium Sulfate Reference At 20° C



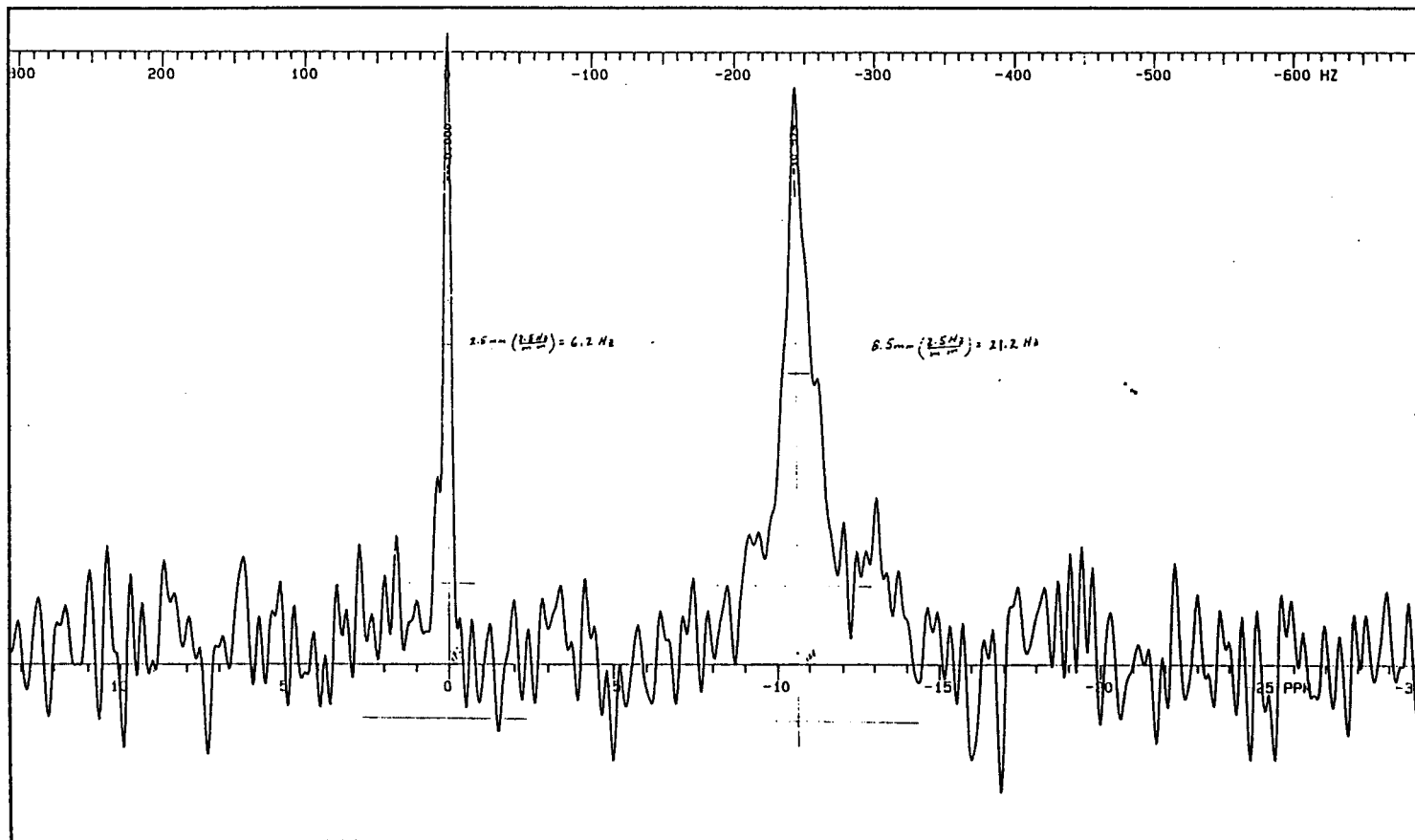
$^{33}\text{S}$  NMR Spectrum of Aqueous meta-Methylbenzenesulfonic Acid And  
Aqueous Ammonium Sulfate Reference At 20° C



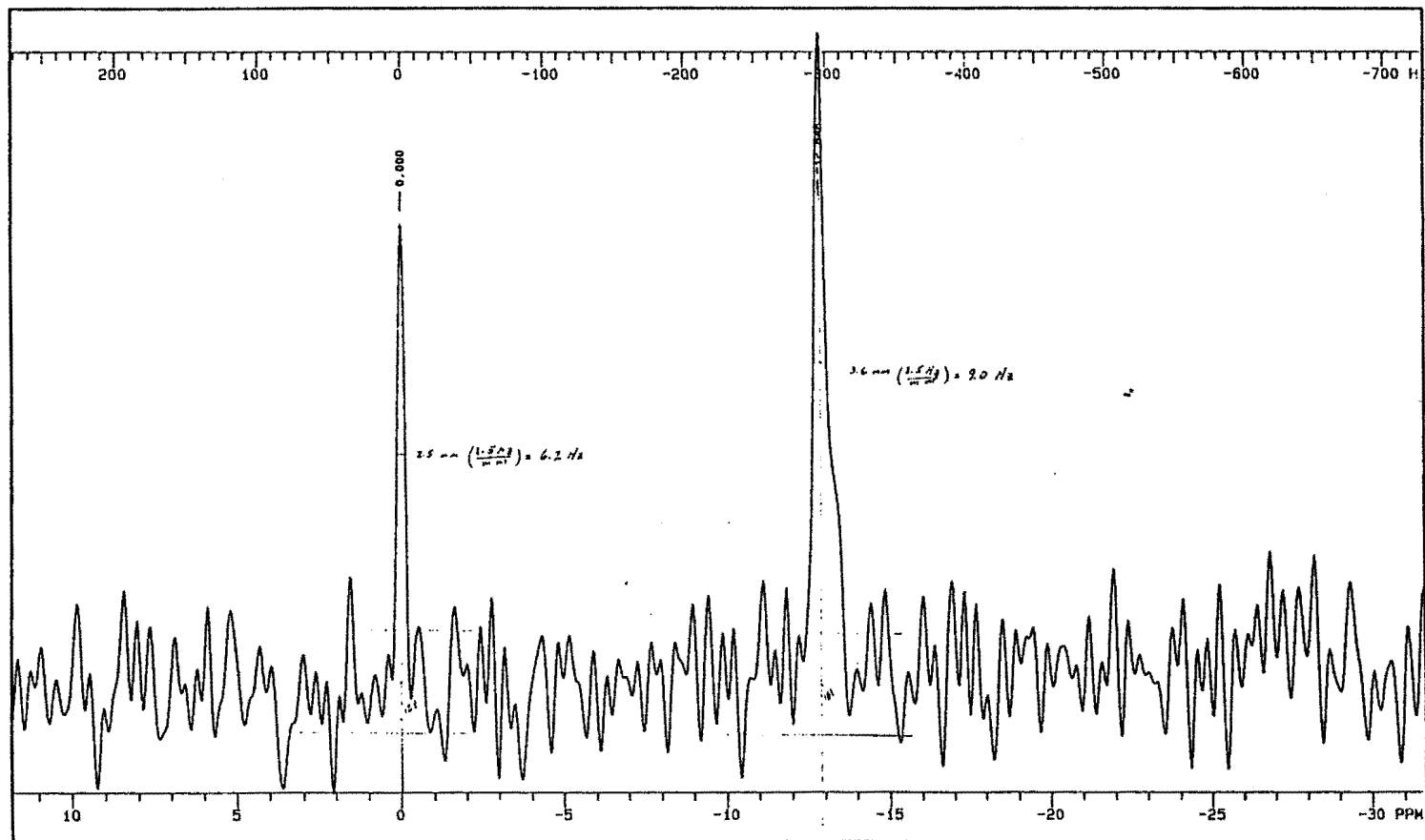
$^{33}\text{S}$  NMR Spectrum of Aqueous meta-Benzenedisulfonic Acid Disodium Salt And  
Aqueous Ammonium Sulfate Reference At 20° C



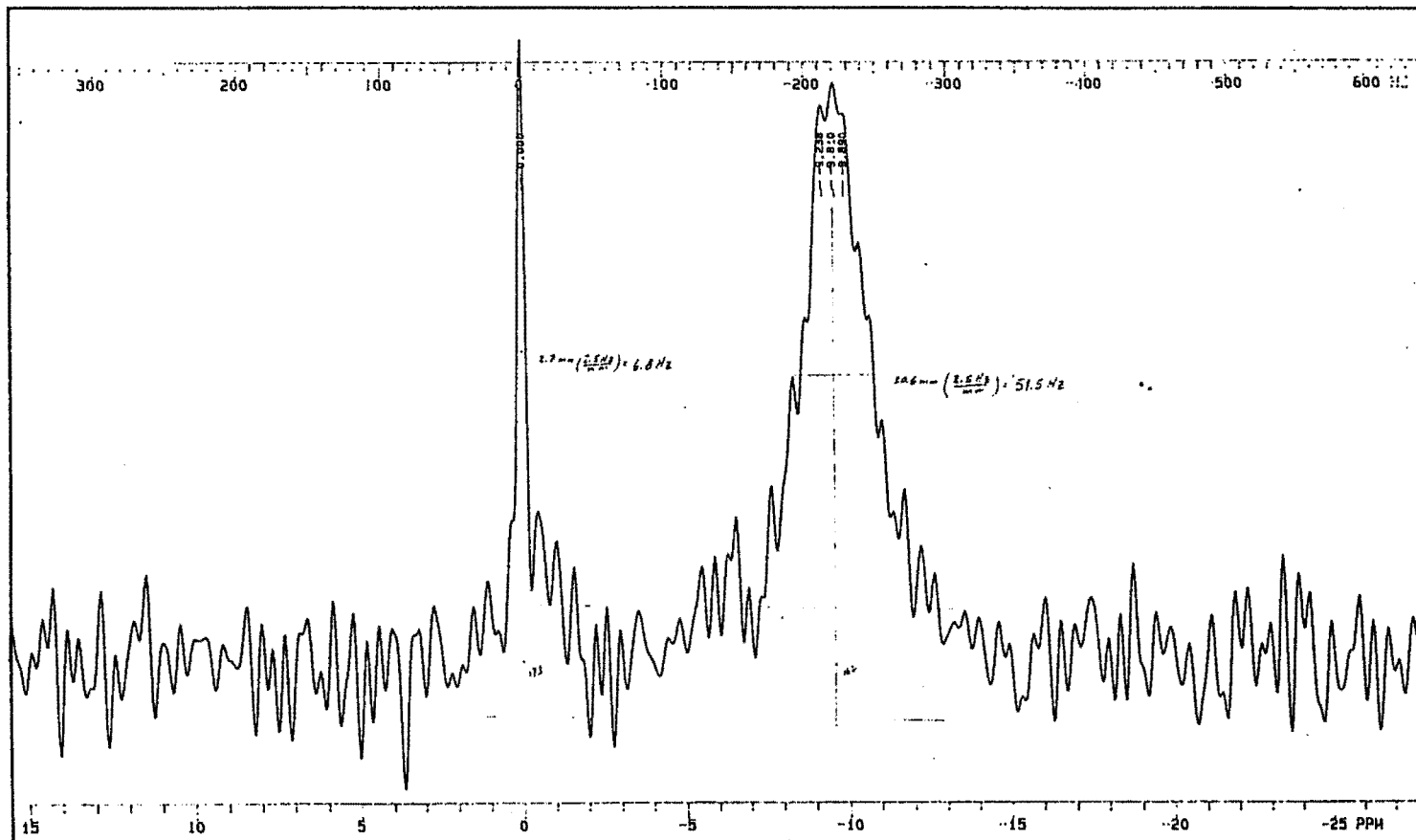
$^{33}\text{S}$  NMR Spectrum of Aqueous para-Methylbenzenesulfonic Acid And  
Aqueous Ammonium Sulfate Reference At 20° C



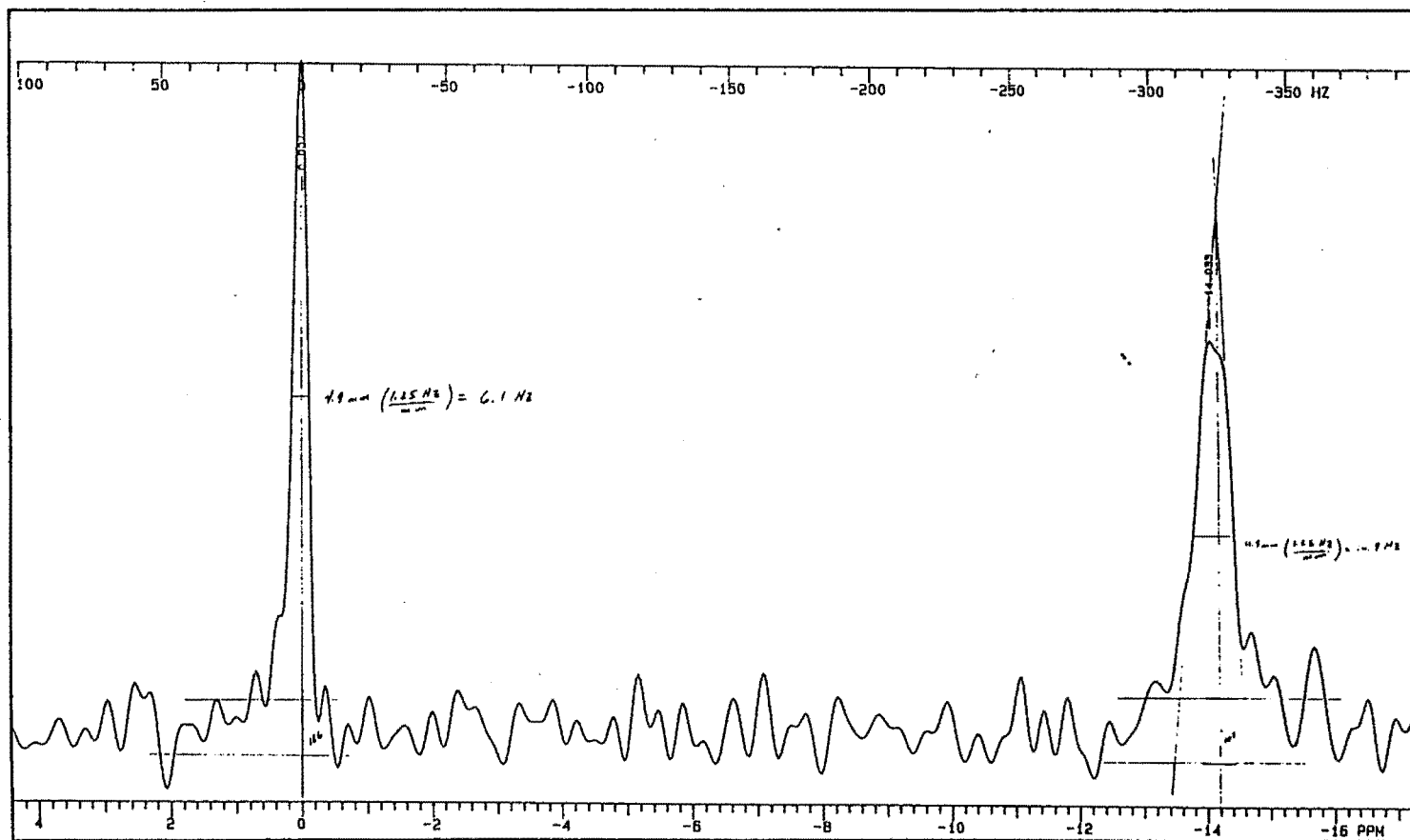
$^{33}\text{S}$  NMR Spectrum of Aqueous para-Bromobenzenesulfonic Acid And  
Aqueous Ammonium Sulfate Reference At 20° C



$^{33}\text{S}$  NMR Spectrum of Aqueous para-Aminobenzenesulfonic Acid Potassium Salt And  
Aqueous Ammonium Sulfate Reference At 20° C

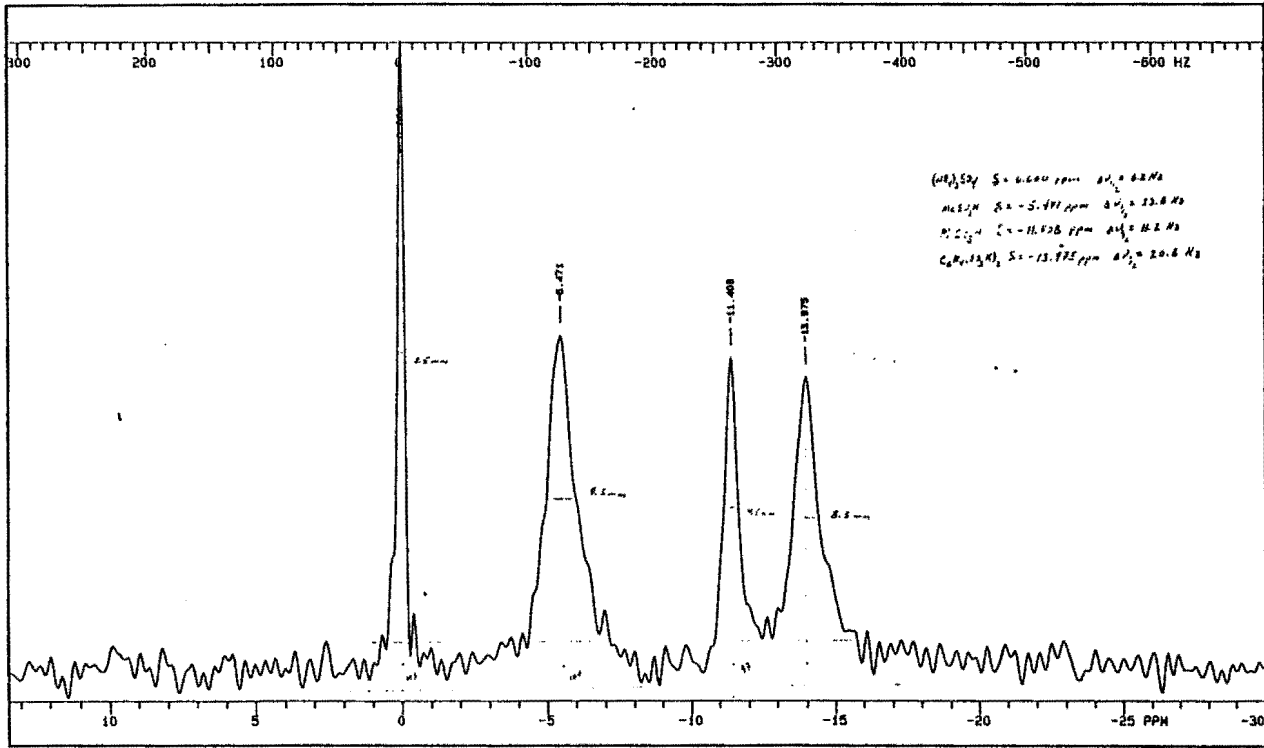


$^{33}\text{S}$  NMR Spectrum of Aqueous para-Ammoniobenzenesulfonic Acid Potassium Salt And  
Aqueous Ammonium Sulfate Reference At 20° C

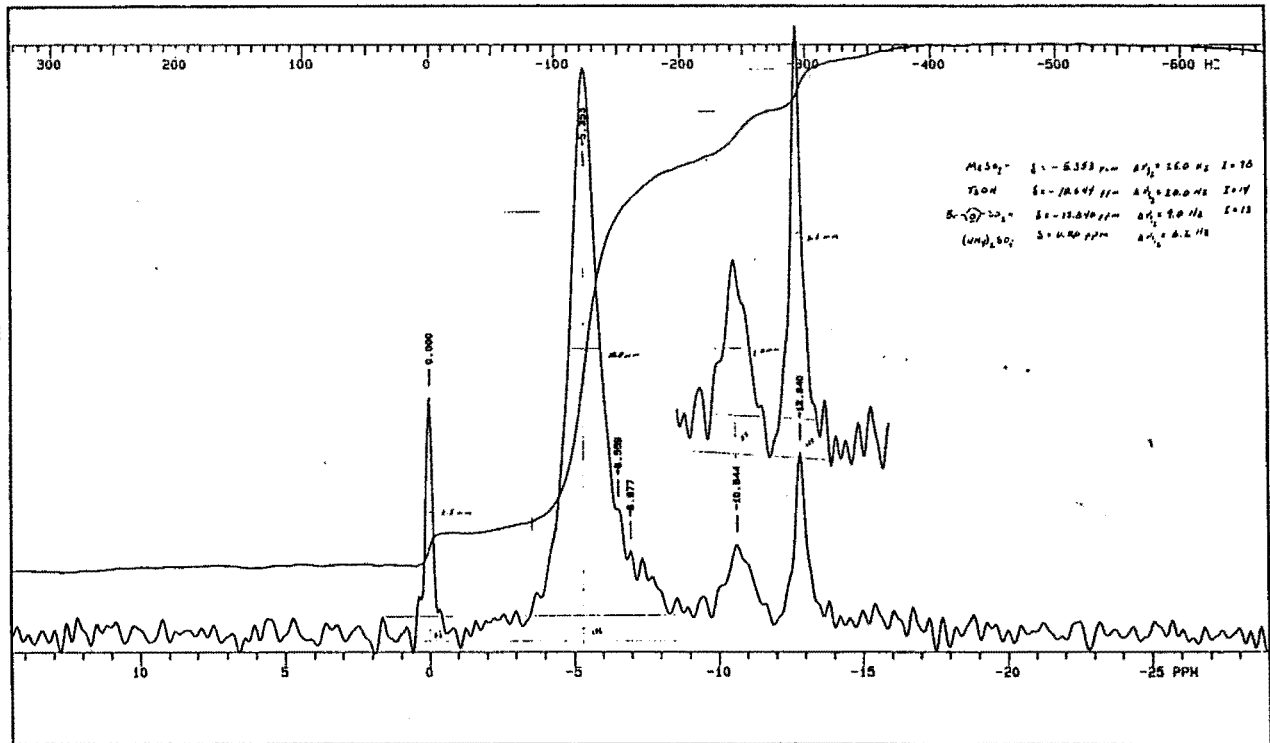


## **APPENDIX**





Mixture 1.



Mixture 2.

The  $^{33}\text{S}$  NMR spectra of two synthetic mixtures of sulfonic acids and a sulfonate salt dissolved in water appear here. Mixture 1 contained ammonium sulfate as the internal reference ( $\delta$  0.00 ppm), methanesulfonic acid ( $\delta$  -5.47 ppm), benzenesulfonic acid ( $\delta$  -11.41 ppm), and dipotassium *p*-benzenedisulfonate ( $\delta$  -13.98 ppm). The sum total concentration of all compounds was approximately 280 mmol/L. The sample solution was adjusted to pH 8 with one drop of 50% aqueous potassium hydroxide. The sample was contained in a 10 mm o. d. NMR sample tube, and broadband proton decoupling (square wave modulated) was used.

Mixture 2 contained methanesulfonic acid ( $\delta$  -5.35 ppm), *p*-methylbenzenesulfonic acid ( $\delta$  -10.64 ppm), and *p*-bromobenzenesulfonic acid ( $\delta$  -12.84 ppm). The solution pH was 2, and each compound was present at the 70 millimolar level. The sample was contained in a 10 mm o. d. NMR sample tube, and the chemical-shift reference was 0.1 M ammonium sulfate ( $\delta$  0.00 ppm) contained in a coaxial 5 mm o. d. NMR sample tube. Broadband proton decoupling (square wave modulated) was used.

The integration of  $^{33}\text{S}$  resonances of arenesulfonic acids in Mixture 2 was 1:1. The ratio of integrated intensities of  $^{33}\text{S}$  resonances of methanesulfonic acid to arenesulfonic acids was 7:1, although the molar ratio of  $^{33}\text{S}$  in all acids was 1:1. Since the total sulfonic acid concentration was 210 millimolar, these acids were completely ionized in water. Therefore, there was no detectable contribution to  $^{33}\text{S}$  relaxation from the protonated acid due to the low concentration and short lifetime of this species. Hence, the nonanalytic integration of alkyl- to arylsulfonic acids was not due to multiexponential decay of the  $^{33}\text{S}$  magnetization.<sup>48</sup> Rather, the disparate integration of the  $^{33}\text{S}$  resonance of methanesulfonic acid was most likely a result of greater nuclear Overhauser enhancement of this signal.<sup>49</sup>

## REFERENCES

1. Hinton, J. F. *Annual Reports On NMR Spectroscopy*, Webb, G. A., Ed.; Academic Press: New York, London, 1987; Vol 19, Chap 1.
2. (a) McFarlane, H. C.; McFarlane, W. *Multinuclear NMR*, Mason, J., Ed.; Plenum Press: New York, 1987; p 623. (b) *ibid*; Chap 15.
3. Harris, R. K. *Nuclear Magnetic Resonance Spectroscopy*, Longman Group UK Limited: Essex, 1986.
4. Abragam, A. *The Principles of Nuclear Magnetism*, Oxford University Press: Oxford, 1961, p 314.
5. Faure, R.; Vincent, E. J.; Ruiz, J. M.; Lena, L. *Org. Magn. Reson.* 1981, 15, 401.
6. Crumrine, D. S.; Gillece-Castro, B. *J. Org. Chem.* 1985, 50, 4408.
7. (a) Harris, D. L.; Evans, Jr., S. A. *J. Org. Chem.* 1982, 47, 3355. (b) Cassidei, L.; Fiandanese, V.; Marchese, G.; Sciacovelli, O. *Org. Magn. Reson.* 1984, 22, 486.
8. Levy, G. C.; Nelson, G. L. *Carbon 13 Nuclear Magnetic Resonance For Organic Chemists*, Wiley Interscience: New York, 1972; p 117.
9. Witanowski, M.; Stefaniak, L.; Januszewski, H. *Nitrogen NMR*, Witanowski, M., Webb, G. A. Eds.; Plenum Press: London, New York, 1973; Chap 4.
10. Modro, T. A.; Yates, K.; Janata, J. *J. Am. Chem. Soc.* 1975, 97, 1492.
11. (a) Cerfontain, H.; Schnitger, B. S. *Recl. Trav. Chim. Pays-Bas* 1972, 91, 199. (b) Maarsen, P. K.; Bregman, R.; Cerfontain, H. *Tetrahedron*, 1974, 30, 1211. (c) Koeberg-Telder, A. Cerfontain, H. *J. Chem. Soc., Perkin Trans. 2*, 1975, 226.

12. Hoffman, R. V.; Belfoure, E. L. *J. Am. Chem. Soc.* **1982**, *104*, 2183.
13. Cassidei, L.; Sciacovelli, O. *J. Magn. Reson.* **1985**, *62*, 529.
14. Hinton, J. F.; Buster, D. *J. Magn. Reson.* **1984**, *57*, 494.
15. (a) March, J. *Advanced Organic Chemistry*, McGraw-Hill Book Company: New York, 1977; p 252. (b) *ibid*, p 254.
16. Crumrine, D. S.; Shankweiler, J. M.; Hoffman, R. V. *J. Org. Chem.* **1986**, *51*, 5013.
17. Values taken from: Hine, J. *Structural Effects On Equilibria In Organic Chemistry*, Wiley-Interscience: New York; 1975.
18. Holz, M. *Progress in NMR Spectroscopy*, **1986**, *18*, 327.
19. (a) Deverell, C. *Progress in NMR Spectroscopy*, **1969**, *4*, 235. (b) Deverell, C. *Mol. Phys.* **1968**, *16*, 491.
20. (a) Hertz, H. G. *Ber. Bunsenges. Phys. Chem.* **1973**, *77*, 531. (b) *ibid.* 688.
21. (a) Melendres, C. A.; Hertz, H. G. *J. Chem. Phys.* **1974**, *61*, 4156. (b) Hertz, H. G.; Holz, M.; Keller, G.; Versmold, H.; Yoon, C. *Ber. Bunsenges. Phys. Chem.* **1974**, *78*, 24. (c) Hertz, H. G.; Holz, M. *J. Phys. Chem.* **1974**, *78*, 1002. (d) Hertz, H. G.; Weingartner, H.; Rode, B. M. *Ber. Bunsenges. Phys. Chem.* **1975**, *79*, 1190.
22. Weingartner, H.; Hertz, H. G. *Ber. Bunsenges. Phys. Chem.* **1977**, *81*, 1204.
23. Struis, R. P. W.; de Bleijser, J.; Leyte, J. C. *J. Phys. Chem.* **1989**, *93*, 7943.
24. Sternheimer, R. M. *Phys. Rev.* **1966**, *146*, 140.

25. Slichter, C. P. *Principles of Magnetic Resonance*, Springer-Verlag: Berlin, Heidelberg, New York, 1978; p 293.
26. Lehn, J. M.; Kintzinger, J. P. *Nitrogen NMR*, Witanowski, M., Webb, G. A. Eds.; Plenum Press: London, New York, 1973; p. 111.
27. Sacco, A.; Holz, M.; Hertz, H. G. *J. Magn. Reson.* **1985**, *65*, 82.
28. Lutz, O. *The Multinuclear Approach To NMR Spectroscopy*, Lambert, J. S., Riddell, F. G., Eds.; Riedel: Boston, 1983; Chap 1.
29. Hinton, J. F.; Shungu, D. *J. Magn. Reson.* **1983**, *54*, 309.
30. Haid, E.; Kohnlein, D.; Kossler, G.; Lutz, O. *J. Magn. Reson.* **1983**, *55*, 145.
31. Belton, P. S.; Cox, I. J.; Harris, R. K. *Magn. Reson. Chem.* **1986**, *24*, 171.
32. Hinton, J. F.; Buster, D. *J. Magn. Reson.* **1984**, *58*, 324.
33. March, J. *Advanced Organic chemistry*, 3rd ed.; Wiley: New York, 1985; p 221.
34. (a) Sigma values for 1, 2, 4, 5-8, 10-12, 15 taken from: Exner, O. *Correlation Analysis of Chemical Data*; Plenum Press: New York, 1988; p 143. (b) Sigma values for 3, 9, 13, 14 taken from: Exner, O. *Correlation Analysis In Chemistry - Recent Advances*; Chapman, N. B.; Shorter, J., Eds.; Plenum Press: New York, 1978; p 439.
35. Sigma values taken from reference 34a p 61.
36. Struis, R. P. W.; de Bleijser, J.; Leyte, J. C. *J. Phys. Chem.* **1989**, *93*, 7932.
37. Neurohr, K. J.; Drakenberg, T.; Forsen, S. *NMR of Newly Accessible Nuclei*. Laszlo, P., Ed.; Academic Press: New York, 1983; Vol. 2, Chap 8.

38. (a) Shannon, R. D.; Prewitt, C. T. *Acta Crystallogr.* 1969, B25, 925. (b) Huheey, J. E. *Inorganic Chemistry*, 2nd ed.; Harper and Row: New York, 1978, p 72.
39. Laszlo, P. *Angew. Chem. Int. Ed. Engl.* 1978, 17, 254 and references therein.
40. (a) Simeral, L.; Maciel, G. E. *J. Phys. Chem.* 1976, 80, 552. (b) Deverall, C.; Richards, R. E. *Mol. Phys.* 1969, 16, 421. (c) Hall, C.; Richards, R. E.; Schulz, G. N.; Sharp, R. R. *Mol. Phys.* 1969, 16, 529.
41. Drago, R. S.; *Physical Methods In Chemistry*, W. B. Saunders: Philadelphia, 1977; p 234.
42. Holz, M.; Weingartner, H.; Hertz, H. G. *J. Solution Chem.* 1978, 7, 705.
43. Criss, C. M.; Held, R. P.; Luksha, E. *J. Phys. Chem.* 1968, 72, 2970.
44. Drushel, W. A.; Felty, A. R. *Am. J. Sci.* 1917, 43, 57.
45. (a) Patt, S. L. *J. Magn. Reson.* 1982, 49, 161. (b) Fukushima, E.; Roeder, S. B. W. *J. Magn. Reson.* 1979, 33, 199. (c) Seiter, C. H. A.; Feigensohn, G. W.; Chan, S. I.; Hsu, M.-C. *J. Am. Chem. Soc.* 1972, 94, 2535.
46. Varian VXR program TEMCAL(E).
47. (a) Belton, P. S.; Cox, I. J.; Harris, R. K. *Magn. Reson. Chem.* 1986, 24, 1004. (b) Patt, S. L. *J. Magn. Reson.* 1982, 49, 161.
48. (a) Hubbard, P. S. *J. Chem. Phys.* 1970, 53, 985. (b) Bull, T. E. *J. Magn. Reson.* 1972, 8, 344. (c) Eliav, U.; Navon, G. *J. Magn. Reson.* 1990, 88, 223. (d) Chung, C.-W.; Wimperis, S. *J. Magn. Reson.* 1990, 88, 440.
49. See reference 3 page 108.



APPROVAL SHEET

The dissertation submitted by David C. French has been read and approved by the following committee:

Dr. David S. Crumrine, Director  
Associate Professor, Chemistry, Loyola University

Dr. A. Keith Jameson  
Professor, Chemistry, Loyola University

Dr. Duarte Mota de Freitas  
Associate Professor, Chemistry, Loyola University

Dr. Charles M. Thompson  
Associate Professor, Chemistry, Loyola University

Dr. Joseph B. Lambert  
Professor, Chemistry, Northwestern University

The final copies have been examined by the director of the dissertation and the signature which appears below verifies the fact that any necessary changes have been incorporated and that the dissertation is now given final approval by the Committee with reference to content and form.

The dissertation is therefore accepted in partial fulfillment of the requirements for the degree of Doctor of Philosophy.

13 November 1980  
Date

David S. Crumrine  
Director's Signature